INFRARED RADIANCE MODEL FOR THE AURORALLY DISTURBED ATMOSPHERE

Richard H. Bishop, et al

Utah State University

Prepared for:

Air Force Cambridge Research Laboratories
Advanced Research Projects Agency

31 August 1973

AFCRL-TR-73-0527

F.G.

1

center for research in aeronomy

Infrared Radiance Model for the Aurorally Disturbed Atmosphere

by

Richard H. Bishop, Ruey Y. Han,
Alan W. Shaw, and Lawrence R. Megill

FINAL REPORT

Period Covered: 1 August 1971 to
31 August 1973

31 August 1973

Contract No. F19628-71-C-0257
Project No. 1366

Sponsored by
Defense Advanced Research Projects Agency
ARPA Order No. 1366
Monitored by
Air Force Cambridge Research Laboratories
Air Force Systems Command, United States Air Force
Bedford, Massachusetts 01730

Contract Monitor: Randall E. Murphy
Optical Physics Laboratory

UTAH STATE UNIVERSITY

LOGAN, UTAH 84322

Unclassified

DOCUMENT CONTROL DATA - R&D

(Security classification of title, body of abstract and indexing annotation must be entered when the overall report is classified)

1. ORIGINATING ACTIVITY (Corporate author)

Center for Research in Aeronomy
Utah State University
Logan, Utah 84322

2a. REPORT SECURITY CLASSIFICATION

Unclassified

2b. GROUP

3. REPORT TITLE

INFRARED RADIANCE MODEL FOR THE AURORALLY DISTURBED ATMOSPHERE

4. DESCRIPTIVE NOTES (Type of report and inclusive dates)

Scientific Final 1 August 1971 - 31 August 1973 Approved 20 Nov 73

5. AUTHOR(S) (First name, middle initial, last name)

Richard H. Bishop Lawrence R. Megill
Ruey Y. Han
Alan W. Shaw

6. REPORT DATE

31 August 1973

7a. TOTAL NO. OF PAGES 149

7b. NO. OF REFS 52

8a. CONTRACT OR GRANT NO. F19628-71-C-0057 NEW ARPA Order No. 1366

b. Project, Task, Work Unit Nos.
1366 n/a n/a

c. DoD Element 62301D

d. Dod Subelement n/a

9a. ORIGINATOR'S REPORT NUMBER(S)

9b. OTHER REPORT NO(S) (Any other numbers that may be assigned this report)

AFCRL-TR-73-0527

10. DISTRIBUTION STATEMENT

A - Approved for public release; distribution unlimited.

11. SUPPLEMENTARY NOTES

This research was supported by the Defense Advanced Research Projects Agency.

12. SPONSORING MILITARY ACTIVITY

Air Force Cambridge Research Laboratories (OP)
L.G. Hanscom Field
Bedford, Massachusetts 01730

13. ABSTRACT

Recently, auroral observations have indicated the strong enhancement of certain infrared bands during periods of auroral activity. A theoretical model has been created in order to study the infrared processes associated with the aurora. The quantitative results of this study depend upon a thorough knowledge of the rates of all processes involved. Some of the rate constants are well known while for others we have made only the crudest approximation. Qualitatively, however, our results indicate that certain infrared bands of CO_2, N_2O, NO, and NO^+ are strongly enhanced during periods of auroral activity. This is primarily the result of two basic energy exchange mechanisms. The energy deposited by the primary auroral electron flux goes into increasing the internal energy of N_2, O_2, and O. That is, the vibrational temperature of N_2 is significantly increased in an aurorally disturbed atmosphere. This energy is then transferred to various infrared active minor constituents such as CO_2, N_2O, NO, etc., through near resonant vibrational-vibrational exchange processes, increasing the higher level vibrational opulations of these species and thereby enhancing their infrared radiative output. In addition to energetic auroral particles as an energy source, we have also considered electric fields. Qualitatively the results are similar except that the energy tends to be deposited at altitudes somewhat higher than in direct precipitation processes.

DD FORM 1 NOV 65 1473

Unclassified
Security Classification

14 KEY WORDS	LINK A		LINK B		LINK C	
	ROLE	WT	ROLE	WT	ROLE	WT
Infrared emissions						
Aurora and airglow						
Atmospheric radiation						
Theoretical investigation						
Computer code						

TABLE OF CONTENTS

TABLE OF CONTENTS (cont.)

LIST OF ILLUSTRATIONS

LIST OF ILLUSTRATIONS (cont.)

LIST OF ILLUSTRATIONS (cont.)

LIST OF ILLUSTRATIONS (cont.)

LIST OF ILLUSTRATIONS (cont.)

LIST OF TABLES

NOTE ADDED IN PROOF

The radiances computed for selected bands of the infrared active minor constituents treated in this study are affected by various input radiative fluxes, as discussed in the report. The values adopted for the terrestrial flux were based on the study of *Corbin et al.*, [1970].

It has recently been suggested [*Murphy*, 1973], and subsequently confirmed [*Degges*, 1974], that the radiative flux from the lower boundary for the present calculations (60 km), as provided by the cited study, is probably significantly in error over portions of the spectral region of interest. In strongly absorbing spectral regions, the effective blackbody temperature at the lower boundary is expected to closely approach the local kinetic temperature. (For example, in the spectral region around 4.3 microns, where the atmosphere is optically very thick at 60 km, the appropriate blackbody temperature should approximate 250°L for the temperature profile assumed in the present study, whereas a value of 220°K was obtained from the work of *Corbin et al.*)

The general impact of the error is to render too small the calculated vibrational populations (and hence band radiances), particularly in the region of the lower boundary. Corrections must be made on a band-by-band basis since the local optical thickness differs from band to band. The significance of the corrections will also depend on the relative importance of the various mechanisms which determine the population of a particular excited level.

It is important to note that the problem with the terrestrial flux does not invalidate the primary conclusion of the study, i.e., that the auroral energy input to the upper atmosphere can significantly enhance certain atmospheric infrared emissions during and immediately after periods of strong auroral activity.

Among all the bands considered in this study, probably the CH_4 band at 3.31 μ is the one which has the biggest error because the absorption of terrestrial flux plays the predominant role in excitation of this band. An approximate estimation indicates that differences as large as one order of magnitude could be caused by the error in terrestrial flux on the calculated band radiance.

INTRODUCTION

The purpose of this study is to investigate the natural infrared background of the earth in the 1 to 25 micrometer region of the electromagnetic spectrum. The study is primarily concerned with the natural infrared background during aurorally disturbed conditions. In order to define this condition, the quiescent background must also be defined. It was originally felt, and has been substantiated by this study, that the auroral energy input would significantly change some of the atmospheric infrared emissions during times of auroral activity.

The emphasis of the work effort was the development of a computer program to physically model the atmosphere in an effort to predict infrared emissions under various conditions of auroral activity. As a starting point, the atmospheric radiance models developed by *Corbin et al.* [1970] under a Honeywell, Inc. contract let by the Air Force Cambridge Research Laboratories were adopted. The so-called low-altitude program was used only to determine terrestrial fluxes as an input to the new program to be developed. The so-called high-altitude program, on the other hand, was used as a starting point for the new program.

The high-altitude programs of *Corbin et al.* [1970] predict infrared emissions for the gases CH_4, CO_2, H_2O, NO, N_2O, and O_3 during quiescent conditions. These programs contain no atmospheric chemistry. The present study undertook to modify these programs by adding additional minor constituent gases, extending the spectral region to include some emissions from the region 1.0 to 5.0 micrometers, and lastly but more importantly, to include a time-dependent accounting of the effect of the auroral energy input on the vibrational populations as well as the number density profiles of the various minor constituents under consideration. This, of course, implies that a number of atmospheric chemical processes were considered.

The high-altitude program of this study includes infrared emissions from CH_4, CO_2, H_2O, NO, N_2O, O_3, NO^+, OH, and CO. The inclusion of NO^+ in the list of gases changes the context of minor constituents

to that of ions and neutral molecules rather than solely neutral molecules. The programs which account for atmospheric chemistry, therefore, must not only be concerned with neutral chemistry but must also be concerned with ion chemistry, as well as the interaction of charged auroral particles with the atmosphere. A major programming effort was also necessary in order to determine the effects that the incoming auroral particles would have on the vibrational temperature of molecular nitrogen. An accurate knowledge of the vibrational population of molecular nitrogen is necessary because of the importance of the many near-resonant vibrational-vibrational energy exchange processes between N_2 and minor constituent gases.

One of the results of the current study is in the form of a plot or a table giving the infrared band radiance in watts/cm^2-steradian for various important bands of the minor constituent gases previously mentioned. The infrared radiance is given in 5-km increments from 60 km up to 150 km (or the point where the number densities of the gas become insignificant) and then in 25-km increments thereafter to 500 km. The direction in which the observer is looking is varied and includes the vertical direction (zenith angle 0°) as well as zenith angles of 20°, 40°, 60°, 70°, 80°, and 90° (horizontal). One other geometry (limb view) is considered and that is one placing the observer outside of the atmosphere and allowing him to view along a path which is tangent, not to the earth's surface, but rather to an atmospheric shell above the earth. The atmospheric shells (points of tangency) are located in 5-km increments from 60 km to 150 km and thereafter in 25-km increments. The height from the surface of the earth to the atmospheric shell, which is tangent to the view path, is called the tangent height. The viewpath of the observer does not stop here but rather extends to a point outside of the atmosphere on the side away from the observer.

A second form of result is presented as a plot or a table giving a compilation of the infrared radiance of all the bands of all the gases. This is done for the limb view case, the vertically looking case, and the horizontally looking case. The table or plot lists the radiance in watts/cm^2-steradian every 0.1 micrometer over the region of interest.

Several auroral and quiescent sets of conditions were studied. In this context a quiescent atmosphere has the meaning that no visible aurora is present. We have examined the infrared output in the 1-25 micron spectral region under this definition of quiescence but with an electron drizzle present. We have also taken a quiescent case but with electric fields being present in the atmosphere. Further, we have studied the infrared emissions from the atmosphere with a class IBC-II and a class IBC-III aurora in progress. A more detailed description of the input parameters during both quiescent and aurorally disturbed conditions will be presented in a following section of this report.

GENERAL DESCRIPTION OF IR BAND MODEL PROGRAM

The purpose of this section of the report is to give a brief but adequate description of the general philosophy used in computing the infrared emissions on a band-by-band basis for each of the minor constituent gases under consideration.

The quantity of infrared radiation emitted by any band is directly proportional to the number density of molecules in the excited state capable of radiating at the band wavelength. It is therefore necessary to have as an input to the model the best information available with regard to the height profile of the number density for each species under consideration. With a knowledge of the height profile and a given temperature model, one may easily calculate, using the Boltzman equation, the populations of the various vibrational levels of a gas. These results represent the local thermodynamic equilibrium (or LTE) case. At auroral altitudes one is often not interested in this case, since many atmospheric conditions do not justify the assumption of local thermodynamic equilibrium. When local thermodynamic equilibrium conditions do not prevail (the NLTE case), one must consider radiative energy exchange processes as well as collisional energy exchange processes in order to determine with reasonable certainty the vibrational populations of a gas.

In order to compute the vibrational populations of a gas under NLTE conditions, one must have as an input to the program such quantities as solar flux, terrestrial flux, and radiative flux from other parts of the atmosphere, as well as excitation and de-excitation rates for the collision processes of vibrational-translational (V-T), translational-vibrational (T-V), and near resonant vibrational-vibrational (V-V) energy exchange. Additional inputs giving information as to the characteristics of the molecule itself are also required. These would include the energy levels and their degeneracies, rotational constants, band transitions, and band strengths.

With this background we may now outline the methodology used in the computation of the emission of a particular infrared band. First the required inputs as described above are read into the computer. A Boltzman or LTE population is determined for each of the vibrational levels. Then, using this population as a starting point, an equation describing both radiative and collisional excitation and de-excitation processes is solved in an iterative fashion, leading to a new value of vibrational population. The new population is now representative of NLTE conditions.

Although a study of how the vibrational populations of various gases change with changing NLTE conditions is of interest in itself, it is more important to relate this to a quantity which can be measured. We desire to know the band radiance expressed in this report as watts/cm^2-steradian that one would observe for various infrared bands for a variety of conditions. If one integrates this quantity over a column with unit area cross section along some optical path length, one obtains the predicted radiance for the chosen band and NLTE conditions. Most of the gases considered are optically thin; however, in the case of the 4.3 μ band of CO_2 this is not true. In this case self absorption must be included in the integration in order to obtain the radiance.

The picture which has been presented thus far appears simple enough on the surface; however, in a detailed analysis, it becomes rather complicated, especially during periods of electron precipitation. Let us briefly consider the procedures involved in handling the energy exchange processes during an auroral distrubance. First a

model is chosen to represent the primary auroral electron flux. With a knowledge of the primary flux, one may calculate the energy deposition rate for the electrons. By applying the proper cross sections, the total production rates of N_2^+, O_2^+, and O^+ may also be calculated These production rates, in addition to various neutral-neutral and ion-neutral chemical reactions, charge exchange, and recombination must be considered in order to determine the height profiles for such quantities as $[N_2^+]$, $[O_2^+]$, $[O^+]$, $[NO^+]$, and $[NO]$. These height profiles are computed on a time-dependent basis in order to study changes which take place shortly after an aurora commences. It has been found that of the minor constituents under consideration the height profiles of $[NO]$ and $[NO^+]$ change in a significant enough manner after auroral commencement to warrant using these new height profiles as an updated input to the program. In addition to the height profiles just described, a production rate for secondary electrons may also be computed. This has been done following the techniques of *Rees, Stewart,* and *Walker* [1969]. With an accurate knowledge of secondary electron production, one may compute the secondary electron flux and then in turn (and with a knowledge of the cross sections) the production rates for $N_2(v=1)$, $O_2(v=1)$, and $O(^1D)$.

From the description just given, it can be seen that a large portion of the auroral energy is at least temporarily deposited in the form of vibrational energy for the molecular N_2 and O_2 and in the form of electronic energy for atomic oxygen. At this point several other energy exchange processes occur. Energy stored in the $O(^1D)$ atom becomes an important production source for $N_2(v=1)$ while both $N_2(v=1)$ and $O_2(v=1)$ exchange energy through near resonant (V-V) processes with all of the minor constituents except OH.

Study has shown that due to the importance of the near resonant (V-V) energy exchange process, several bands are particularly enhanced during auroral activity. These include the bands of CO_2, NO, N_2O, and NO^+.

Thus it is seen that in order to accurately predict infrared emissions (particularly for the bands mentioned above) one must have available an accurate knowledge of the vibrational population of molec-

ular nitrogen. The methods used in determining the vibrational population of N_2 will be presented in detail in a later section.

INPUT PARAMETERS FOR THE INFRARED BAND MODELING PROGRAM

The height profiles of the number densities of the various minor constituent gases as well as the height profiles for [O], [O_2], and [N_2] and the temperature were obtained from a variety of sources. This also holds true for the molecular constants, the band strengths, the input fluxes, etc. It is therefore the purpose of this section of the report to collect together what are considered the more important of these parameters and to state the source of the values used.

Number Density Height Profiles

The height profiles of [CH_4], [CO_2], [H_2O], [N_2O], [O_3] noon, [O_3] predawn, [OH] day, [OH] night, and [CO] are shown in Figures 1-9 respectively. The height profiles of [CH_4], [CO_2], [H_2O], and [N_2O] were adopted from *Corbin et al.* [1970]. It was necessary to modify the [O_3] predawn height profiles of *Corbin et al.* in order to make them compatible with the [OH] profiles of *Shimazaki* and *Laird* [1970]. To explain this further, it was assumed in this report that OH is predominantly formed by the process $H + O_3 \rightarrow OH + O_2$. We have used the height profiles of both [H] and [OH] (day and night) from *Shimazaki* and *Laird* [1970]. The [O_3] profile used by *Corbin et al.* was somewhat larger at higher altitudes than that of *Shimazaki* and *Laird* and had we used it, it would have led to a population inversion of [OH] as it is modeled in this program. On the other hand, the profiles by *Shimazaki* and *Laird* do not have quite the structure at lower altitudes as those of *Corbin et al.* Therefore, it was decided to simply modify the height profiles of *Corbin et al.* in the higher altitude region. The one remaining height profile is [CO]. It was assumed that CO constitutes 7.0×10^{-8} times the total number density as suggested by *Goody* [1964].

Figures 10-13 show the height profiles of [NO] and [NO^+] during an electron drizzle but no aurora and during an IBC-III aurora respec-

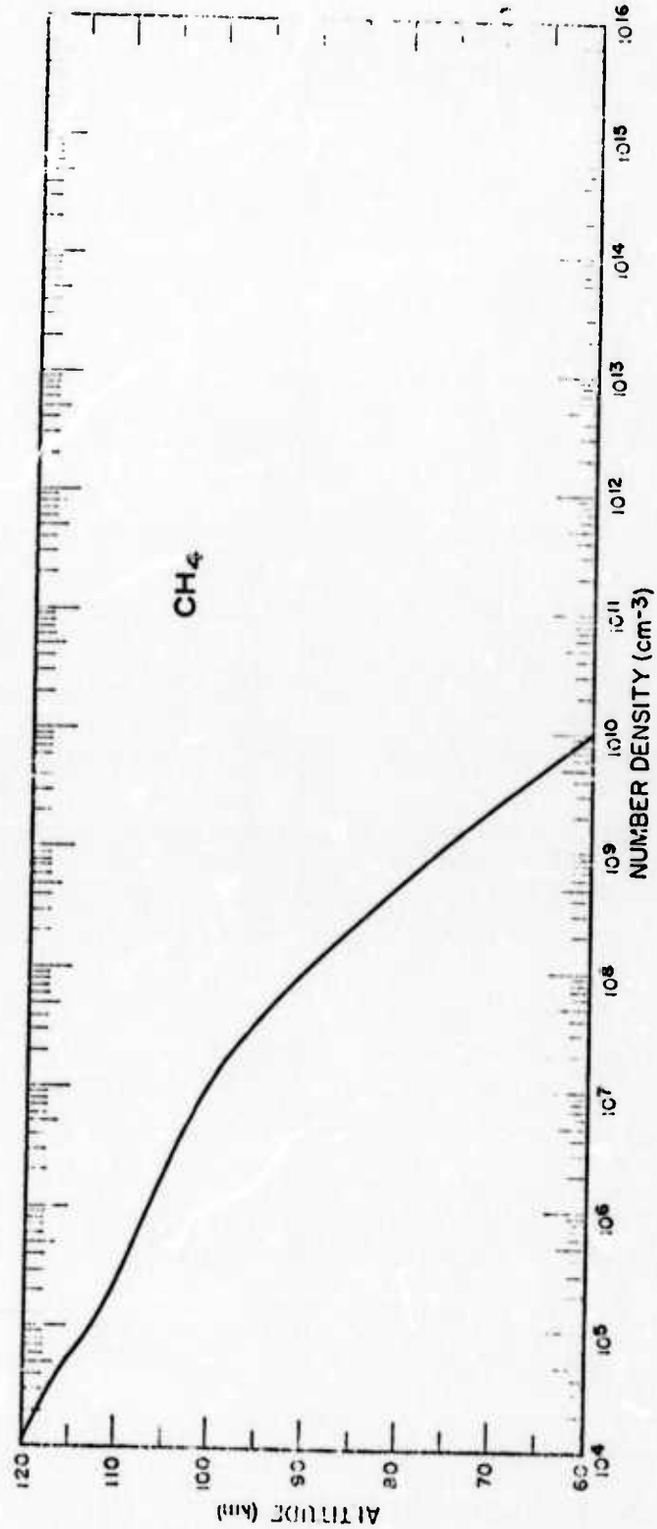

Figure 1. Height profile of CH_4.

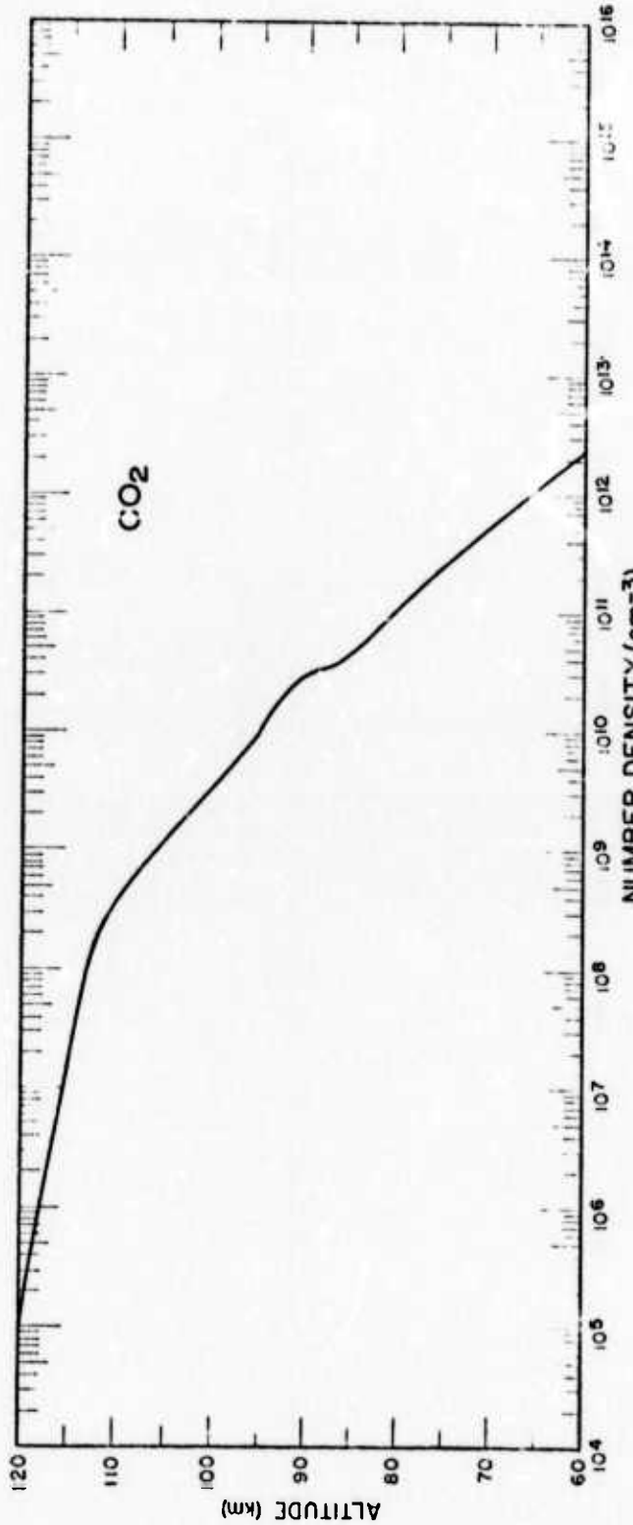

Figure 2. Height profile of CO_2.

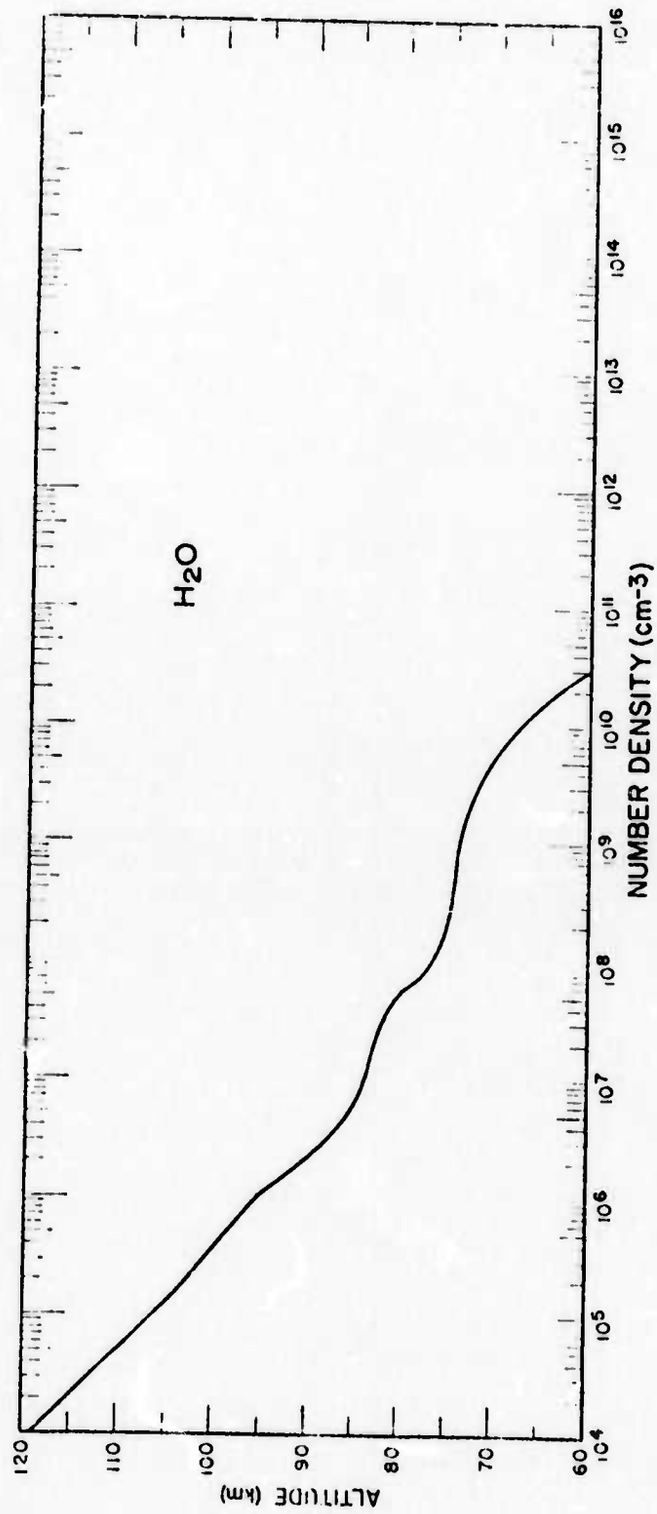

Figure 3. Height profile of H_2O vapor.

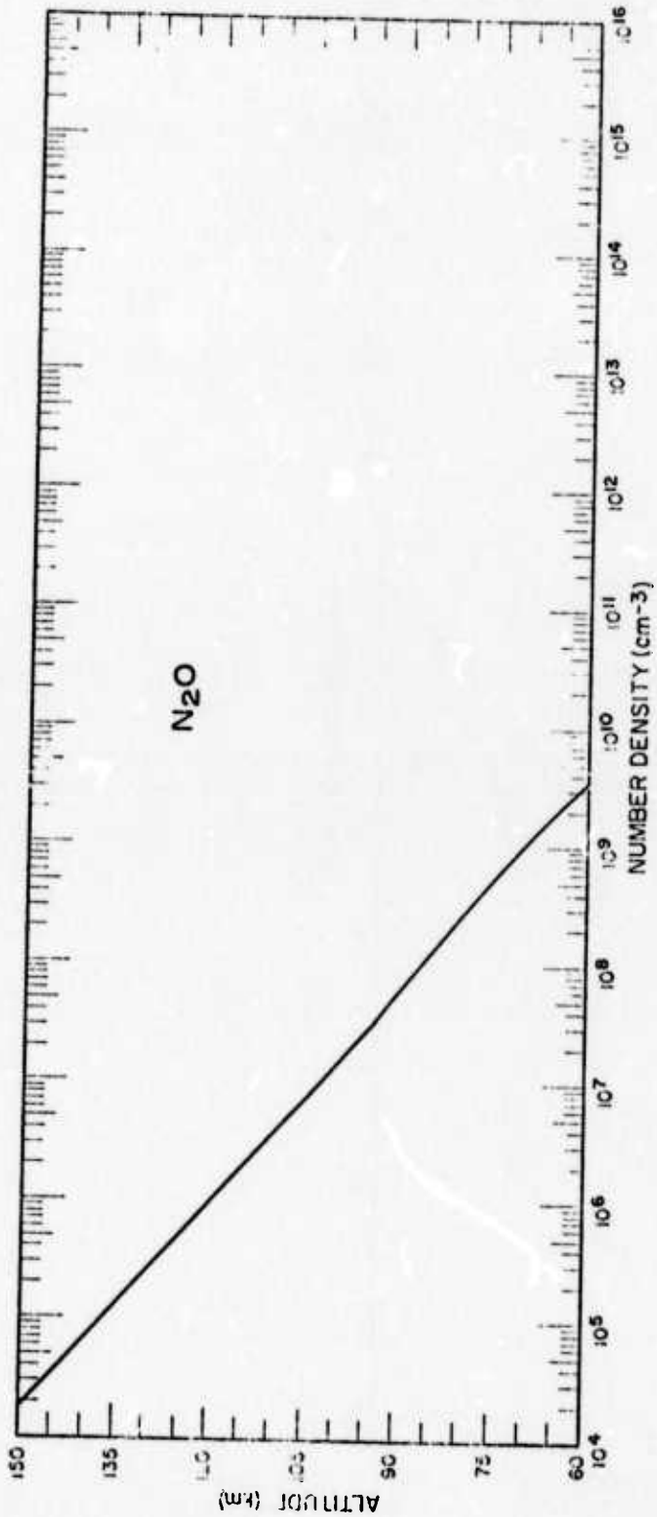

Figure 4. Height profile of N_2O.

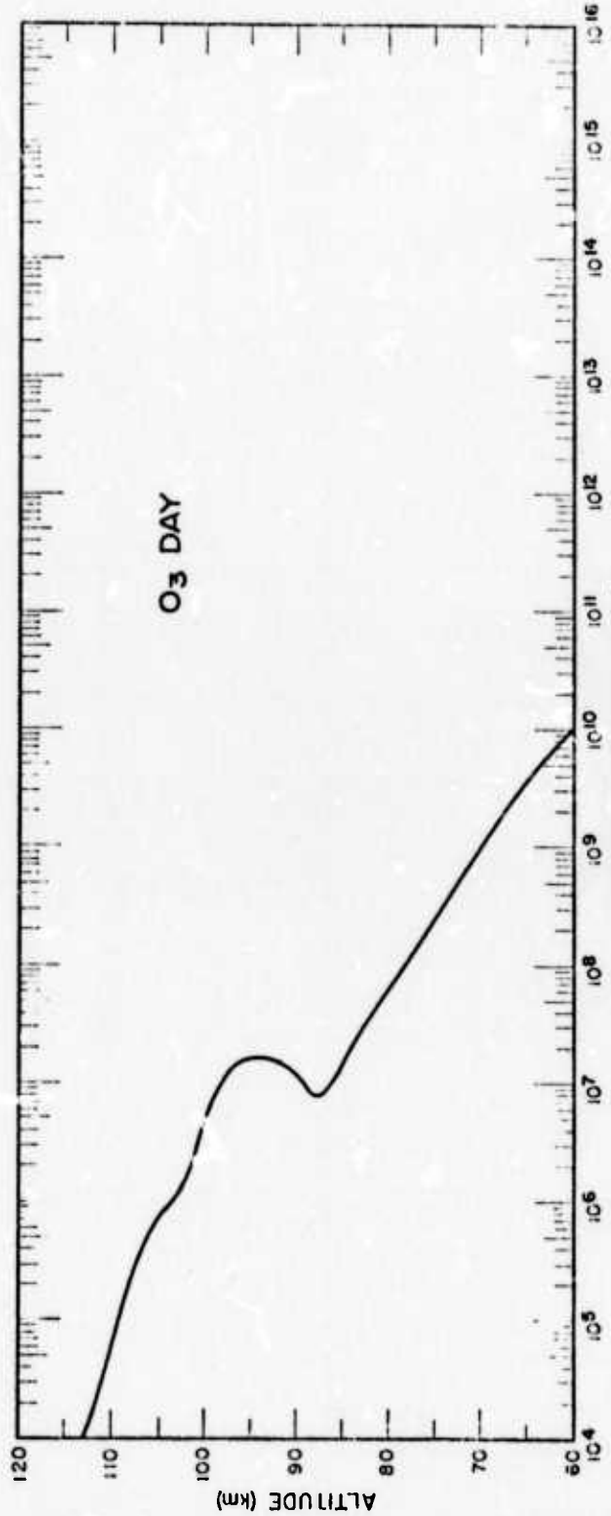

Figure 5. Daytime height profile of O_3.

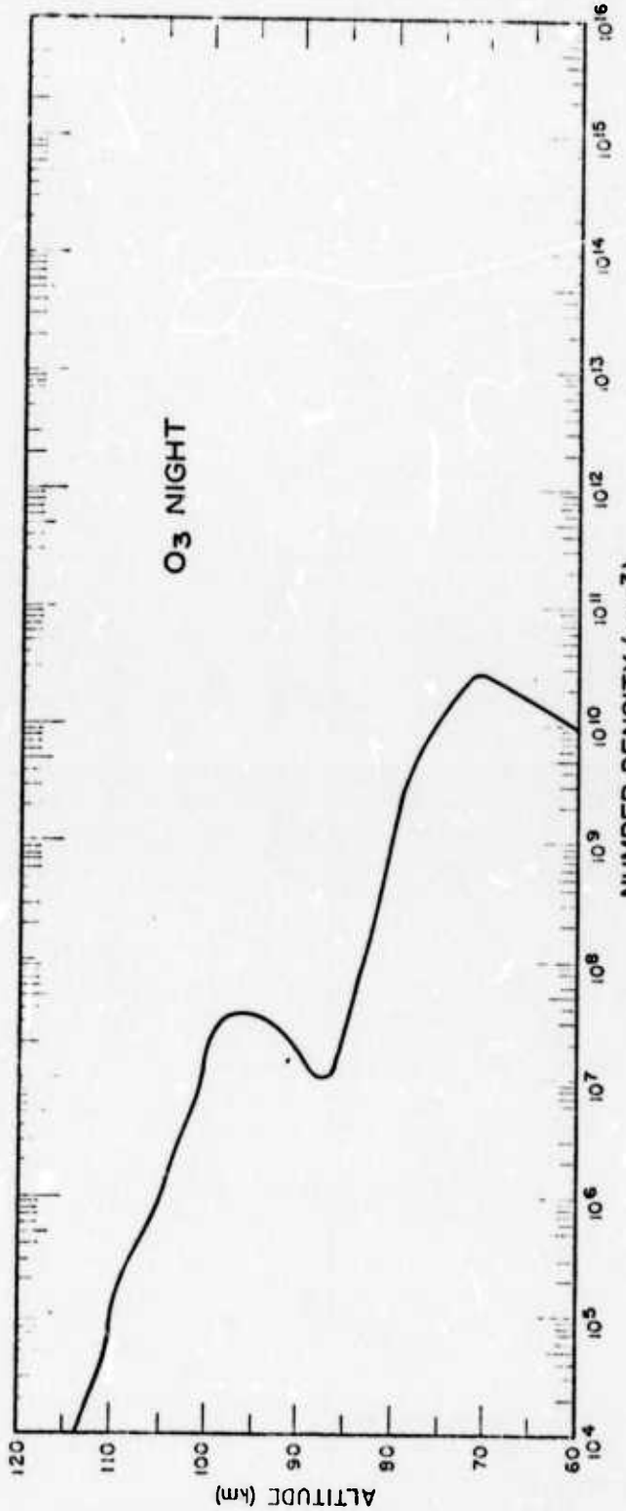

Figure 6. Pre-dawn height profile of O_3.

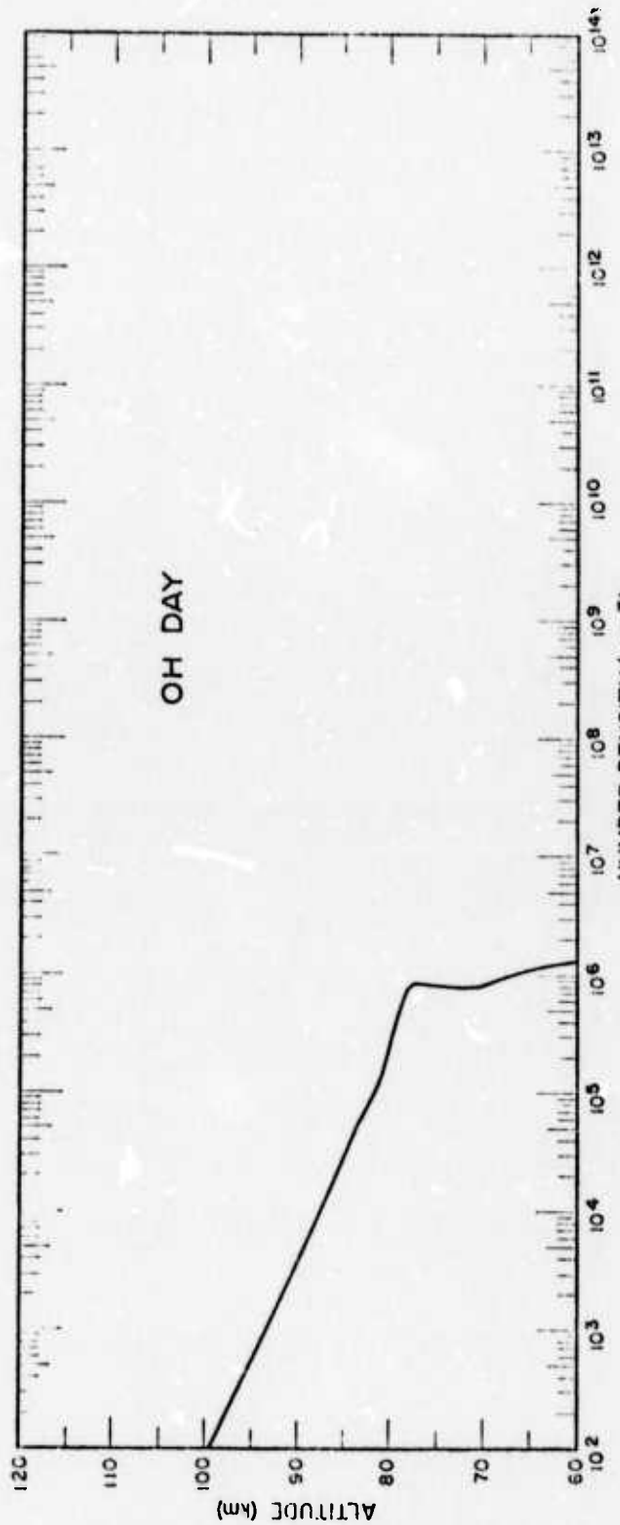

Figure 7. Daytime height profile of OH.

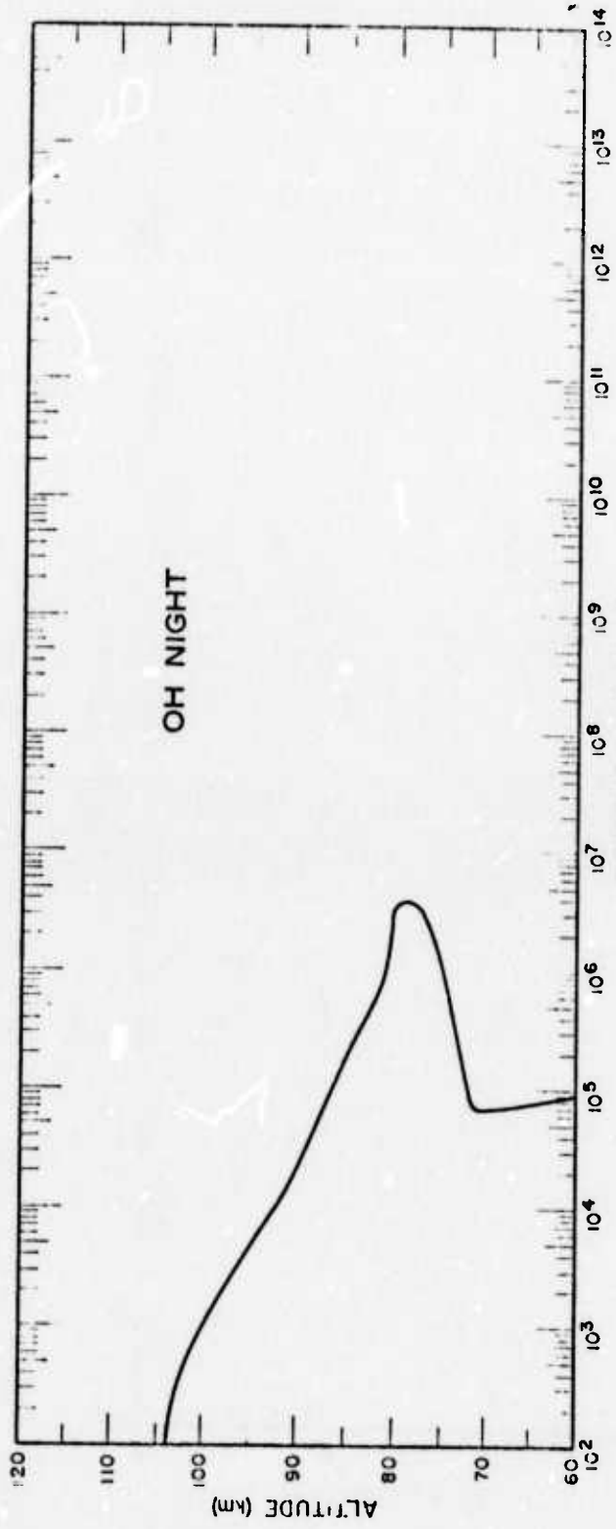

Figure 8. Nighttime height profile of OH.

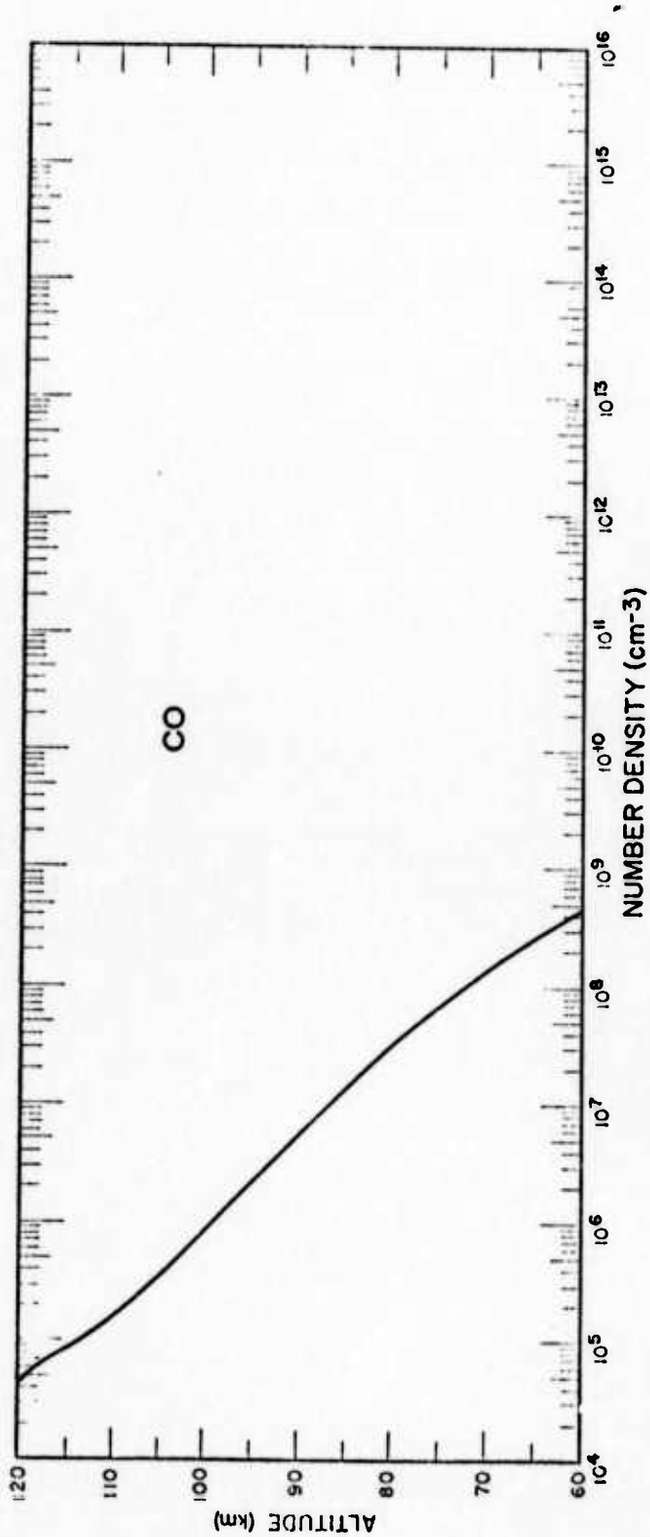

Figure 9. Height profile of CO.

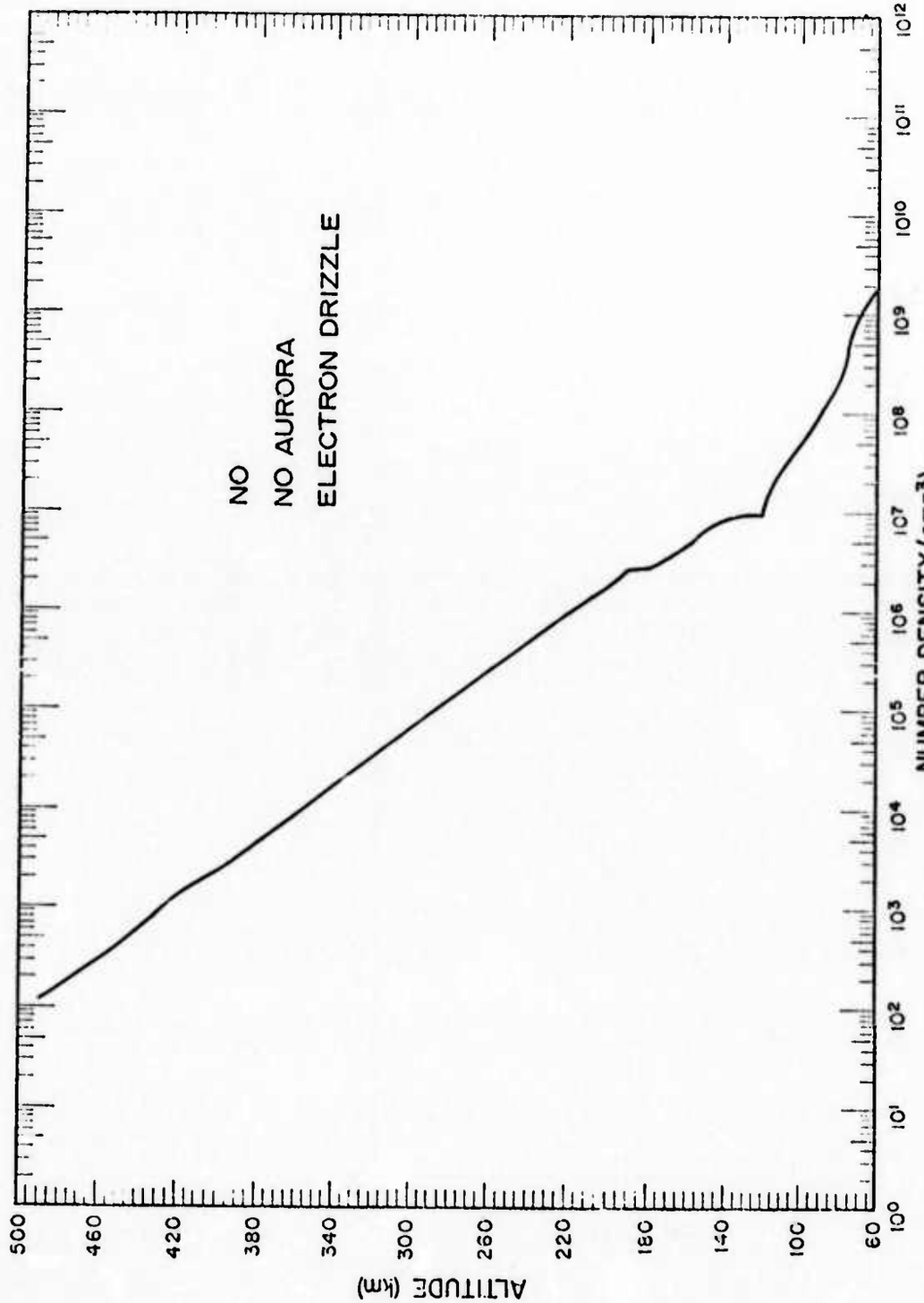

Figure 10. Height profile of NO, no aurora but with an electron drizzle present.

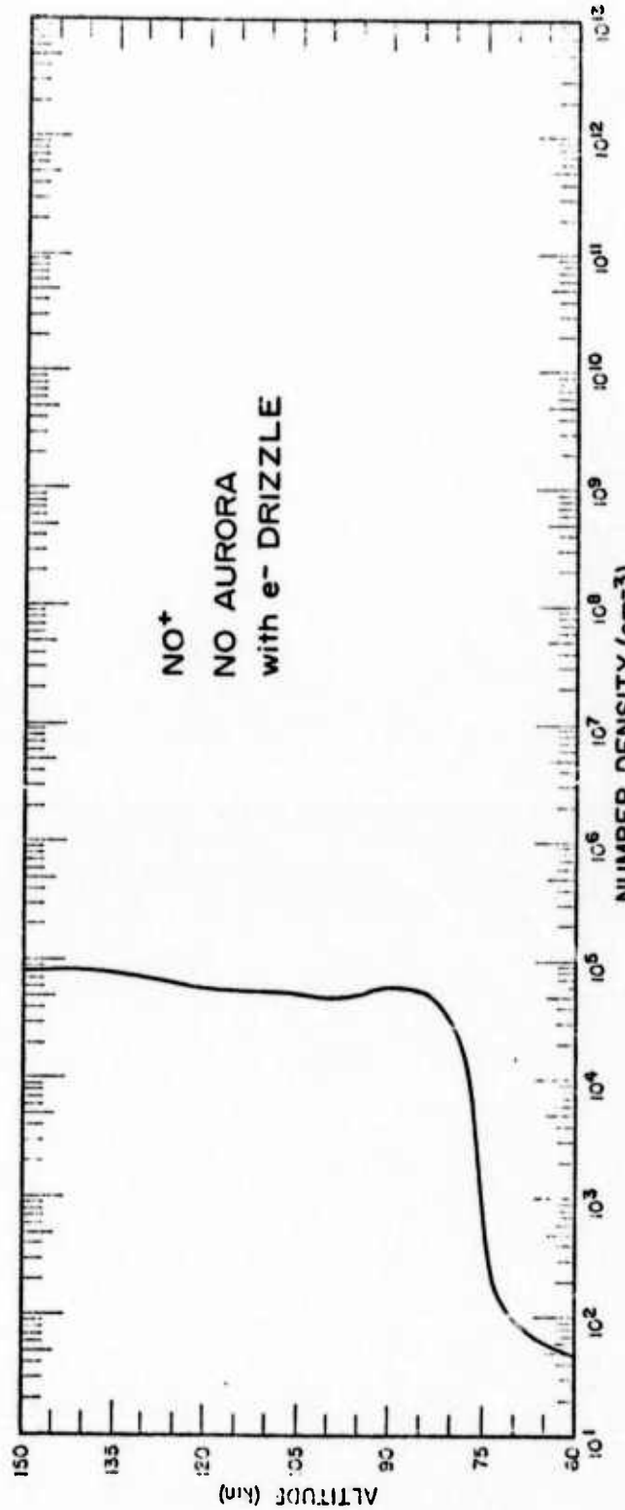

Figure 11. Height profile of NO^+, no aurora but with an electron drizzle present.

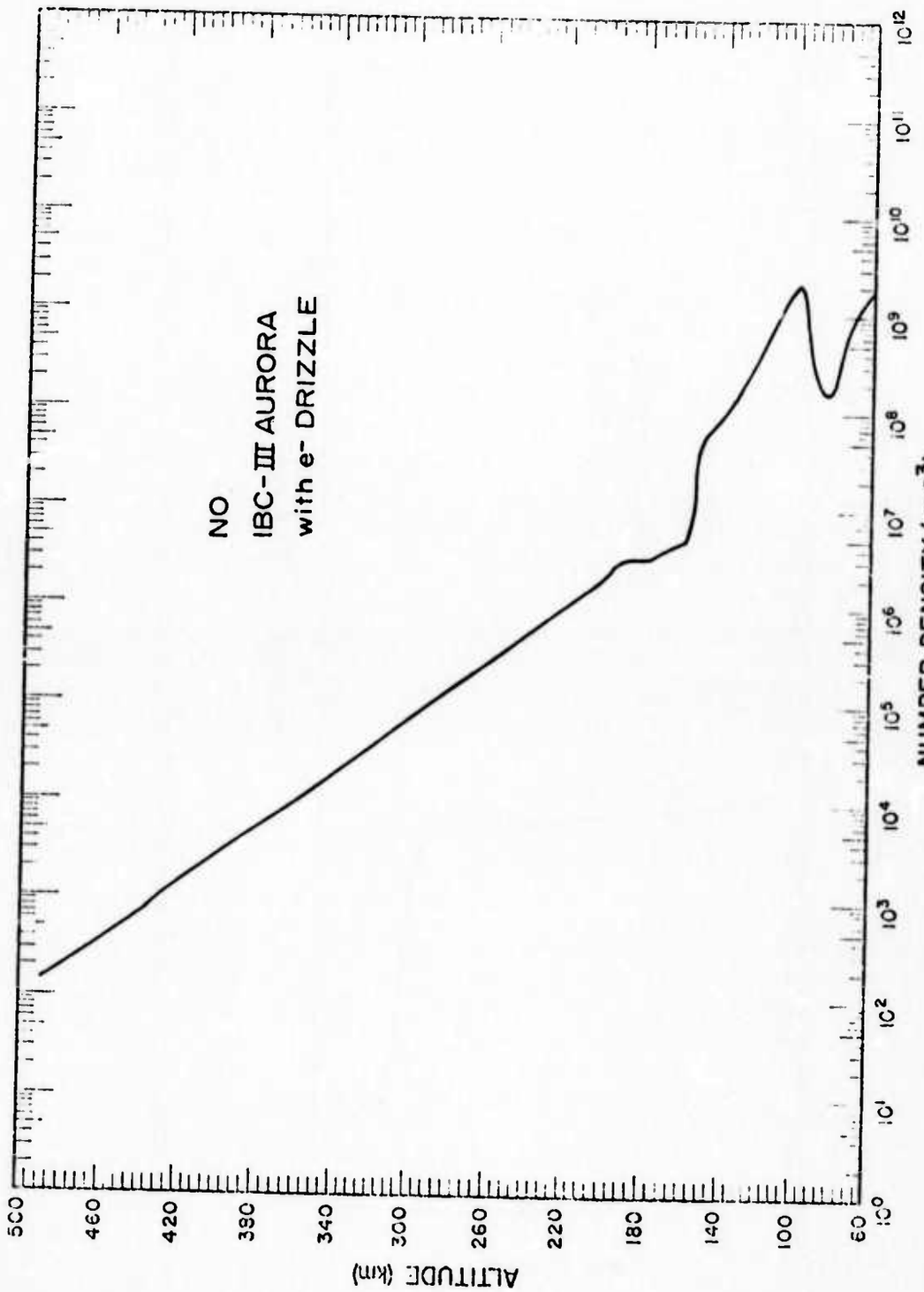

Figure 12. Height profile of NO five minutes after auroral commencement.

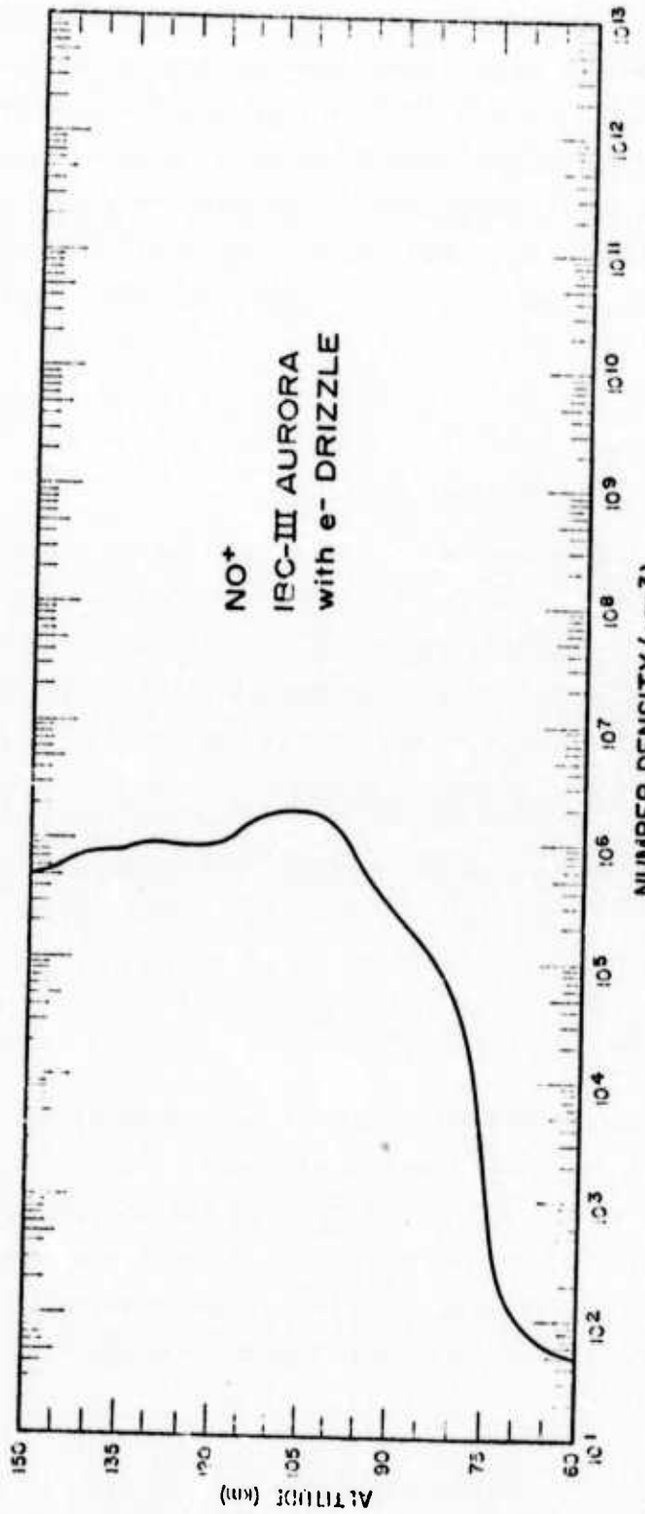

Figure 13. Height profile of NO five minutes after auroral commencement.

tively. These height profiles are computed in the chemistry subprogram which will be explained in detail in a later section of this report.

The height profiles of $[N_2]$, $[O_2]$, and $[O]$ are shown in Figures 14, 15, and 16. These profiles have been extracted from *Adams* [1970]. The height profile of the total number density is shown in Figure 17. Figure 18 shows the temperature model used. This model is the spring/fall mid-latitude model from the *U.S. Standard Atmosphere Supplement* [1966].

Rotational Constants

Of the molecules under consideration in this report, all are linear with the exception of CH_4, H_2O, and O_3. The rotational constants B_v of a diatomic molecule for a given vibrational level v are different from the rotational constants for the equilibrium positions, B_e. To find B_v an averaging process is used which can be shown to yield

$$B_v = B_e - \alpha_e(v + \tfrac{1}{2}) + \ldots \qquad (1)$$

where α_e is a constant which depends upon the anharmonicity of the vibrations as well as B_e and other factors. For linear polyatomic molecules the expression for B_v becomes

$$B_v = B_e - \sum \alpha_i \left(v_i + \frac{d_i}{2}\right) + \ldots \qquad (2)$$

Here the subscript v has become the set of quantum numbers v_1, v_2, $v_3, \ldots$ and $d_i = 1$ or 2 for nondegenerate and doubly degenerate vibrations respectively. Table 1 is a compilation of the rotational constant, B_v for all of the minor constituents along with the source of these constants. Also listed in this table are the wave numbers of the vibrational levels. These were taken either from the listed source or *Corbin et al.* [1970].

Band Strengths

The integrated absorption S'_{lu} with dimensions cm^{-1} sec^{-1} may be written in the following manner:

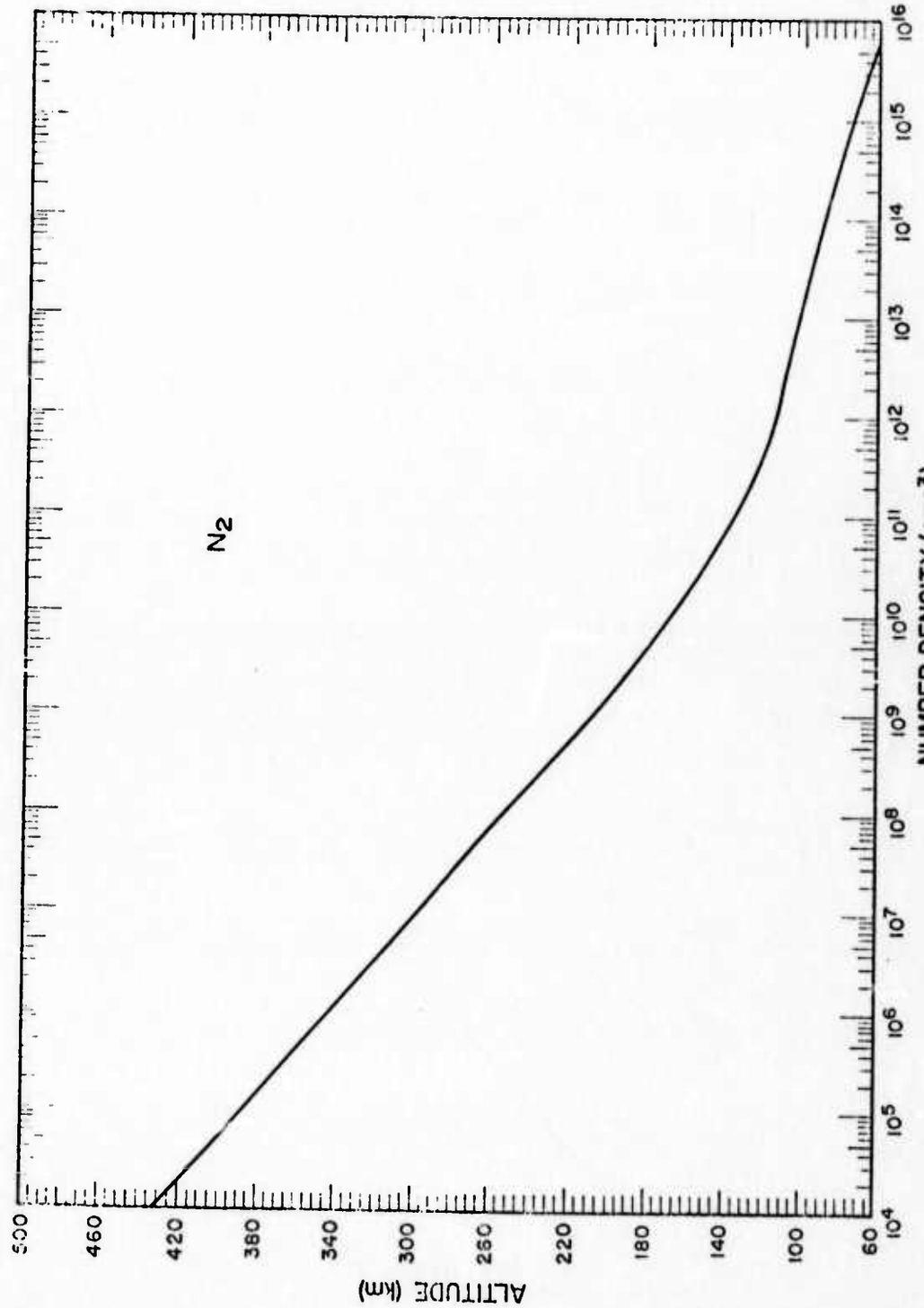

Figure 14. Height profile of molecular nitrogen.

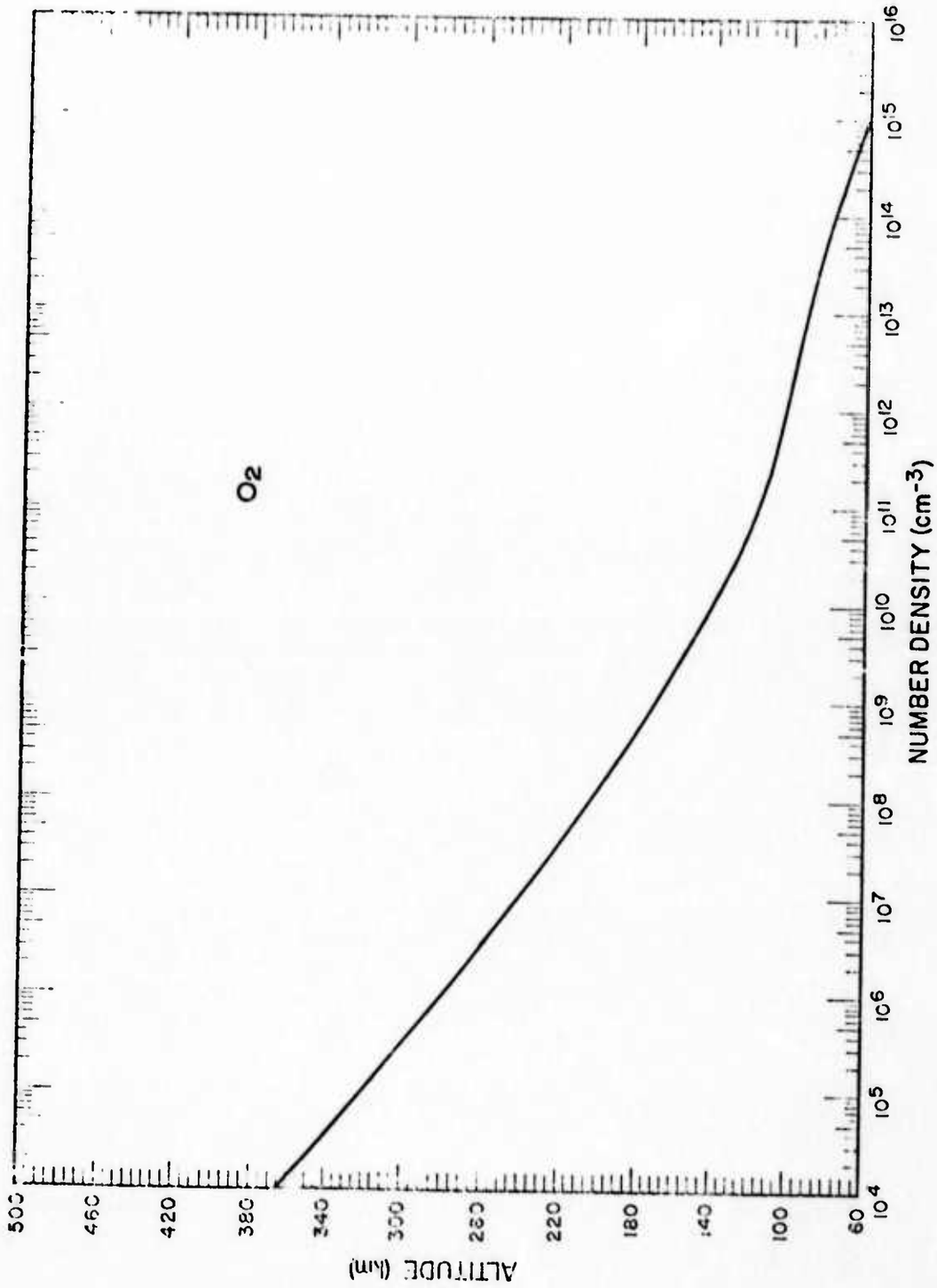

Figure 15. Height profile of molecular oxygen.

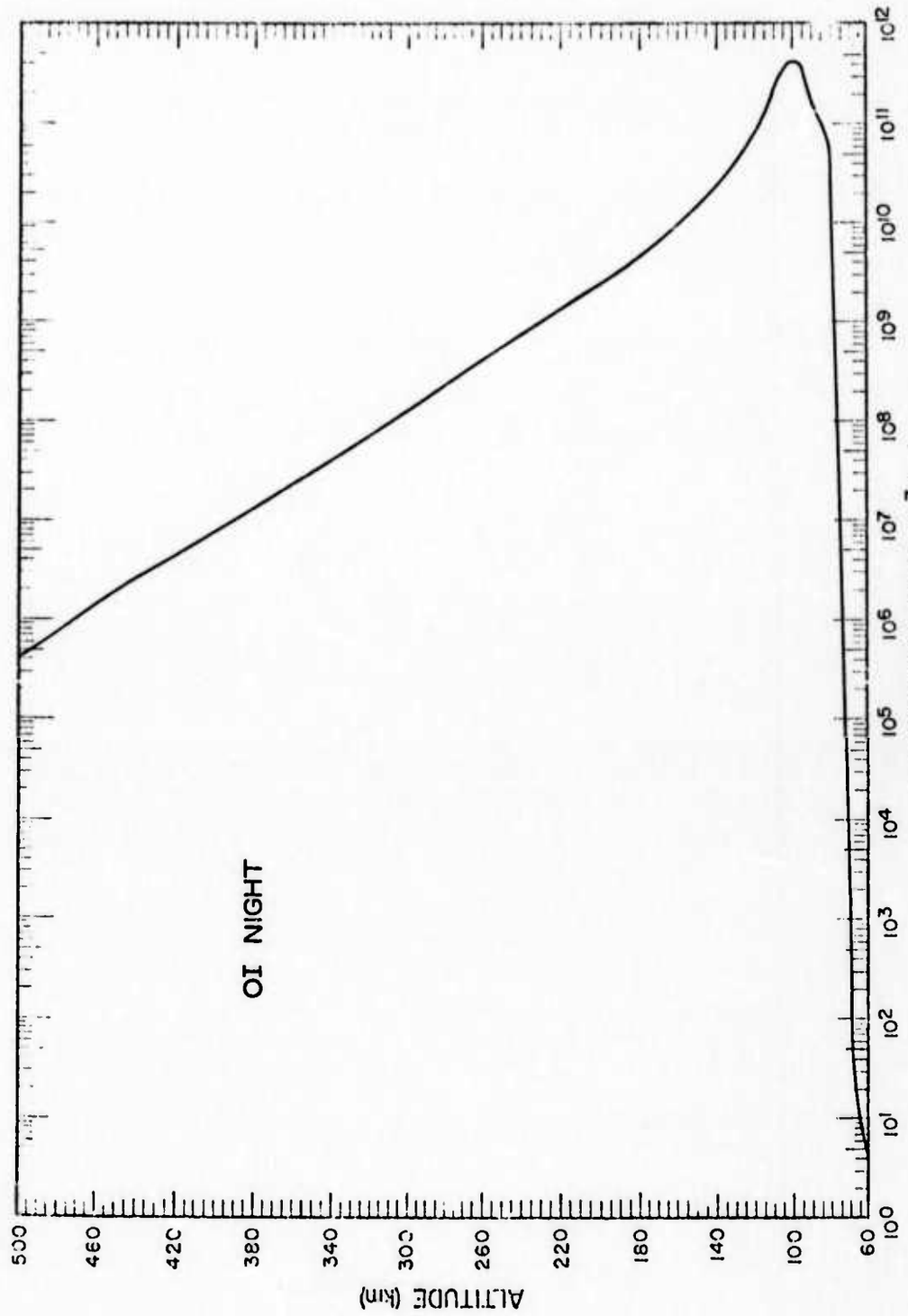

Figure 16. Height profile of atomic oxygen.

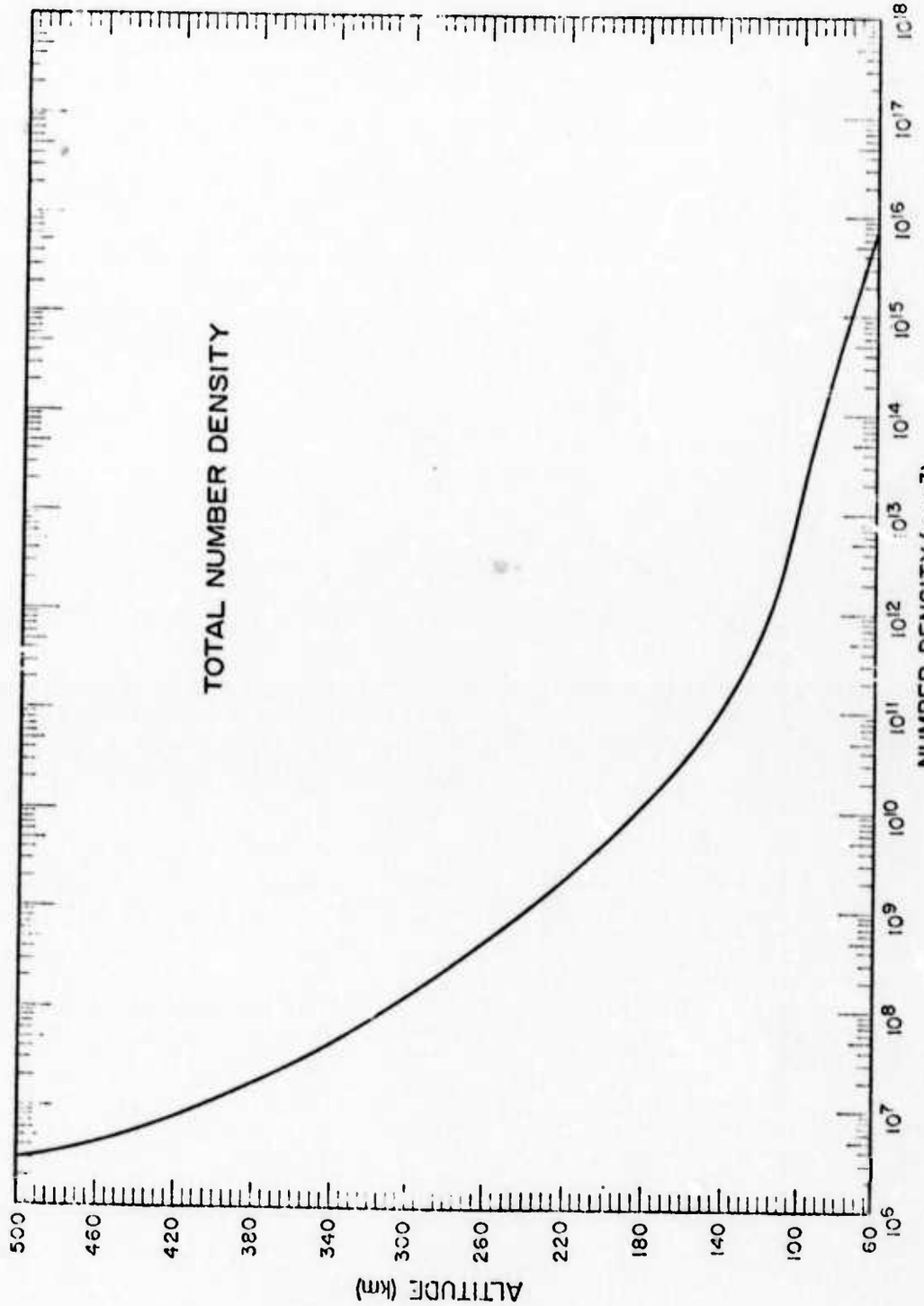

Figure 17. Height profile of the total number density.

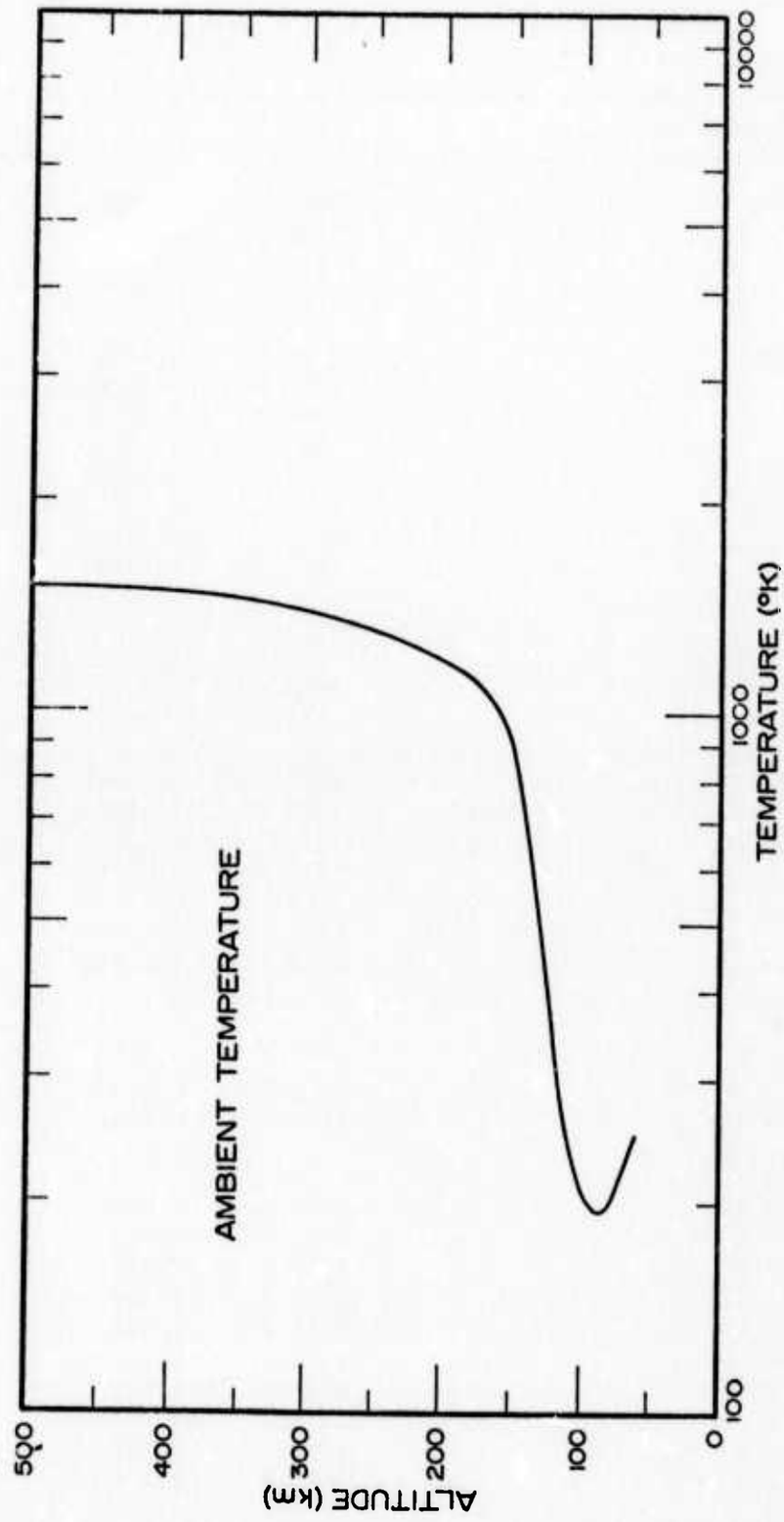

Figure 18. Temperature height profile.

TABLE 1

MOLECULAR CONSTANTS

Molecule	ν_1 ν_2 ν_3 ν_4	RCM	B_v	Source
CH_4	0 0 0 0	0000.0	0.3400	*Corbin et al.* [1970]
	0 1 0 0	1526.0	0.3500	
	0 0 1 0	3018.4	0.3500	
	0 0 0 1	1306.2	0.3500	
CO_2	0 0 0	0000.0	0.38918	*Herzberg* [1945]
	1 0 0	1388.2	0.38862	
	0 0 1	2348.0	0.38628	
	$0\ 1^1\ 0$	667.4	0.38980	
	$0\ 2^0\ 0$	1285.4	0.38990	
	$0\ 2^2\ 0$	1335.1	0.39042	
	$0\ 3^1\ 0$	1932.5	0.30104	
	$0\ 3^3\ 0$	2003.3	0.39104	
NO				
v = 0		0000.0	1.6961	*Albritton* [1973]
v = 1		1878.0	1.6785	
v = 2		3727.0	1.6610	
N_2O	0 0 0	0000.0	0.41892	*Thomson and Williams* [1953]
	1 0 0	1285.0	0.41549	
	0 0 1	2223.5	0.41984	
	0 1 0	588.8	0.41916	
	0 2 0	1173.0	0.41941	
	0 3 0	1758.8	0.41966	
	0 4 0	2338.5	0.41991	
NO^+				
v = 0		0000.0	1.9887	*Field* [1973]
v = 1		2344.0	1.9696	
v = 2		4660.0	1.9508	
OH				
v = 0		0000.0	18.513	*Herzberg* [1971]
v = 1		3562.0	17.805	
v = 2		6976.0	17.097	
v = 3		10222.0	16.389	
v = 4		13315.0	15.681	
v = 5		16260.0	14.973	
v = 6		19061.0	14.265	
v = 7		21725.0	13.557	
v = 8		24258.0	12.849	
v = 9		26663.0	12.141	

TABLE 1 (cont.)

Molecule	ν_1 ν_2 ν_3 ν_4	RCM	B_v	Source
CO				
v = 0		0000.0	1.9255	*Mantz et al.*
v = 1		2143.0	1.9050	[1971]
v = 2		4260.0	1.8875	
H_2O	0 0 0	0000.0	0.3000	*Corbin et al.*
	0 1 0	1594.7	0.3000	[1970]
O_3	0 0 0	0000.0	0.3000	*Corbin et al.*
	0 0 1	1043.0	0.3000	[1970]

$$S'_{1u} = \int_{\Delta\nu_{1u}} k_{L,\nu} d_\nu = (N_1 B_{1\to u} - N_u B_{u\to 1}) \frac{h\nu_{1u}}{c} \tag{3}$$

where $k_{L,\nu}$ (in cm^{-1}) is the spectral absorption coefficient per unit length, and where N_u (N_1) is the number density in the upper (lower) quantum state and $B_{1\to u}$ ($B_{u\to 1}$) is the Einstein coefficient for induced absorption (emission). The parameter ν_{1u} is the frequency (sec^{-1}) of the band center. Often it is advantageous to define a spectral absorption coefficient P_ω (in cm^{-1}. atm^{-1}) where ω is the wave number ($\omega = \nu/c$). It is the integral of P_ω that leads to the band strength S_{1u} as

$$S_{1u} = \int_{\Delta\omega_{1u}} P_\omega d\omega = \frac{S'_{1u}}{pc} \tag{4}$$

In this expression, p is the partial pressure of the absorber (in atm). Needless to say, P_ω ($k_{L,}\nu$) is nonzero only for a narrow wave number (frequency) range $\Delta\omega_{1u}$ ($\Delta\nu_{1u}$).

The band strengths for all but NO^+, OH, and CO were taken from *Corbin et al.* The band strengths of NO^+ were obtained from *Stair* and *Gauvin* [1967]. Those for OH and CO were taken from *Penner* [1959]. Table 2 lists the various bands of interest and their respective band strengths.

TABLE 2

MOLECULAR BAND STRENGTHS AND
COLLISIONAL ENERGY EXCHANGE COEFFICIENTS

Constituent	Band No.	Wavelength Band-Center (μ)	V-T Coefficient	V-V Coefficient	Band Strength (cm^{-2} atm^{-1}) and Temperature (°K)	
CH_4	1	7.66	10^{-15}	2×10^{-15}	185.0000	273
	2	3.31	10^{-15}	2×10^{-15}	320.0000	273
	3	6.55	10^{-15}	2×10^{-15}	2.4000	[illegible]
	4	5.54	10^{-15}	2×10^{-15}	0.0100	300
CO_2	1	14.93	Temperature Dependent		194.0000	300
	2	16.18	(See *Taylor and*		4.2700	300
	3	14.98	*Bitterman* [1969])		15.0000	300
	4	15.45			1.0000	300
	5	16.74			0.1400	300
	6	14.97			0.8500	300
	7	13.87			6.2000	300
	8	10.42			0.0720	299
	9	4.26			2700.0000	299
H_2O	1	6.27	5×10^{-11}	2×10^{-15}	300.0000	273
NO	1	5.32(1-0)	4×10^{-15}	2×10^{-15}	125.0000	273
	2	2.68(2-0)	4×10^{-15}	2×10^{-15}	2.1100	273
	3	5.41(2-1)	4×10^{-15}	2×10^{-15}	0.0310	273
N_2O	1	16.98	10^{-15}	2.5×10^{-13}	33.0000	303
	2	7.78	10^{-15}	2.5×10^{-13}	260.0000	303
	3	4.50	10^{-15}	2.5×10^{-13}	1856.0000	303
O_3	1	9.59	10^{-14}	10^{-14}	360.0000	273
NO^+	1	4.27	8×10^{-15}	6×10^{-15}	500.0000	300
	2	2.15	8×10^{-15}	6×10^{-15}	3.0000	300
	3	4.32	8×10^{-15}	6×10^{-15}	0.0100	300
OH	1(7-5)	1.87	10^{-17}	10^{-16}	4.0000	300
	2(4-2)	1.58	10^{-17}	10^{-16}	4.0000	300
CO	1	4.67	10^{-16}	10^{-15}	260.0000	300
	2	2.35	10^{-16}	10^{-15}	1.7900	300

Input Radiative Fluxes

Radiative input fluxes come from three sources: the sun, the earth, and other parts of the atmosphere. In the computational model, the solar and the terrestrial fluxes have fixed input values for each band, whereas the flux from other parts of the atmosphere is computed in the program itself. The input values for the solar flux for all bands except NO^+, OH, and CO were obtained from *Corbin et al.* [1970], whereas the solar flux for the bands of these gases were adapted from *Gast* [1965]. The input values for the terrestrial flux were also obtained from *Corbin et al.* for all but the same three molecules. For the vibration-rotational bands of these molecules the so-called "low altitude computer program" [*Corbin et al.* 1970] was run and values obtained from this source. For band-center wavelengths below the operational limit of this program (5μ), an extrapolation was made.*

Collisional Energy Exchange Coefficients

Four basic collisional energy exchange processes have been considered in this study. They are vibrational-translational (V-T), translational-vibrational (T-V), vibrational-vibrational (V-V), and internal vibrational mode exchange. Of these, the latter is used only for CO_2 and the temperature dependent values for this coefficient come from *Taylor* and *Bitterman* [1969].

The V-T and T-V coefficients become important to the excitation and de-excitation of N_2 and O_2 (between v = 0 and v = 1 levels) in the upper E-region and the F-region. The V-T coefficients were chosen to be an input parameter to the program and the T-V coefficients were found by solving a detailed balance problem as part of the overall computer program. The V-T values used by *Corbin et al.* were used for all gases except NO^+, CO, and OH. No information could be found regarding this parameter for NO^+. As a result, an estimated value of twice the V-T coefficient for NO was used. The same problem of a lack of available information was encountered for CO and OH. This resulted in estimates being used for these gases also.

*The reader is referred to the Note Added in Proof, p. x.

Of the collisional energy exchange processes, the V-V exchange process is probably the most important. This is because near resonant exchange conditions exist between N_2 and the following gases: CO_2, NO, N_2O, NO^+, and CO. Also, but less importantly, near resonant exchange conditions exist between O_2 and CH_4, H_2O, and O_3. Again the values used by *Corbin et al.* were adopted for all but NO^+ and CO (OH having no near resonant V-V exchange with either N_2 or O_2). A lack of information was again a problem for the determination of an input value. An estimated value of three times the NO value was used for NO^+ and an estimate consistant with the other constituents was used for CO. The values of collisional energy exchange coefficients are listed in Table 2.

PHYSICS OF THE PROGRAM EXCHNG

Aurora and Drizzle Fluxes

When energetic electrons enter into the atmosphere, they cause ionization and initiate many excitation processes. In all these processes, the transfer of energy occurs from one particle to another and from one form into the other. The excitation in the vibration-rotation mode thus caused makes important contributions to the infrared emissions in the upper atmosphere. The more important sources of these energetic electrons are aurora and electron drizzles.

Three "standards" were chosen for the primary electron fluxes and represent IBC-I, -II, and -III auroras. These are all expressed in exponential form as

$$\phi(E) = \phi_o \cdot e^{-E/E_o} \qquad (5)$$

where E = the energy of the primary electron,

ϕ_o = the low-energy flux limit as E approaches zero, and

E_o = the e-folding energy.

Table 3 lists the values of ϕ_o and E_o used in this report for the three IBC auroras.

Excepting auroras, there is an additional source of energetic electrons for the high-latitude ionosphere, which we term as an electron drizzle. The satellite measurement made by *Burch* [1968] gave evidence

TABLE 3

THE VALUES OF ϕ_o AND E_o FOR IBC-I, -II, and -III AURORAS

IBC	ϕ_o (electrons cm^{-2} $ster^{-1}$ sec^{-1} kev^{-1})	E_o (kev)
I	10^7	3.5
II	10^8	8.5
III	10^9	12.5

The values of ϕ_o and E_o for IBC-I and -II were given by *Ulwick et al.* [1967]. The values for IBC-III are chosen arbitrarily. The primary electron fluxes for the IBC-I, -II, and -III auroras are plotted in Figure 19.

to the existence of an electron drizzle and indicated that its energy spectrum is softer than that of most auroras and ranged approximately from 50 ev to 10 kev. This long term bombardment of energetic electrons can make some significant contribution to the ionization and excitation in the normal high-latitude ionosphere in the nighttime. According to *Burch's* measurement, the drizzle flux can be approximated by

$$\phi(E) = 4.0 \times 10^7 (E)^{-2} \quad \text{(electrons } cm^{-2} \text{ ster}^{-1} \text{ sec}^{-1} \text{ kev}^{-1}\text{)} \qquad (6)$$

with E, the electron energy, ranging from 0.05 kev to 10 kev.

Chemical Model

After the ionization of the major species N_2, O_2 and O in the ionosphere by the primary electron flux, the ions and electrons thus produced will immediately undergo a series of secondary reactions. The primary and secondary reactions involved in variations of ion and electron concentrations listed below are the important ones considered in our calculation.

N_2 + (energetic electron) $\rightarrow N_2^+ + e$

O_2 + (energetic electron) $\rightarrow O_2^+ + e$

O + (energetic electron) $\rightarrow O^+ + e$

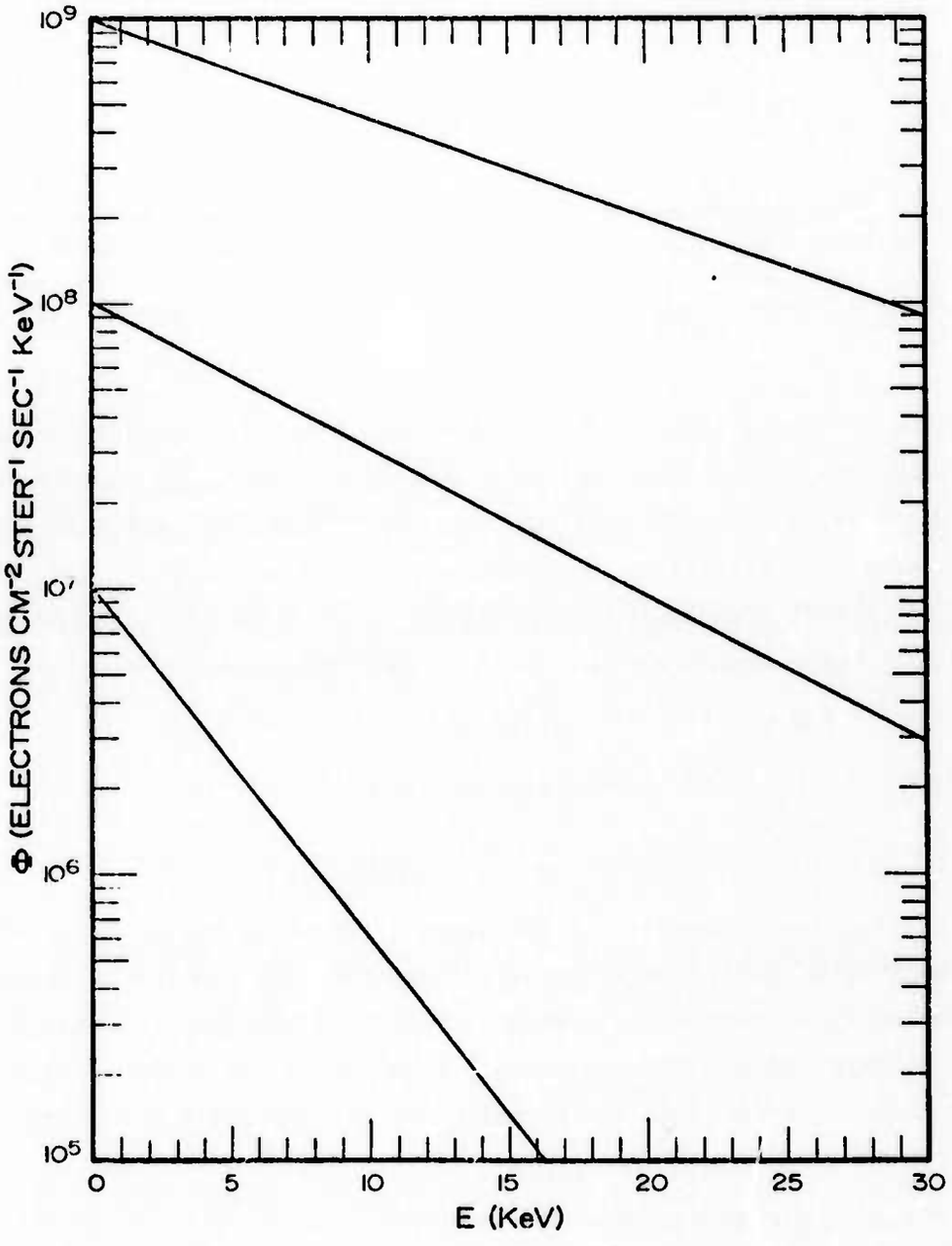

Figure 19. Primary electron fluxes for IBC-I, -II, and -III auroras.

$O^+ + N_2 \rightarrow NO^+ + N$ (7)

$1.0 \times 10^{-12} \cdot (T/300)^{-1}$ [*Dunkin et al.* 1968]

$O^+ + O_2 \rightarrow O_2^+ + O$ (8)

$2.0 \times 10^{-11} \cdot (T/300)^{-.5}$ [*Dunkin et al.* 1968]

$O^+ + NO \rightarrow NO^+ + O$ (9)

2.4×10^{-11} [*Fehsenfeld et al.* 1965]

$N_2^+ + O \rightarrow O^+ + N_2$ (10)

1.0×10^{-12} [*Ferguson* 1967]

$N_2^+ + O \rightarrow NO^+ + N(^2D)$ (11)

1.4×10^{-10} [*Fehsenfeld et al.* 1970]

$N_2^+ + O_2 \rightarrow O_2^+ + N_2$ (12)

5.0×10^{-11} [*Dunkin et al.* 1968]

$N_2^+ + NO \rightarrow NO^+ + N_2$ (13)

5.0×10^{-10} [*Goldan et al.* 1966]

$O_2^+ + N_2 \rightarrow NO^+ + NO$ (14)

5.0×10^{-16} [*Ferguson* 1967]

$O_2^+ + NO \rightarrow NO^+ + O_2$ (15)

6.3×10^{-10} [*Fehsenfeld et al.* 1970]

$O_2^+ + N \rightarrow NO^+ + O$ (16)

1.8×10^{-10} [*Goldan et al.* 1966]

$e + O_2^+ \rightarrow O + O$ (17)

$2.1 \times 10^{-7} \cdot (T/300)^{-1}$ [*Biondi* 1969]

$e + N_2^+ \rightarrow N + N(^2D)$ (18)

$2.8 \times 10^{-7} \cdot (T/300)^{-.33}$ [*Biondi* 1969]

$$e + NO^+ \rightarrow N(^2D) + O \qquad (19)$$

$4.1 \times 10^{-7} \cdot (T/300)^{-1}$ [*Biondi* 1969]

$$N(^2D) + O_2 \rightarrow NO + O \qquad (20)$$

6.0×10^{-12} [*Lin* and *Kaufman* 1970]

$$N + NO \rightarrow N_2 + O \qquad (21)$$

2.2×10^{-11} [*Phillips* and *Schiff* 1962]

This reaction set does not include the excitation processes due to secondary electrons. These processes are taken into account separately. The only neutral reactions included in this model are $N(^2D) + O_2$ and $N + NO$. The reaction of $N(^2D) + O_2$ is the major source for NO. The production of $N(^2D)$ comes mainly from dissociative recombination reactions of N_2^+ and NO^+. According to *Nicholes* [1970], the production of $N(^4S : {}^2D : {}^2P)$ from the reaction of $N_2^+ + e$ is in the ratio 40 = 40 = 10. The quantum yield of production of $N(^2D)$ from the reaction $NO^+ + e$ is assumed to be unity in the calculations presented here.

Time-dependent calculations are applied to this chemical model to determine the concentrations of the electrons and various ions with the aurora and electron drizzle input. Production rates of N_2^+, O_2^+, and O^+ due to primary electron flux of aurora and drizzle must be evaluated before one can make any time-dependent calculation of concentrations.

Calculation of Production Rates of N_2^+, O_2^+, and O^+ due to Primary Electron Flux of Aurora and Drizzle

The ionization rate coeffi ient due to primary electron flux is a function of altitude because energetic electrons with different energies have diffcrent limits on their penetration depth into the atmosphere. The maximum penetration depth for electrons with energy E kev can be calculated by using the following formula [*Gerard* 1970]

$$X_m = 4.6 \times 10^{-6} \cdot (E)^{1.65} \quad (gm/cm^2) \qquad (22)$$

This penetration depth is given as the mass of air penetrated through in a unit area of column. The actual altitude corresponding to a vertical penetration depth in the atmosphere can be found in a functional relationship, $X = X(h)$, where h is the altitude and X is the penetration depth. This functional relationship is tabulated in Table 4. Therefore, the minimum energy, E_{min}, needed for electrons to penetrate down to a particular altitude can be found by using the above formula and Table 4. The linear ionization rate at an altitude h due to primary energetic electrons with energy E kev is given by *Lazarev* [1967] as

$$q(h,E) = \frac{\Omega\phi E}{X_m \Delta\varepsilon} d(\chi)\rho \qquad (cm^{-3}\ sec^{-1}\ kev^{-1}) \tag{23}$$

where $E(kev) \geq E_{min}(kev)$

ϕ = the electron flux

ρ = mass density of air at altitude h

$\Delta\varepsilon$ = average energy dissipation of primary electrons for a single ionization to produce an electron-ion pair, 34 ev needed for air

Ω = the solid angle extended by a cone with a half vertex angle of 80°

and $d(\chi) = 4.2\chi \exp(-\chi^2 - \chi) + 0.48 \exp(-17.4\chi^{1.37})$, called the dimensionless energy

with $\chi = X(h)/X_m(E)$

The total production rate of ions is obtained by the integration

$$Q(h) = \int_{E_{min}}^{\infty} q(h,E)dE \qquad (cm^{-3}\ sec^{-1}) \tag{24}$$

The individual production rates for N_2^+, O_2^+, and O^+ from the ionization of N_2, O_2, and O by primary electron flux are given as

$$Q_i(h) = \frac{\sigma_i n_i}{\sigma_{N_2} n_{N_2} + \sigma_{O_2} n_{O_2} + \sigma_O n_O} Q(h) \qquad (cm^{-3}\ sec^{-1}) \tag{25}$$

where the subscript i represents the ith species N_2, O_2, or O; n's are the concentrations; and σ's are the ionization cross sections. Values

TABLE 4

THE PENETRATION DEPTH AND DENSITY OF THE ATMOSPHERE [*Rees* 1963]

h (km)	X (gm cm^{-2})	ρ (gm cm^{-3})
60	2.34 - 1	3.04 - 7
64	1.37 - 1	1.89 - 7
68	7.76 - 2	1.15 - 7
72	4.20 - 2	6.71 - 8
76	2.17 - 2	3.71 - 8
80	1.08 - 2	1.94 - 8
84	5.16 - 3	9.59 - 9
88	2.46 - 3	4.56 - 9
92	1.19 - 3	2.17 - 9
96	5.88 - 4	9.93 - 10
100	3.10 - 4	4.48 - 10
108	1.04 - 4	1.32 - 10
114	5.18 - 5	5.70 - 11
120	2.75 - 5	2.61 - 11
126	1.65 - 5	1.30 - 11
132	1.08 - 5	7.05 - 12
140	6.90 - 6	3.47 - 12
150	4.40 - 6	1.70 - 12
162	2.96 - 6	9.00 - 13
192	1.41 - 6	2.94 - 13
230	7.05 - 7	1.16 - 13
252	5.02 - 7	7.60 - 14
276	3.59 - 7	5.00 - 14
300	2.65 - 7	3.42 - 14

Note: Entries in the Table N ± n are to be read as N X $10^{\pm n}$

calculated for Q_{N_2}, Q_{O_2}, and Q_O are sent into the program SIXBIT [*Adams* and *Megill* 1970]. In this program the ionization reactions due to the energetic electrons in aurora and drizzle are treated in the same way as other chemical and photochemical reactions for the time-dependent calculation of concentrations of ions and electrons.

Time-Dependent Calculations of the Electron and Ion Concentrations

The generalized reaction kinetics program SIXBIT was originally developed for the time-dependent calculation of concentrations of reactants and products in a chemical model. This program was modified to calculate temporal variations of electron and ion concentrations with energetic electron input. In addition to the subroutine added for the calculation of production rates of N_2^+, O_2^+, and O^+ due to primary electron flux, new subroutines for the computation of secondary electron flux, the estimation of the electron temperature, vibrational excitation and de-excitation rates of N_2 and O_2, and electronic excitation rate of $O(^1D)$ were also added. The modified program is called EXCHNG.

All the following calculations are made for altitude ranges from 60 km to 150 km in the nighttime. Several steps are taken in the calculations. The electron and ion concentrations for quiescent conditions in the nighttime were taken from *Jones* and *Rees* [1972] as the initial profiles and the calculation were made with constant drizzle input. The time-dependent calculation was made to continue until quasi steady state for the concentrations was reached. In the next step, the quasi steady-state profiles with drizzle input were taken as the initial profiles in time-dependent calculations with constant aurora input. The quasi steady state is also reached for this calculation. Following this procedure the results obtained for IBC-II and -III auroras are plotted in Figures 20 and 21. A separate calculation was made with constant IBC-II aurora input starting with the initial quiescent profiles from *Jones* and *Rees*. The initial profiles and the steady-state profiles with constant aurora input are plotted in Figure 22.

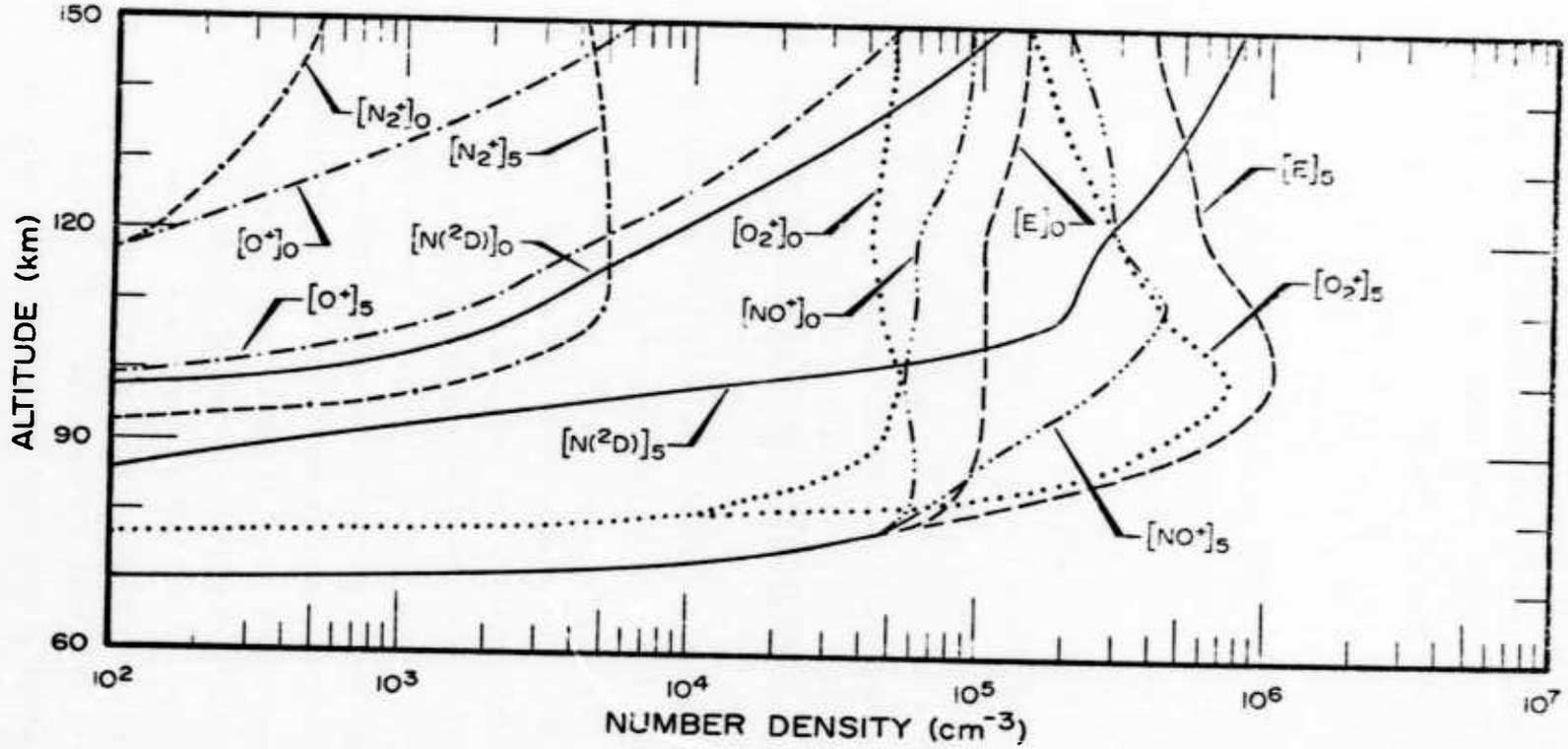

Figure 20. Height profiles five minutes after commencement of an IBC-III aurora starting from an electron drizzle.

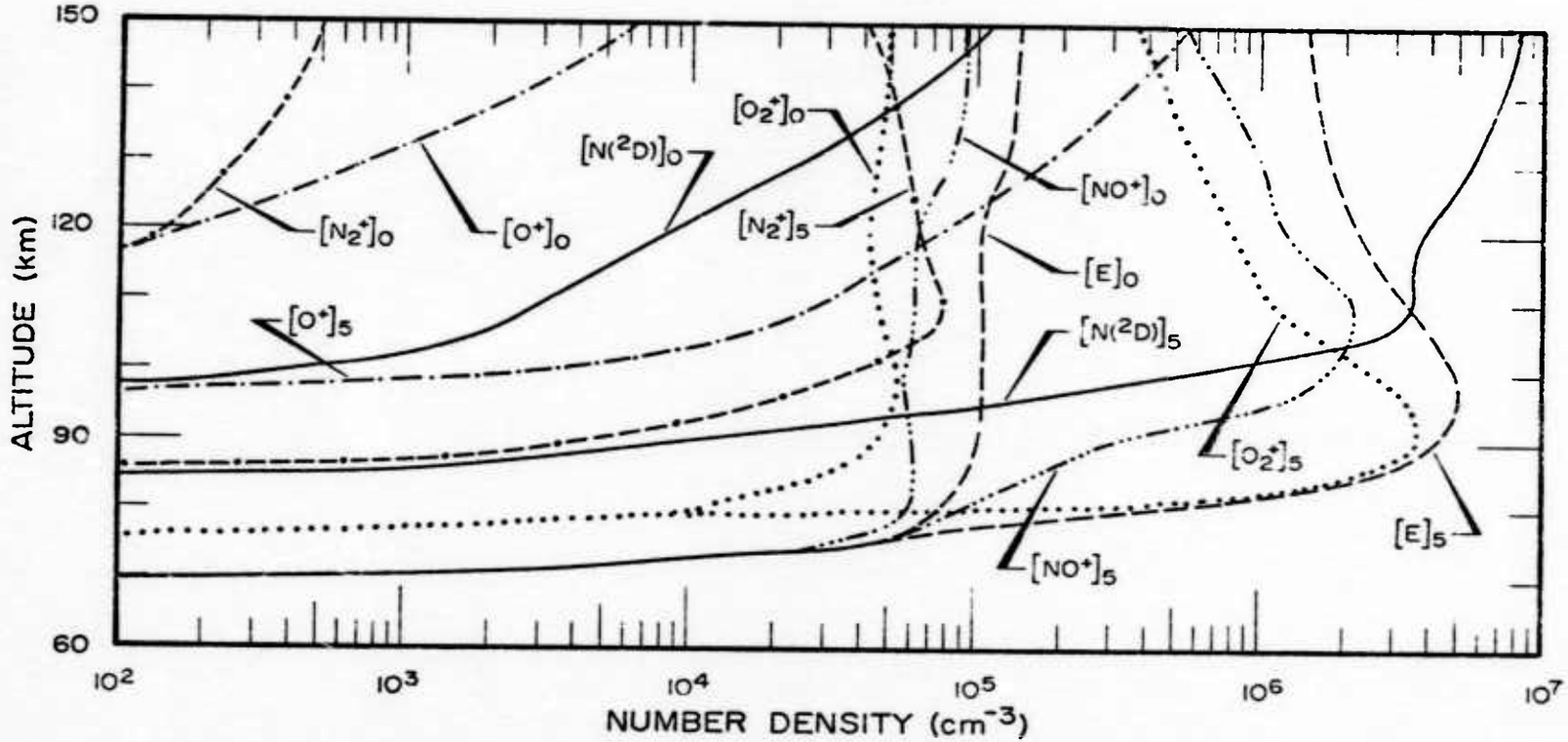

Figure 21. Height profiles five minutes after commencement of an IBC-III aurora starting from an electron drizzle.

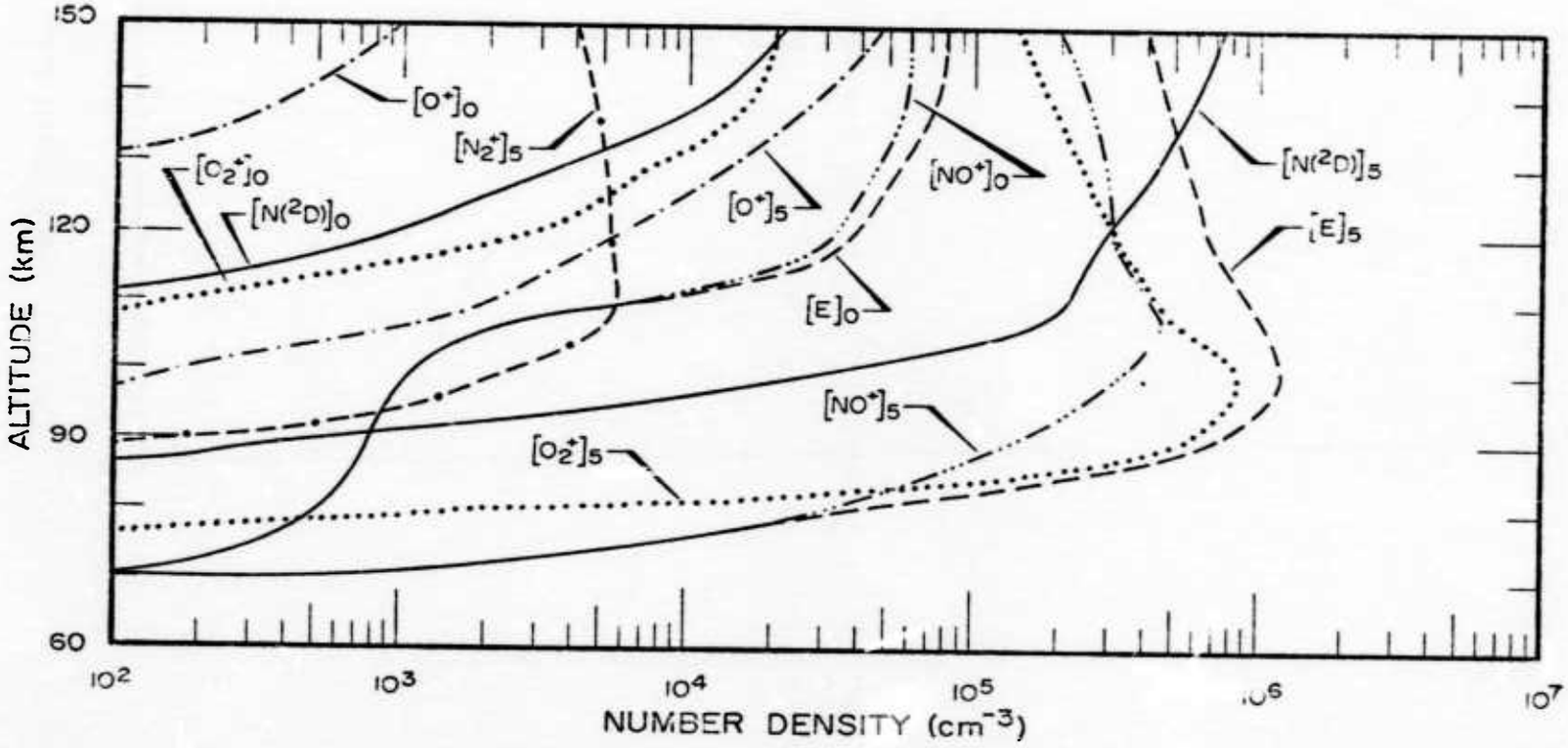

Figure 22. Height profiles five minutes after commencement of an IBC-II aurora starting from quiescent conditions.

Calculation of Secondary Electron Flux

This calculation follows the method suggested by *Rees et al.* [1969]. The production rate of secondary electrons is evaluated by the following expression

$$\eta(E_s) = \frac{G(W_{N_2})}{2.53} Q_{N_2} + \frac{G(W_{O_2})}{2.77} Q_{O_2} + \frac{G(W_O)}{2.71} Q_O \qquad (26)$$

(electrons cm^{-3} sec^{-1} ev^{-1})

where Q_i is the rate of ionization due to primary electrons, and E_s is the energy of the secondary electrons. G(W) is a function of W given as

$$G(W) = \frac{\exp[-\frac{W}{31.5} - 339 \cdot \exp(-\frac{W}{2.49})]}{W} \times \ln \left(\frac{31.6 + \sqrt{1000 - W}}{31.6 - \sqrt{1000 - W}}\right) \qquad (27)$$

(ev^{-1})

with $W = I + E_s$

and I = the ionization potential, 15.6 ev for N_2, 12.1 ev for O_2, and 13.6 ev for O.

With the assumption that energy loss is a continuous function of energy, the differential flux of secondary electrons is

$$\phi(E_s) = \frac{\int_{E_s}^{\infty} \eta(E_s)\, dE_s}{L(E)_{elect.} + L(E)_{neut.}} \qquad (\text{electrons } cm^{-2} \text{ sec}^{-1} \text{ ev}^{-1}) \qquad (28)$$

where $L(E)_{elect.}$ and $L(E)_{neut.}$ are the terms of energy loss to ambient electrons and to neutrals, respectively, per unit distance traveled by the secondary electrons. The function $L(E)_{elect.}$ is given in *Rees'* paper as

$$L(E)_{elect.} = \frac{1.95 \times 10^{-12}\, n(e)}{E} \qquad (ev\ cm^{-1}) \qquad (29)$$

where n(e) is the ambient electron density in units of electrons/cm^3. For the function $L(E)_{neut.}$, the approximate analytical expression for E down to 25 ev is given by *Green* and *Peterson* [1968] as

$$L(E)_{neut.} = \frac{q_o}{2R_e} \sum_i z^+ \left[\left(\frac{E}{A}\right)^{\Omega} + \left(\frac{E}{B}\right)^{M} + \left(\frac{E}{C}\right)^{\Lambda}\right]^{-1} \cdot n_i \qquad (ev\ cm^{-1}) \qquad (30)$$

where $q_o = 6.514 \times 10^{-14}$ ev^2 cm^2

$R_e = 13.6$ ev

and Ω, M, Λ, A, B, C, and z^+ are the parameters which are listed in Table 5 for N_2, O_2, and O, and n_i is the concentration of ith species, N_2, O_2, or O. For E in the range from 25 ev to 1 ev, *Green's* approximation [1972] is used in the calculation of $L(E)_{neut.}$. The energy of the secondary electrons in this range is mainly lost to electronic and vibrational excitation, the Rydberg series, and the ionization continuum of N_2, O_2, and O in the upper atmosphere. Therefore, the energy loss functions will be discussed individually in these three categories.

TABLE 5

PARAMETERS USED IN GREEN AND PETERSON'S APPROXIMATE ANALYTIC EXPRESSION OF THE ELECTRON ENERGY LOSS TO N_2, O_2, AND O

[*Green* and *Peterson* 1968]

Parameter	N_2	O_2	O
Ω	0.783	0.771	0.758
M	-0.328	-0.518	-0.500
Λ	-3.14	-3.59	-3.5
A (ev)	100	100	100
B (ev)	217	123	765
C (ev)	54.6	54.1	50
z^+	14.1	15.2	7.15

1. Loss due to electronic and vibrational excitation

$$L(E)_e = \sum_{ij} n_i \bar{W}_{ij} \sigma_{ij}(E) \quad \text{for } E \geq \bar{W}_{ij} \quad (\text{ev cm}^{-1}) \qquad (31)$$

where E = the energy variable, which is the energy of the secondary electrons in the discussion considered here

subscript i = the ith species, N_2, O_2, or O

subscript j = the jth vibrational level or electronic state

n_i = the concentration of the ith species

$\overline{W}_{ij}$ = the excitation energy of the jth vibrational level or electronic state of the ith species relative to the lowest vibrational level in the ground electronic state

$\sigma_{ij}(E)$ = the excitation cross section of the jth vibrational level or electronic state of the ith species

The excitation cross section has an expression

$$\sigma_{ij}(E) = \frac{q_o (f_o C_o)}{W_{ij}^2} \left[\frac{W_{ij}}{E}\right]^{\Omega} \left[1 - \left(\frac{W_{ij}}{E}\right)^{\beta}\right]^{\nu} \qquad (cm^2) \qquad (32)$$

where $q_o = 4\pi a_o^2 Ry^2 = 6.514 \times 10^{-14}$ cm^2 ev^2

(a_o is the Bohr radius and Ry is the Rydberg energy, 13.6 ev), and $f_o C_o$, W_{ij}, Ω, β, and ν are the input parameters which have different values for the various vibrational levels or electronic states for different species. All parameters for the different vibrational levels or electronic states of N_2, O_2, and O are listed in Table 6.

2. Loss due to Rydberg series

$$L(E)_R = \sum_{ij} n_i WI_{ij} \sigma_{ij}(E) \qquad (ev\ cm^{-1}) \qquad (33)$$

where E, the subscripts i and j, n_i and $\sigma_{ij}(E)$ have the same meaning as those in category (1) but WI_{ij} is the ionization potential for the jth Rydberg series of the ith species.

The expression for the cross section has the form

$$\sigma_{ij}(E) = q_o \sum_{n=n_i}^{(n_f-1)} \frac{(f_o C_o)_n}{W_{ijn}^2} \left[\frac{W_{ijn}}{E}\right]^{\Omega} \left[1 - \left(\frac{W_{ijn}}{E}\right)^{\beta}\right]^{\nu}$$

$$+ q_o \frac{(f_o C_o)_R}{W_{ijR}^2} \left[\frac{W_{ijR}}{E}\right]^{\Omega} \left[1 - \left(\frac{W_{ijR}}{E}\right)^{\beta}\right]^{\nu} \qquad (cm^2) \qquad (34)$$

where $q_o = 6.514 \times 10^{-14}$ cm^2 ev^2

$$(f_o C_o)_n = \frac{f_o^*}{(n - \delta)^3} \qquad (n_i \leq n < n_f)$$

$$(f_o C_o)_R = \frac{f_o^*}{2(n_f - \delta - \tfrac{1}{2})^2}$$

TABLE 6

THE PARAMETERS USED IN CALCULATION OF THE ENERGY LOSS OF SECONDARY ELECTRONS TO NEUTRALS DUE TO VIBRATIONAL AND ELECTRONIC EXCITATION [*Green* 1972]

Excited State	W_{ij}(ev)	β	ν	$\bar{W}_{ij}$(ev)	Ω	$f_o C_o$
N_2						
N_2(v=1-3)	1.850	1.000	1.000	0.570	7.000	0.273200
N_2(v=4-8)	2.150	1.000	1.000	1.680	9.000	0.241300
$A^3\Sigma_u^+$	6.168	1.000	1.000	6.168	3.000	0.226000
$B^3\pi_g$	7.353	3.000	1.000	7.353	3.000	0.177500
$C^3\pi_u$	11.031	3.000	1.000	11.031	3.000	0.281200
$E^3\Sigma_g^+$	11.900	3.000	1.000	11.900	3.000	0.047800
$a^1\pi_g$	8.548	1.000	1.000	8.548	1.000	0.136200
$a^1\Sigma_g$	12.250	2.300	1.000	12.250	1.000	0.027200
$b^1\pi$	12.500	1.000	3.000	12.800	0.750	0.672000
$b^1\Sigma_u$	13.300	1.000	3.000	14.000	0.750	0.334000
$2p^2(^3P)3s\ ^4P$	21.000	1.000	2.000	24.000	0.750	0.200000
$2p^2(^1D)3s\ ^3P$	21.000	1.000	2.000	24.000	0.750	0.047000
$2p^2(^3P)3s\ ^2P$	21.000	1.000	2.000	23.000	0.800	0.085000
$2p^2(^1D)3s\ ^2D$	22.000	1.000	2.000	25.000	0.850	0.064000
O_2						
	9.900	1.000	3.000	9.900	0.850	0.080000
$a^1\Delta_g$	0.980	1.000	3.000	0.980	0.750	0.000990
$b^1\Sigma_g^+$	1.640	3.000	1.000	1.640	3.000	0.000500
$c^1\Sigma_u^-$	4.500	1.000	1.000	4.500	0.900	0.021000
	8.400	1.000	2.000	8.400	0.750	0.230000
	16.100	1.000	3.000	19.000	0.900	0.067000
	19.200	1.000	3.000	22.000	0.750	0.016000
	17.600	1.000	3.000	21.000	1.000	0.032000
	14.600	1.000	3.000	18.000	0.750	0.085000

TABLE 6 (cont.)

Excited State	W_{ij}(ev)	β	ν	$\bar{W}_{ij}$(ev)	Ω	$f_o C_o$
O						
$O(^1D)$	1.850	1.000	2.000	1.960	1.000	0.010000
$O(^1S)$	4.180	0.500	1.000	4.180	1.000	0.004200

$$W_{ijn} = WI_{ij} - \frac{Ry}{(n - \delta)^2} (ev)$$

(Ry = Rydberg energy)

$$W_{ijR} = (W_{ijn_f} + WI_{ij})/2 \quad (ev)$$

and f_o^*, δ, n_i, n_f, Ω, β, and ν are the input parameters. In the above expression of $\sigma_{ij}(E)$, the last term represents an effective state which is the result of the summation over all the terms with $n \geq n_f$. The parameters needed in the calculation of this loss function are given in Table 7. n_i and n_f have the values 3 and 5 respectively for the above.

TABLE 7

THE PARAMETERS USED IN CALCULATION OF ENERGY LOSS OF SECONDARY ELECTRONS TO NEUTRALS DUE TO THE EXCITATION OF RYDBERG SERIES [*Green* 1972]

Rydberg Series	WI_{ij}(ev)	β	ν	δ	Ω	f_o^*
N_2						
$X^2\Sigma_g^+$	15.580	1.000	3.000	0.700	0.750	14.349999
$A^2\pi_u$	16.730	1.000	3.000	1.040	0.750	1.646000
$B^2\Sigma_u^+$	18.750	1.000	3.000	0.870	0.750	1.000000
$D^2\pi_g$	22.000	1.000	3.000	1.530	0.750	0.700000
$C^2\Sigma_u^+$	23.600	1.000	3.000	0.800	0.750	0.700000

TABLE 7 (cont.)

Rydberg Series	WI_{ij}(ev)	β	ν	δ	Ω	f_o^*
O_2						
$X^2\pi_g$	12.100	1.000	3.000	1.080	0.750	1.200000
$a^4\pi_u$	16.100	1.000	3.000	1.000	0.750	2.500000
$A^2\pi_u$	16.900	1.000	3.000	1.070	0.750	2.099999
$b^4\Sigma_g^-$	18.200	1.000	3.000	0.690	0.750	1.799999
	23.000	1.000	3.000	1.000	0.750	0.700000
O						
	13.600	1.000	3.000	1.160	0.750	0.289500
	13.600	1.000	2.000	1.240	3.000	0.270200
	13.600	1.000	1.000	0.810	3.000	0.077200
	13.600	2.000	1.000	0.690	0.750	0.011600
	13.600	1.000	3.000	0.010	0.750	0.400500
	13.600	1.000	2.000	0.010	3.000	0.373800
	16.900	1.000	3.000	1.210	0.750	0.481500
	16.900	1.000	2.000	1.180	3.000	0.449400
	16.900	2.000	1.000	0.920	0.750	0.019300
	16.900	1.000	1.000	0.920	3.000	0.128400
	16.900	2.000	1.000	0.810	0.750	0.019300
	16.900	1.000	1.000	0.780	3.000	0.128400
	16.900	2.000	1.000	0.780	0.750	0.019300
	16.900	1.000	1.000	0.780	3.000	0.128400
	16.900	1.000	3.000	0.040	0.750	0.298500
	16.900	1.000	2.000	0.040	3.000	0.278600
	16.900	1.000	3.000	0.040	0.750	0.459000
	16.900	1.000	2.000	0.040	3.000	0.428400
	16.900	1.000	3.000	0.040	0.750	0.237000
	16.900	1.000	2.000	0.040	3.000	0.221200
	18.500	1.000	3.000	1.250	0.750	0.297000
	18.500	1.000	2.000	1.190	3.000	0.277200
	18.500	2.000	1.000	1.040	0.750	0.011900
	18.500	1.000	1.000	1.040	3.000	0.079200

TABLE 7 (cont.)

Rydberg Series	WI_{ij}(ev)	β	ν	δ	Ω	f_o^*
	18.500	2.000	1.000	0.770	0.750	0.011900
	18.500	1.000	1.000	0.770	3.000	0.079200
	18.500	2.000	1.000	0.770	0.750	0.011900
	18.500	1.000	1.000	0.730	3.000	0.079200
	18.500	1.000	3.000	0.050	0.750	0.235500
	18.500	1.000	2.000	0.050	3.000	0.219800
	18.500	1.000	3.000	0.050	0.750	0.678000
	18.500	1.000	2.000	0.050	3.000	0.632800

3. Loss due to ionization continuum

$$L(E)_i = \sum_{ij} n_i \int_o^{T_M} W_{ij} S_{ij}(E,T)\,dT \qquad (\text{ev cm}^{-1}) \tag{35}$$

where E, the subscripts i and j, n_i have the same meaning as those in categories (1) and (2), but $W_{ij} = I_{ij} + T$ with I_{ij} representing the ionization energy for the jth continuum state of the ith species.

T = kinetic energy of the electron released from the ionized molecule

$T_M = (E - I_{ij})/2$, the possible maximum value of T

$S_{ij}(E,T)$ = the differential ionization cross section for a continuum state j of the ith species

The integration in the above expression for $L(E)_i$ yields

$$\int_o^{T_M} W_{ij} S_{ij}(E,T)\,dT = q_o A_o \left(\frac{I_{ij}}{E}\right)^P \sum \frac{a_r}{\phi_r}\left[\left(\frac{E + I_{ij}}{2E}\right)\phi_r - \left(\frac{I_{ij}}{E}\right)\phi_r\right] \quad (\text{ev cm}^2) \tag{36}$$

where $q_o = 6.514 \times 10^{-14}$ cm^2 ev^2

$a_r = C_r^{\nu}(-1)^r$ with C_r^{ν} as the number of combinations of ν distinct things taken r at a time

$\phi_r = \Omega - P + \Gamma_r$

$\Gamma_r = \beta r$

and A_o, P, Ω, β, and ν are the input parameters.
Table 8 presents the values of various parameters needed in the calculation of $L(E)_i$.

The total energy loss of the secondary electrons to neutrals within the energy range from 25 ev to 1 ev is the summation of the above three losses.

$$L(E)_{neut.} = L(E)_e + L(E)_R + L(E)_i \qquad (ev\ cm^{-1}) \qquad (37)$$

TABLE 8

PARAMETERS USED IN THE CALCULATION OF ENERGY LOSS OF SECONDARY ELECTRONS TO NEUTRALS DUE TO THE IONIZATION CONTINUA [*Green* 1972]

Ion State	I_{ij}(ev)	β	ν	P	Ω	$A_o(ev^{-1})$
N_2						
$X^2\Sigma_g^+$	15.58	1.00	2.0	1.20	0.80	0.37000
$A^2\pi_u$	16.73	1.00	1.0	1.20	0.83	0.16000
$B^2\Sigma_u^+$	18.75	0.15	1.0	1.20	0.94	0.36800
$D^2\pi_g$	22.00	1.00	2.0	1.20	0.83	0.05600
$C^2\Sigma_u^+$	23.60	1.00	2.0	1.20	0.83	0.06000
O_2						
$X^2\pi_g$	12.10	1.00	2.0	1.10	0.80	0.05800
$a^4\pi_u$	16.10	1.00	2.0	1.10	0.80	0.15000
$A^2\pi_u$	16.90	1.00	2.0	1.10	0.80	0.15000
$b^4\Sigma_g^-$	18.20	1.00	2.0	1.10	0.80	0.13000
	23.00	1.00	2.0	1.10	0.80	0.06400
	18.00	1.00	3.0	1.10	0.93	0.40000
	22.00	1.00	3.0	1.10	0.93	0.25000
O						
	13.60	1.00	2.0	1.20	0.85	0.26500
	16.90	1.00	2.0	1.20	0.85	0.33000
	18.50	1.00	2.0	1.20	0.85	0.18000

Calculation of the Electron Temperature, Vibrational Excitation, and De-excitation Rates of N_2 and O_2 and the Electronic Excitation Rate of $O(^1D)$

After the secondary electron flux is determined, the electron temperature can be calculated by making the energy input to the ambient electrons by the secondary electrons

$$E_{in} = \int_o^\infty L(E_s)_{elec.} \phi(E_s)\, dE_s \qquad (ev\ cm^{-3}\ sec^{-1}) \tag{38}$$

equal to the energy loss from the heated ambient electrons to the neutral molecules. This energy loss is calculated by following the method suggested by *Megill* [1965].

$$E_{loss} = \nu(u)\, g(u)(u - u_o)\, [M][E] \qquad (ev\ cm^{-3}\ sec^{-1}) \tag{39}$$

where u = average energy of the ambient electrons, $3/2kT_e$, with T_e as the electron temperature and k as the Boltzman constant

u_o = average thermal energy of the neutrals, $3/2kT_o$ with T_o as the temperature of neutral particles

$g(u)$ = average fractional energy loss per collision

$\nu(u)$ = average collision frequency between ambient electrons and neutral particles normalized to a neutral particle density of one per cm^3

$[M]$ = total number density of neutral particles

$[E]$ = number density of the ambient electrons

Both $g(u)$ and $\nu(u)$ are functions of the average energy of ambient electrons and are plotted in Figure 23. The condition of steady state is assumed for the average energy of ambient electrons, that is

$$E_{in} = E_{loss}$$

The electron temperature, T_e, which is included in the above equation through u, can be solved numerically from this equation.

Calculation of the excitation rates of N_2 and O_2 into the first vibrational level in their ground state by collision with secondary electrons is simply made by the integrations

$$\nu_{ex}(N_2) = \int \phi(E_s) \cdot \sigma_{N_2}(E_s)\, dE_s \qquad (sec^{-1}) \tag{40}$$

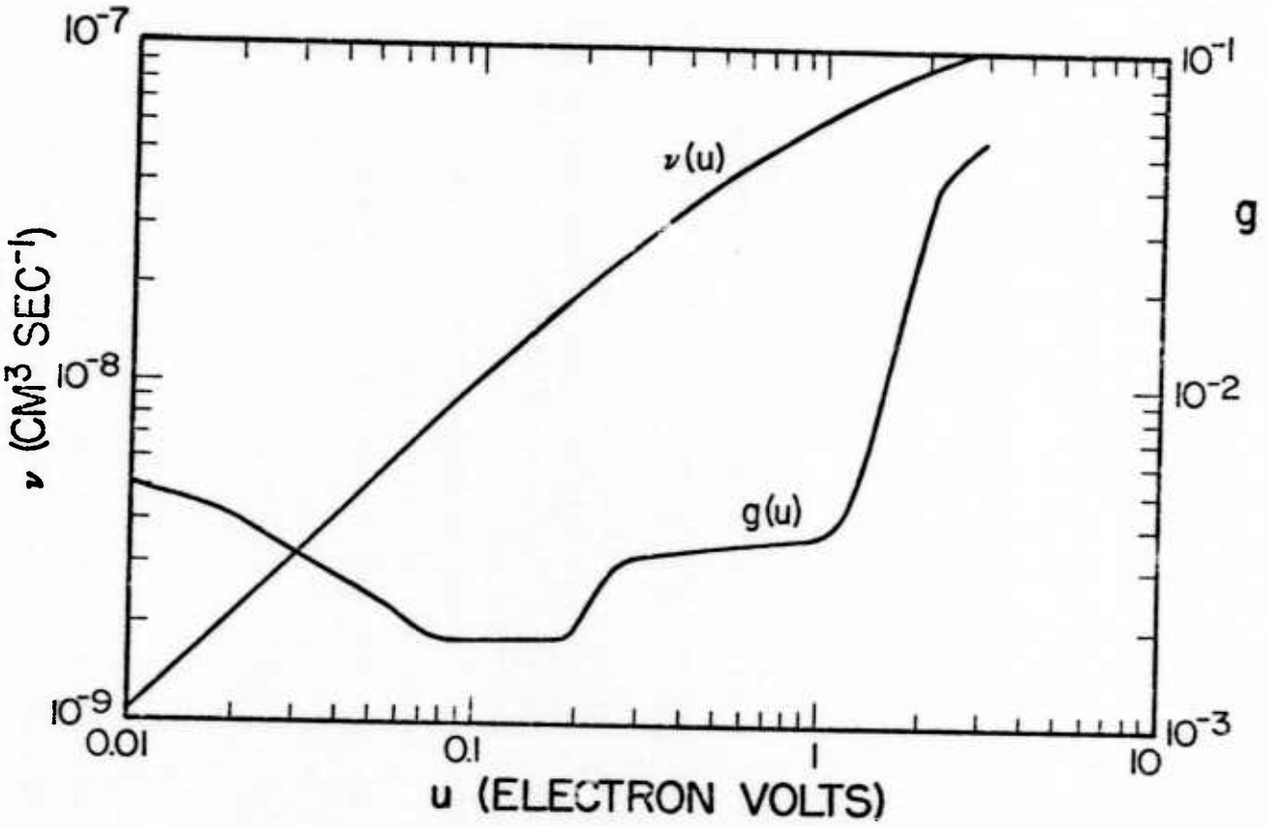

Figure 23. Average collision frequency ν and average functional energy loss g plotted in a function of the average energy of the ambient electrons.

$$\nu_{ex}(O_2) = \int \phi(E_s) \cdot \sigma_{O_2}(E_s)\, dE_s \qquad (sec^{-1}) \qquad (41)$$

where $\sigma_{N_2}(E_s)$ is the excitation cross section for N_2 given by *Chen* [1964] and $\sigma_{O_2}(E_s)$ is the one for O_2 given by *Linder* and *Schmidt* [1971]. A similar integration yields the excitation rate of O into its ^1D state.

$$\nu_{ex}(O(^1D)) = \int \phi(E_s) \cdot \sigma_{O(^1D)}(E_s)\, dE_s \qquad (sec^{-1}) \qquad (42)$$

where $\sigma_{O(^1D)}$ is the excitation cross section for $O(^1D)$.

An expression for this cross section is given by *Green* [1972] as

$$\sigma_{O(^1D)}(E) = \frac{q_o (f_o C_o)}{W^2} \left(\frac{W}{E}\right)^{\Omega} \left[1.0 - \left(\frac{W}{E}\right)^{\beta}\right]^{\nu} \qquad (cm^2) \qquad (43)$$

where $q_o = 6.514 \times 10^{-14}$ cm^2 ev^2

$f_o C_o = 0.01$

$W = 1.85$ ev

$\Omega = 1.00$

$\beta = 1.00$

$\nu = 2.00$

The deactivation rate for the vibrational level (v = 1) of N_2 by collisions with slow ambient electrons, K_d, is evaluated by using the analytic approximation to the cross section given by *Chen* [1964], as shown below for different energy intervals

$$\sigma_1 = 5 \times 10^{-13} \left(1 - \frac{1.5}{E}\right) \exp\left(-\frac{E}{0.3}\right) (cm^2) \quad (1.5 \text{ ev} \leq E) \qquad (44)$$

$$\sigma_2 = 0.3 \times 10^{-16} \exp\left(-\frac{E}{0.1}\right) (cm^2) \quad (0 \leq E \leq 0.2 \text{ ev}) \qquad (45)$$

$$\sigma_3 = 0.05 \times 10^{-16} \ (cm^2) \quad (0.2 \text{ ev} < E < 1.5 \text{ ev}) \qquad (46)$$

where σ's are given in the units of cm^2 and E is the kinetic energy of ambient electrons.

The sum over the three energy intervals gives

$$\sigma = \sigma_1 + \sigma_2 + \sigma_3 \quad (cm^2)$$

The deactivation rate is given by

$$K_d = \int v\sigma(E)\, f(E)\, dE \qquad (cm^3\ sec^{-1}) \tag{47}$$

where $f(E) = \left(\frac{2m_e}{\pi}\right)^{\frac{1}{2}} (kT_e)^{-3/2} \cdot v \cdot e^{-E/kT_e} \qquad (ev^{-1})$

(the Maxwell distribution of kinetic energy)

$v = \sqrt{2E/m_e}$ (the velocity of ambient electrons)

m_e = electron mass

T_e = electron temperature

k = Boltman constant

Finally, the above integration gives rise to the following expression for K_d

$$K_d \simeq 3.34 \times 10^{-5} \frac{(T_e)^{\frac{1}{2}}}{(1159 + T_e)^2} + 3.11 \times 10^{-12}(T_e)^{\frac{1}{2}} \quad (cm^3\ sec^{-1}) \tag{48}$$

ELECTRIC FIELD EXCITATION OF INFRARED EMISSIONS

Recent measurements [*Westcott et al.* 1969; *Hepner et al.* 1971] indicate that the auroral regions are quite often subjected to the presence of relatively large electric fields. These fields are generally meridional in nature and vary considerably with time. Fields as high as 100 mv/meter are fairly often observed. A field as large as 200 mv/meter would be very large when a field of 10 mv/meter is near what one would expect for "quiet" times.

The geographic extent of these fields is at present uncertain, except that at times fields have been observed at widely separate points; e.g., Point Barrow, Alaska, and Fairbanks, Alaska. One could, therefore, expect that these field structures are of great extent compared to auroral features -- hundreds of kilometers as compared to several kilometers for auroral forms. It is not clear at present whether or not these fields exhibit the characteristics of current sources or voltage sources. In other words, does the electric field remain constant in an auroral

arc when the ionization and consequently the conductivity is increased greatly? There are no definitive answers to this question at present, although relatively simple arguments concerning the total amount of charge available in the magnetosphere would argue for a current source.

It is of interest to consider the energy inputs of a system such as this. *Heaps* [1972] and *Harris* [1972] have done this by studying the ohmic heat input to the atmosphere as well as the ion drag and some of the motions consequent to these energy and momentum inputs.

In this section we explore the way in which energy is placed into vibrationally excited states of the O_2 and N_2 molecules by collisions with ions driven by the electric fields. We have assumed that the process

$$A^+ + BC \rightarrow A^+ + BC^{\ddagger} \tag{49}$$

is the only type of process that proceeds. We know that the process is much more complicated than this, because in drifting experiments in which ions drift in their parent gases, much more complicated processes occur. For example, N_2^+ drifting in N_2 results in the ions N^+, N_2^+, N_3^+, and N_4^+ [*Bloomfield* and *Hasted* 1966]. One item that is quite clear is that processes like this are continually breaking and making bonds. These are processes which are likely to create significant amounts of vibrational energy. To the knowledge of these authors, no quantitative information exists as to cross sections for processes like equation (49). We have, therefore, adopted a set of cross sections which we think are possible. Indeed, we feel that these are on the conservative side in the sense that our estimates are probably smaller than the cross sections themselves. We have considered excitation of $O_2(v=1)$, $N_2(v=1)$, and $O_2(^1\Delta_g)$ by O^+, N_2^+, NO^+, and O_2^+ ions. The cross sections assumed for each of the processes is given in Table 9.

The calculation that we have made is considered to be a very conservative one. Conservative again in the sense that we expect that we calculate excitation rates smaller than those which may actually occur. We assume that the ion is accelerated by the electric field until it

TABLE 9

CROSS SECTIONS IN cm^2

ION	STATE EXCITED		
	$O_2(v=1)$	$N_2(v=1)$	$O_2(^1\Delta_g)$
O^+	10^{-16}	10^{-16}	10^{-16}
N_2^+	10^{-16}	10^{-15}	10^{-16}
NO^+	10^{-16}	10^{-16}	10^{-16}
O_2^+	10^{-15}	10^{-16}	10^{-15}

collides with another molecule or until it is forced into cyclical motion by the magnetic field. The calculations assume a mean free path determined by

$$L = \frac{1}{[M]\sigma} \tag{50}$$

where [M] is the sum of the O, O_2, and N_2 densities. The cross section is assumed to be 10^{-14} for all species and ions for purposes of mean free path calculations. This cross section is analogous to a diffusion cross section for electrons. If the mean free path is longer than a gyro-radius of the ion, then the maximum energy which the ion can attain is determined by the magnetic field. At each altitude, both the mean free path and the gyro-radius are calculated for each ion. The energy as a function of time is then calculated using the appropriate equations. In all cases the ions are considered to start from a zero velocity. The fraction of their energy that is spent above the threshold energy of the state being considered is then calculated. The appropriate equations are given in Table 10. For example, in considering the excitation of $N_2(v=1)$, we use a threshold of .3 ev. The average velocity is also calculated. We then form the rate of excitation per molecule as

$$R(j) = \left[\sum_i \sigma(i,j)\ v_i[n_i]\ T_f(i,j)\right] \tag{51}$$

TABLE 10

ION ENERGY CALCULATIONS

Physical Parameters	Equations	
Gyro-radius of ion	$R = eE/M\omega^2$	
Mean free path of ion	$d = 1/(\sigma \cdot [\text{Ion}])$	
	$d > R$	$d < R$
Average velocity of ions	$AVEL = 1.414E/B$	$AVEL = \sqrt{eED/2M}$
Average energy of ion	$AENR = ME^2/B^2$	$AENR = eEd/4$
Maximum energy of ion	$MENR = 2ME^2/B^2$	$MENR = eEd$
Fractional time ion have energy > EXR	$TA = (1/\pi)\sin^{-1}(K.E./ME^2/B^2)-1)$	$TA = 1 - ED/MENR$
Excitation rate per molecule	$EXR = (\sigma \cdot [\text{Ion}]\ TA\ AVEL)$ for each ion	

where $w \equiv eB/M$

$e \equiv$ electronic charge

$E \equiv$ electric field strength

$B \equiv$ magnetic field strength

$[\text{Ion}] \equiv$ concentration of ions

$\sigma \equiv$ cross section

$M \equiv$ mass of ion

where j represents the state being considered; $\sigma(i,j)$ is obtained from Table 9; v_i and $[n_i]$ are the average velocity and number density of the ith ion; $T_f(i,j)$ is the fraction of its time which the ith ion spends with enough energy to excite the jth state.

The results of these calculations are then entered as excitation rates of the N_2 and O_2 vibrational states in the program previously described, and the resulting infrared emissions are calculated. The $O_2(^1\Delta_g)$ excitation rate was also calculated using this technique, but the results will not be presented in this report. Figures 24, 25, and 26 show the results of these calculations for electric fields of 0.05,

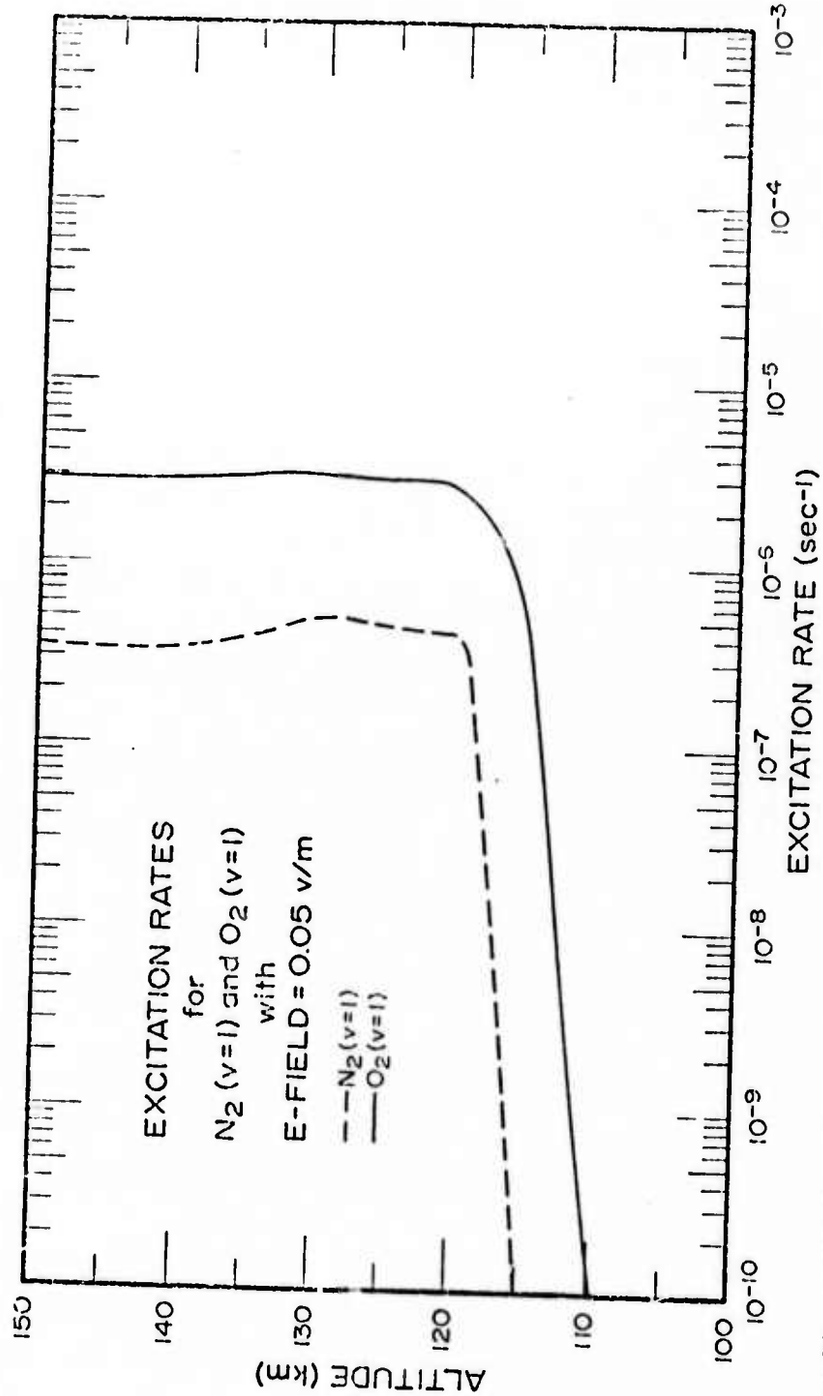

Figure 24. Height profile of the N_2 and O_2 excitation rates as a result of an electric field intensity of 0.05 volts/meters.

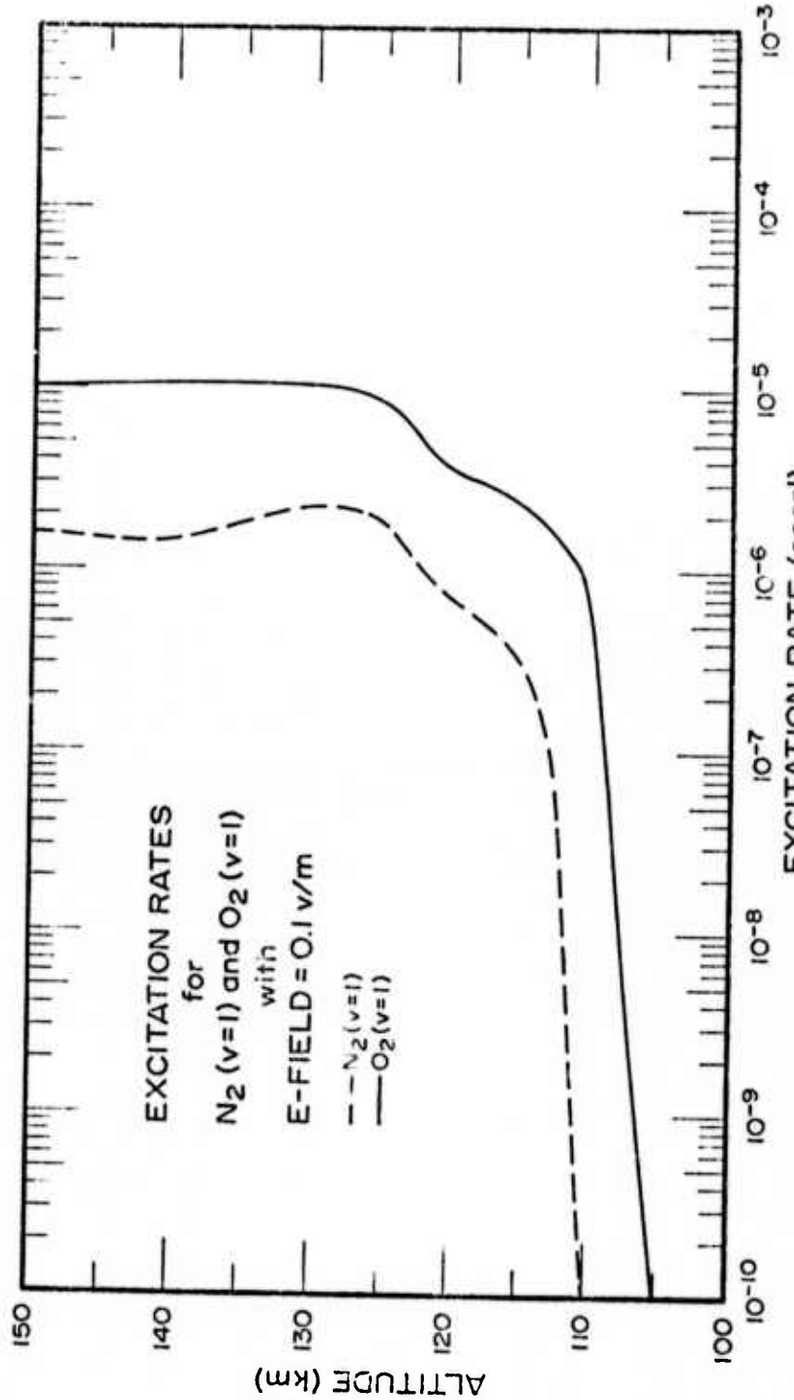

Figure 25. Height profile of the N_2 and O_2 excitation rates as a result of an electric field intensity of 0.1 volts.meter.

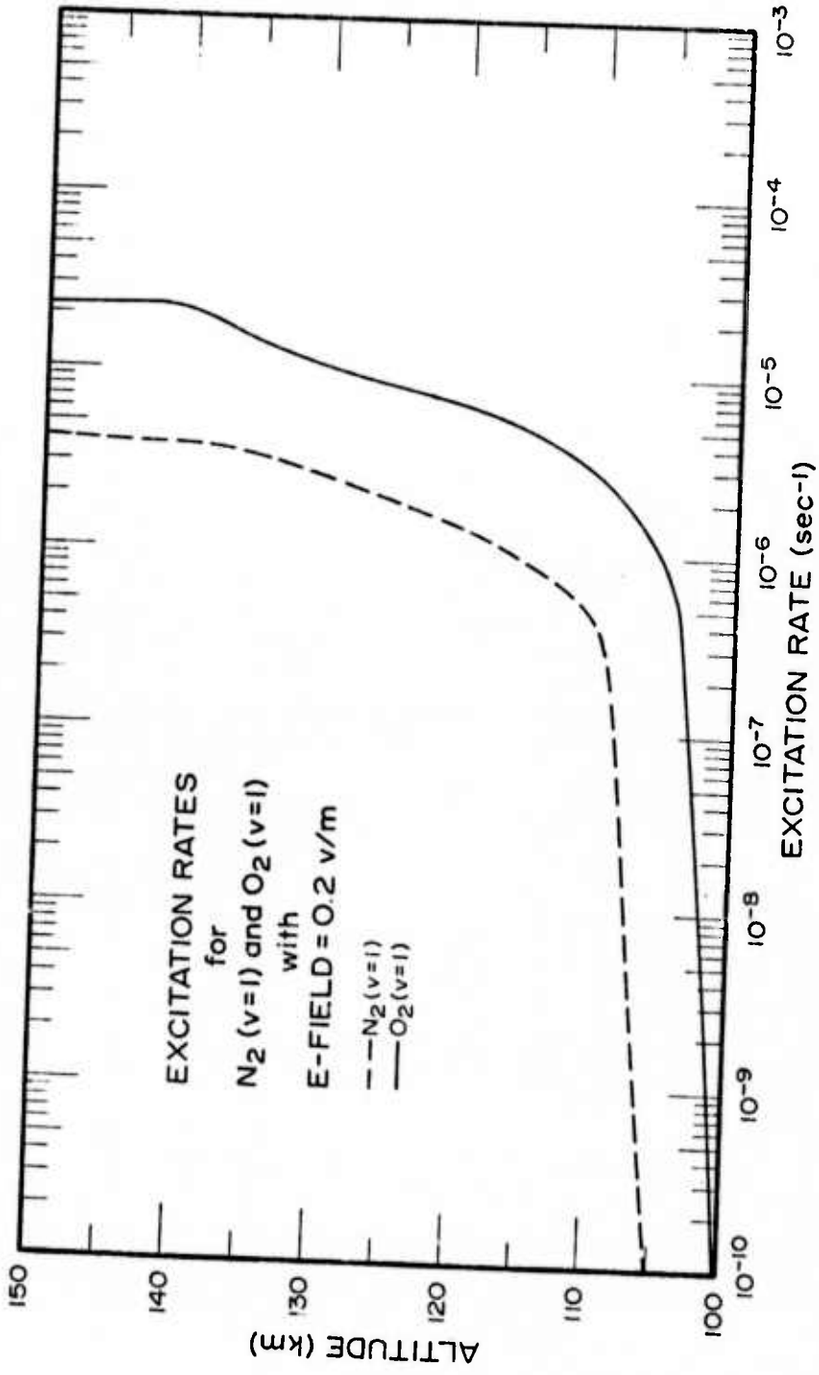

Figure 26. Height profile of the N_2 and O_2 excitation rates as a result of an electric field intensity of 0.2 volts/meter.

0.1, and 0.2 volts/meter. By referring to Figure 77, one can see the marked affect of the electric field on N_2 vibrational temperature. This is a plot of the steady state ratio of $N_2(v=1)$ as opposed to that which would be calculated from the assumption of a Boltzmann distribution.

As was stated earlier, a number of conservative assumptions have been made in these calculations. We have ignored the initial ion energies which, for auroral altitudes, may represent a maxwellian distribution function with average energies of several hundredths of an electron volt. When one is considering the excitation of states as low as 0.2 ev (for excitation of $O_2(v=1)$), inclusion of this energy would increase the calculated excitation rate substantially. A larger term that has been ignored is the substantial increase in random kinetic energy as measured in the drift frame of reference. This energy can, depending on the relative mass of the ions, become substantial if only elastic collisions occur [*Megill* and *Carleton* 1964]. Inelastic processes may well dominate in the auroral situation so that accurate evaluation of this term is difficult. The effect of neglecting this term is, again, to underestimate the intensities.

IR BAND MODEL PROGRAM (PROGRAM BCKGND) PHYSICS

A very general description of the methods used in computing the band radiance for each of the infrared bands under consideration was given in a previous section of this report. It is the purpose of this section to consider the physics of this program in more depth.

Since this research used the IR band model program of *Corbin et al.* [1970] as a starting point, much of the physics described in their report will also be applicable here. On the other hand, many new ideas and the associated physical processes have been incorporated in the original work with the consequent change in overall philosophy. Therefore, a complete physical description will be made even though it may mean duplicating some of the physical description found in the report by *Corbin et al.* [1970].

General Concepts

Ultimately, it is the population of the various vibrational states of a molecule which determines the infrared radiation from that molecule. Molecules may be vibrationally excited by one of several means; absorption of radiation, fluorescent excitation, chemiluminescent processes, or by one of several collisional excitation processes. These processes, in any kind of steady state, are balanced by radiative or collisional de-excitation.

In the lower regions of the atmosphere where collisional frequencies are high, collisional excitation and de-excitation processes are the more important. As one proceeds higher in the atmosphere, collisional frequencies decrease and radiative processes become more and more important. In order for a model to predict IR band radiance over a wide altitude region, it is necessary to include all processes over all altitudes. This is especially true when one considers the variation of excitation and de-excitation cross-sections for the same processes from species to species.

In the proceeding sections it was shown that electrons and/or electric fields tend to put a substantial amount of their energy into the vibrational energy of N_2 and O_2 as well as into $O(^1D)$. Physically this energy input has been computed in the form of production rates. Additionally, the reverse processes also take place for N_2 and O_2. That is, a certain amount of vibrational energy is lost to the ambient electrons. For these processes, the computational input is in the form of a loss rate. In the case of $O(^1D)$, much of this energy is transferred to N_2 and some, of course, to O_2.

These production and loss rates for $N_2(v=1)$, $O_2(v=1)$, and $O(^1D)$ are obtained from the computer program EXCHNG described earlier. The values obtained depend upon the auroral classification used. A primary electron flux was assumed as representative of an IBC-I, -II, and -III aurora and from this flux the production and loss rates were determined. The auroral classifications and representative primary electron flux are listed in a preceding section. In addition to these aurorally disturbed conditions, three categories of "quiescent" condi-

tions were examined. These categories included a totally quiet condition, a condition whereby an electron drizzle of flux $4 \times 10^7 \times E^{-2}$ cm^{-2} sec^{-1} $ster^{-1}$ kev^{-1} exists, and a condition which is totally quiet but in which an electric field exists in the ionosphere. Field values of 0.05, 0.1, and 0.2 volts/meter were used as representative. The electric fields, as in the case of electron precipitation, tend to put energy into the vibrational states of N_2 and O_2 since these are the major constituents. Production rates for $N_2(v=1)$ and $O_2(v=1)$ resulting from the electric fields were computed as described in a previous section.

Atmospheric disturbances represent additional energy inputs to the atmospheric system. It is the fact that a considerable amount of this energy ends up as vibrational energy in N_2 and O_2 that makes a close examination of the energy exchange processes of these vibrationally excited molecules important. Further, it makes the near resonant V-V exchange process probably the most important collisional process.

From the point of view of radiative transfer, the procedure of *Corbin et al.* [1970] of treating the radiative transfer problem for a single molecular vibrational-rotational band with a Doppler lineshape as if it were a single line was adopted. As they point out, this procedure greatly simplifies things for NLTE conditions.

Excited N_2, O_2, and O Calculations

Any energy deposited in the ^1D state of atomic oxygen will undergo a transfer, at least to some extent, to N_2 and O_2. It is therefore necessary for one to determine the population of $O(^1D)$ before considering the population of $N_2(v=1)$ and $O_2(v=1)$.

Rather than attempt to solve time-dependent equations for the excited states, it was decided to assume that an equilibrium had been reached between the production and loss terms. That is, rather than solve

$$\frac{d[O(^1D)]}{dt} = \text{Production terms-loss terms}$$

the time dependence would be removed by assuming quasi steady state, i.e.

$$\frac{d[O(^1D)]}{dt} = 0$$

In so doing, the resulting equation to be solved for the population of $O(^1D)$ is

$$[O(^1D)] = (k_1[e][O(^3P)] + k_2[O_2^+][e]) \; / \; (q_1[N_2] + q_2[O_2]) \qquad (52)$$

The two production terms (k's) are obtained from the program EXCHNG as described in a previous section. The loss rate terms (q's) which are used are $q_1 = 9.0 \times 10^{-11}$

$q_2 = 4.0 \times 10^{-11}$

which are in general agreement with *Young et al.* [1968].

Once the population for $O(^1D)$ has been determined, it is possible to compute with reasonable accuracy the population of $N_2(v = 1)$. In making this calculation, it is assumed that all levels with $v \geq 2$ rapidly decay to the $v = 1$ level. Therefore, one need only be concerned with two vibrational levels; $v = 0$ and $v = 1$. The assumption of a quasi steady state condition leads one to an equation for $N_2(v=1)$, i.e. $N_2^\ddagger$, as follows:

$$[N_2^\ddagger] = (k_{TV}[M] + k_e + k_O[O(^1D)] + k_{CO_2}[CO_2^\ddagger] + k_{O_2}[O_2^\ddagger] + k_E)[N_2]/(q_e +$$

$$q_{CO_2}[CO_2] + q_{NO}[NO] + q_{N_2O}[N_2O] + q_{NO^+}[NO^+] + q_{H_2O}[H_2O] +$$

$$q_{O_2}[O_2] + q_{VT}[M] = q_O[O(^3P)]) \qquad (53)$$

Most of the rate constants above are self explanatory, however, a few may need some explanation.

k_{TV} = production rate due to T-V energy exchange
q_{VT} = loss rate due to V-T energy exchange
k_e = production rate due to secondary electrons
q_e = loss rate due to ambient electrons
k_E = production rate attributable to electric fields
$[M]$ = total number density - all species

Figures 27 through 30 show the production rate k_e and the loss rate q_e as a function of height. The first two figures are for the case of an electron drizzle but no aurora, while the second two are for the case of an IBC-III aurora five minutes after commencement.

The same assumptions which were made for N_2 were also made in order to facilitate computation of $O_2(v=1)$, i.e. $O_2^{\ddagger}$. The quasi steady state condition leads to an equation for $O_2^{\ddagger}$ as follows:

$$[O_2^{\ddagger}] = (k_{TV}[M] + k_{N_2}[N_2^{\ddagger}] + k_e + k_O[O(^1D)] + k_E)[O_2]/(q_e + q_{H_2O}[H_2O] + q_{O_3}[O_3] + q_{N_2}[N_2] + q_{VT}[M] + q_{AEX}[O(^3P)]) \quad (54)$$

Here the production and loss terms take on the same meanings as outlined above. The values of the constants, needless to say, are no longer the same. The one addition is the q_{AEX} term which accounts for the atom interchange reaction $O + O_2^{\ddagger} \rightarrow O^* + O_2$ as discussed by *Deggs* [1971].

Radiative Transfer Considerations

Contributions to the broadening of an absorption line are in general due to five processes. Each of these processes acts to broaden the absorption line. Under certain conditions, all five may be important. On the other hand, it may well be that one particular process dominates all the others. The five processes are listed below.

1. Doppler Broadening - the result of molecular or atomic motion (velocity broadening)
2. Natural Broadening - the result of excited states having a finite lifetime.
3. Lorentz Broadening - the result of collisions with foreign gas molecules.
4. Holtzmark Broadening - the result of collisions with absorbing molecules of the same kind.
5. Stark Broadening - the result of collisions with electrons and ions.

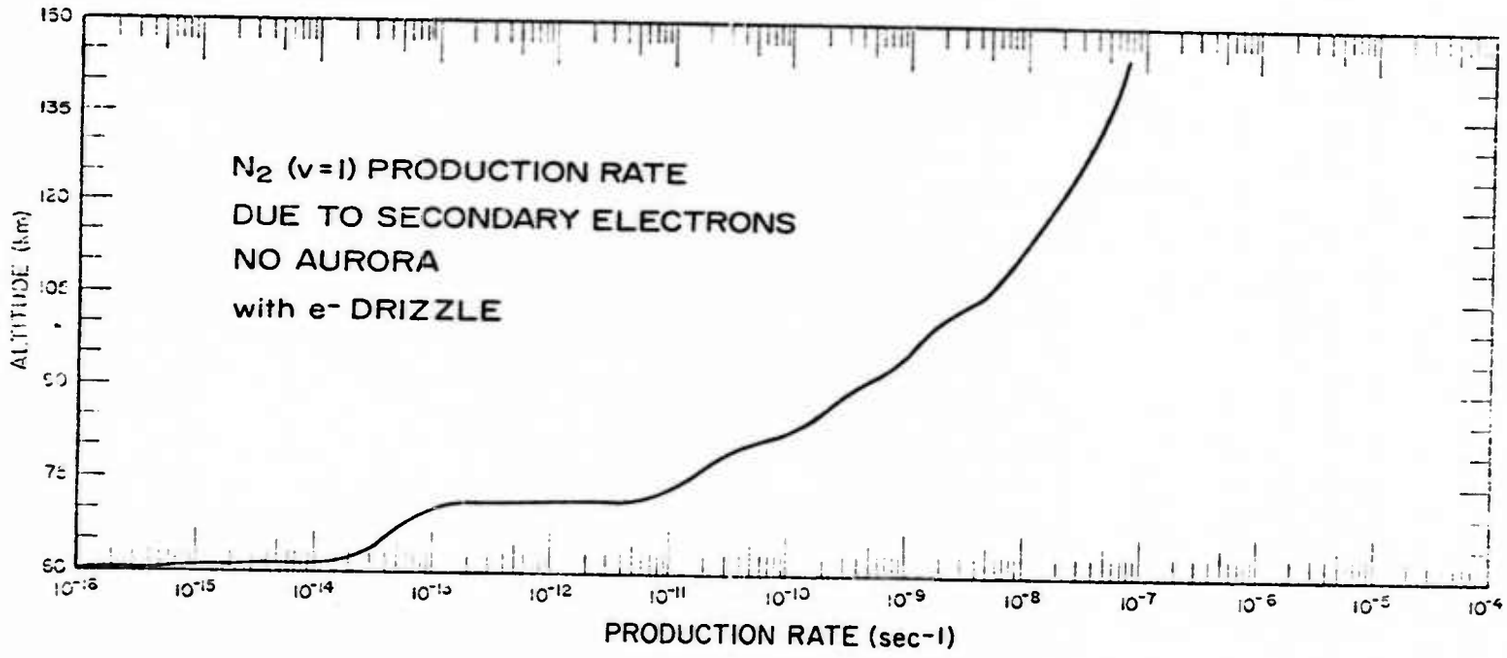

Figure 27. Height profile of the excitation rate of $N_2^{\ddagger}$ as a result of collisions with secondary electrons: no aurora is occurring, however, an electron drizzle exists.

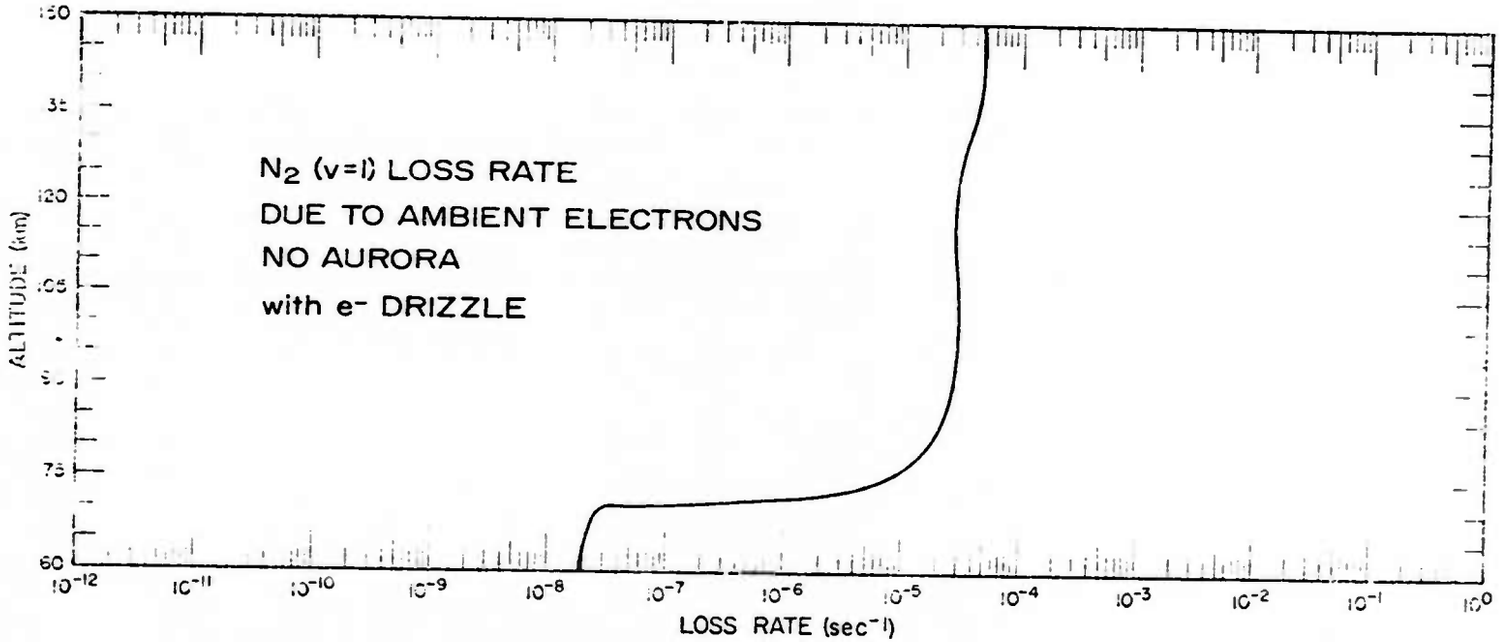

Figure 28. Height profile of the de-excitation rate of $N_2^{\ddagger}$ as a result of collisions with ambient electrons, no aurora is occurring; however, an electron drizzle exists.

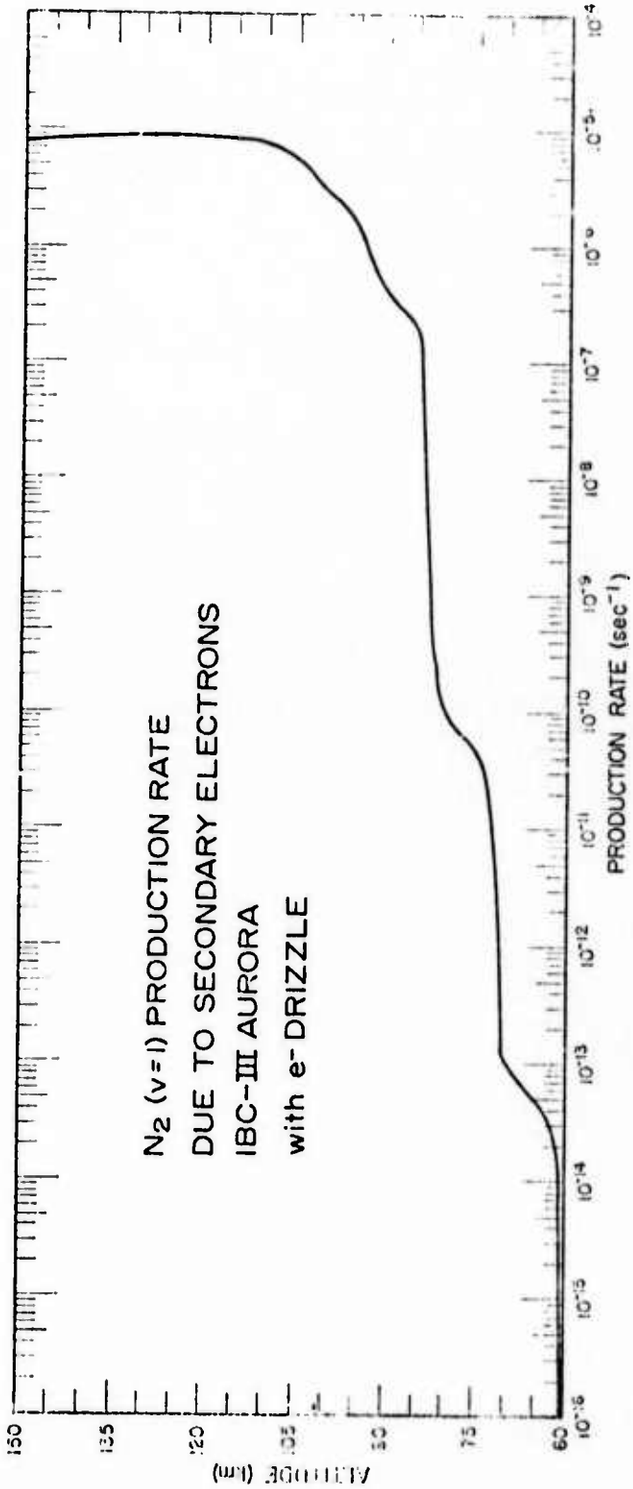

Figure 29. Height profile of the excitation rate of N_2^+ as a result of collisions with secondary electrons five minutes after commencement of an IBC-III aurora.

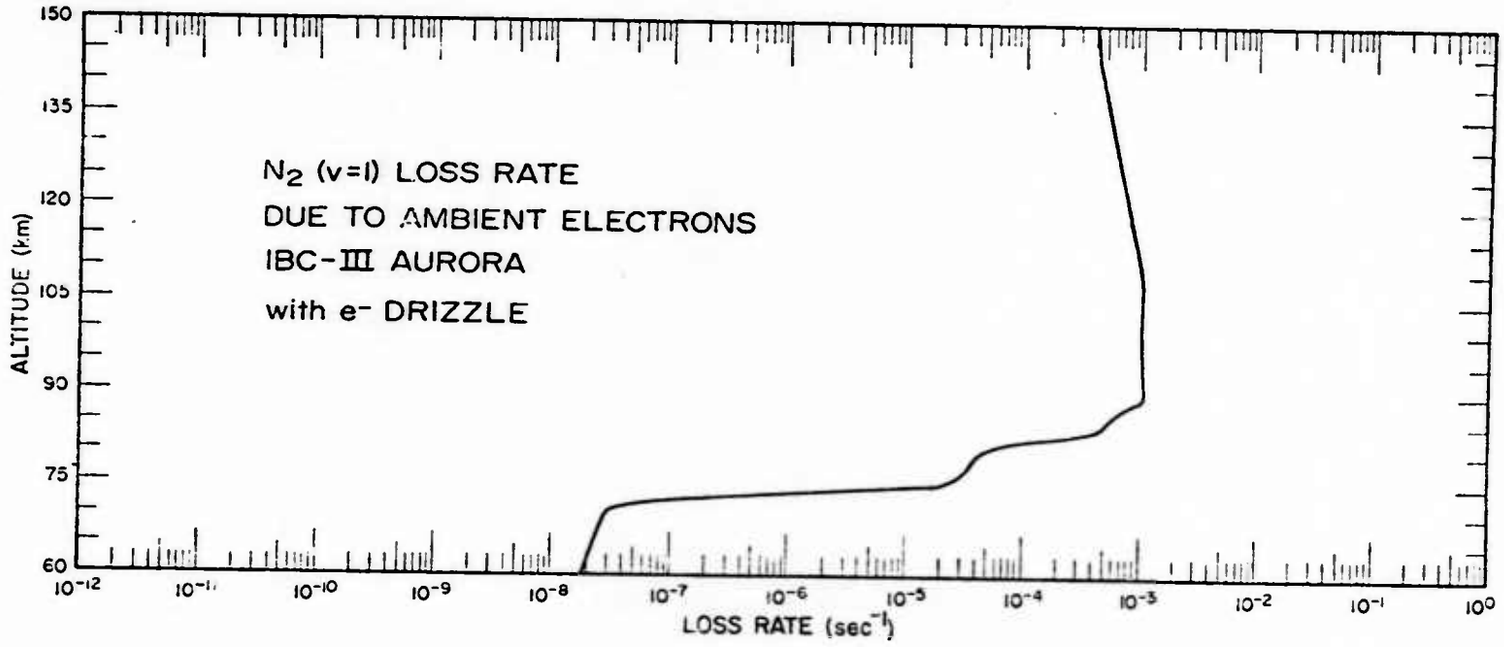

Figure 30. Height profile of the de-excitation rate of $N_2^{\ddagger}$ as a result of collisions with ambient electrons five minutes after commencement of an IBC-III aurora.

Lorentz and Holtsmark Broadening are often referred to as pressure broadening. Broadening as the result of collisions becomes unimportant with respect to Doppler Broadening at altitudes above approximately 70 km [*Kuhn* and *London* 1969]. Of the two remaining processes, unless the optical thickness is quite large ($k_o l > 1000$) the central region of the line will dominate the absorption process. That is to say, the edges of the absorption line may be neglected and the entire line may be well approximated with a purely Doppler lineshape. If, however, the absorbing gas is optically very thick, then only in the edges would a measurable amount of light be transmitted. For this optically thick case, Natural Broadening must be considered.

A study of the vibrational rotational bands of the minor constituents under consideration indicates, however, that the only band of significant optical thickness is the 4.3 μ band of CO_2. Even this band does not approach the requirements [*Mitchell* and *Zemansky* 1971] to utilize Natural Broadening as a lineshape factor. Therefore, the computational model assumes a Doppler lineshape factor.

The spectral absorption coefficient of a Doppler broadened line is [*Mitchell* and *Zemansky* 1971]

$$k_\nu = k_o \exp\left[-\frac{2(\nu - \nu_o)}{\Delta\nu_D}\sqrt{\ell n 2}\right]^2 \tag{55}$$

where $$\Delta\nu_D = \frac{2\sqrt{2R\ell n 2}}{C} \cdot \nu_o \sqrt{\frac{T}{M}}$$

is the Doppler breadth. T and M are the absolute temperature and the molecular weight respectively. k_o is the maximum absorption coefficient which occurs at $\nu = \nu_o$. k_o may be found from

$$\int^{\infty} k_\nu d_\nu = \tfrac{1}{2}\sqrt{\frac{\pi}{\ell n 2}}\, k_o \Delta\nu_D$$

which yields the expression

$$k_o = \frac{2}{\Delta\nu_D}\sqrt{\frac{\ell n 2}{\pi}}\,\frac{\lambda_o^2}{8\pi}\,\frac{g_2}{g_1}\,\frac{N}{\tau} \tag{56}$$

or $$k_o = \frac{2}{\Delta\nu_D}\sqrt{\frac{\ell n 2}{\pi}}\frac{\pi e^2}{mc} Nf \qquad (57)$$

Here the parameter g_2/g_1 is the ratio of the statistical weights of the upper to the lower state. τ is the lifetime of molecule in the upper state and, hence, the Einstein A coefficient is $A = 1/\tau$. The parameter f is the absorption oscillator strength. Under conditions when $h\nu_{1u} >> kT$, f and the band strength are related by a constant as [*Penner* 1959]

$$S_{1u} = 2.3795 \times 10^7 \, f \qquad (58)$$

Even though the optical thickness of the various vibrational-rotational bands is small enough to adequately describe the lineshape by Doppler broadening, it is not small enough to neglect. The effect of optical thickness is a reduction of the radiant flux being transmitted through the medium. Let us consider the radiative exchange process in more detail.

For a parallel beam of incident intensity I_ν, the amount of energy absorbed by a gaseous column of length ℓ per unit time is [*Mitchell* and *Zemansky* 1961]

$$F = \int_o^\infty I_\nu \, (1 - e^{-k_\nu \ell}) \, d\nu \qquad (59)$$

If the gas is Doppler broadened, this expression on a per unit length basis becomes

$$F = \int_o^\infty I_\nu \, (1 - \exp[-k_o \exp\{-\left[\frac{2(\nu - \nu_o)}{\Delta\nu_D}\sqrt{\ell n 2}\right]^2\}])d\nu \qquad (60)$$

If we define $w = \frac{2(\nu - \nu_o)}{\Delta\nu_D}\sqrt{\ell n 2}$

then $$dw = \frac{2\sqrt{\ell n 2}}{\Delta\nu_D} \, d\nu$$

Now the line will absorb only near its center frequency ν_o hence we may write

$$F = I(\nu_o) \frac{\Delta\nu_D}{2\sqrt{\ell n 2}} \int_{-\infty}^{\infty} [1 - \exp(-k_o e^{-w^2})] dw \tag{61}$$

$$F = I_o(\nu_o) \frac{\Delta\nu_D}{2\sqrt{\ell n 2}} \sqrt{\pi} k_o \left[1 - \frac{k_o}{2!\sqrt{2}} + \frac{k_o^2}{3!\sqrt{3}} - \ldots .\right] \tag{62}$$

$$F = I_o(\nu_o) \frac{\pi e^2}{mc} Nf \left[1 - \frac{k_o}{2!\sqrt{2}} + \frac{k_o^2}{3!\sqrt{3}} - \ldots .\right] \tag{63}$$

Let us define $S(k_o) = \left[1 - \frac{k_o}{2!\sqrt{2}} + \frac{k_o^2}{3!\sqrt{3}} - \ldots .\right]$ (64)

A factor $L(k_o)$ may be defined as

$$L(k_o) \equiv k_o S(k_o) = \frac{1}{\sqrt{\pi}} \int_{-\infty}^{\infty} [1 - \exp(-k_o e^{-w^2})] dw \tag{65}$$

If one now takes the derivative of $L(k_o)$ with respect to k_o, it will give a transmission factor for an optical depth k_o as [*Ivanov* and *Shcherbakov* 1965]

$$M_1(k_o) = \frac{dL(k_o)}{dk_o} = \frac{1}{\sqrt{\pi}} \int_{-\infty}^{\infty} \exp[-w^2 - k_o e^{-w^2}] dw \tag{66}$$

In a similar manner one may obtain transmission factors for cases other than for a parallel beam continuum source. Specifically, $N_1(k_o)$ and $N_2(k_o)$ are used in this report and represent transmission factors for a continuum surface source and a doppler lineshape layer source. Expressions for $N_1(k_o)$ and $N_2(k_o)$ are [*Deggs* 1972]

$$N_1(k_o) = \int_o^{2\pi} d\phi \int_o^{\pi/2} \cos\theta \sin\theta M_1\left(\frac{k_o}{\cos\theta}\right) d\theta \tag{67}$$

$$N_2(k_o) = \int_o^{2\pi} d\phi \int_o^{\pi/2} M_2\left(\frac{k_o}{\cos\theta}\right) \sin\theta d\theta \tag{68}$$

where $$M_2(k_o) = \frac{1}{\sqrt{\pi}} \int_{-\infty}^{\infty} \exp[-2w^2 - k_o e^{-w^2}] dw \tag{69}$$

The computational procedure used to determine radiative absorption was adopted from *Corbin et al.* [1970]. In essence, the effect of optical

thickness is accounted for by multiplying the radiant flux (whether it be solar, terrestrial, or computed flux radiated from some small atmospheric volume) by one of the three transmission factors. These factors, $M_1^B(\tau)$, $N_1^B(\tau)$, and $N_2^B(\tau)$, are dimensionless and are computed for all vibrational-rotational bands (the superscript B designates the factor for a band rather than a line) by means of a best fit polynomial expression. The choice of factors is determined by the kind of radiation source. That is to say, $M_1^B(\tau)$ is used for both solar flux and for the particular infrared radiance of a vibration-rotational band which we are trying to find. Specifically, $M_1^B(\tau)$ is used when the radiant flux is in the form of a parallel beam. On the other hand, the terrestrial flux is essentially a black body source which is 2π steradians in extent. $N_1^B(\tau)$ is the proper factor to use with this type of source. The third and last source of radiant flux is that generally categorized as other parts of the atmosphere. Here the source of radiation has a Doppler lineshape profile which is assumed to be exactly that of the absorbing line. In addition, this source of radiation is handled in the computational model on a layer by layer basis. The proper factor for this type of source is $N_2^B(\tau)$.

As previously stated, $M_1^B(\tau)$, $N_1^B(\tau)$, and $N_2^B(\tau)$ are computed by means of best fit polynomials developed by *Corbin et al.* [1970]. The particular polynomial to be used is determined by (1) the optical thickness τ and (2) whether the band is parallel or perpendicular transition. Nevertheless, all bands with these same characteristics are treated in the same manner. At first this may be viewed with some skepticism, however, in light of the optical thinness of almost all lines, this factor turns out to be either 1 or very close to it. Therefore, it is felt that little error is introduced by this method of treating the problem.

One further consideration is necessary with regard to the factors $M_1^B(\tau)$, $N_1^B(\tau)$, and $N_2^B(\tau)$. The superscript B indicates that the factor is for a vibrational-rotational band, whereas in general it is written on a line by line basis. The physics of transforming these factors to a band basis will be explained below. However, some of the technique

is not obvious in the computer program because it is included in the best fit polynomials for evaluating $M_1^B(\tau)$, $N_1^B(\tau)$, and $N_2^B(\tau)$.

Since the relative line-strength of each line in a vibrational-rotational band varies with respect to the other lines, so will the optical thickness of each line. In order to greatly simplify computation, only one value of optical thickness (τ_o) is used for the whole band. This means that only one computation of either $M_1^B(\tau)$, $N_1^B(\tau)$, or $N_2^B(\tau)$ is necessary and that that value will then be on a band basis. Thus a reasonable method of choosing τ_o is all that is outwardly required. Inwardly, on the other hand, the polynomial fit method shields from view the process used to obtain it. That is in order to obtain $M_1^B(\tau)$ for example, the product $\tau M_1(\tau)$ is computed for each line and then summed for all lines where the product is more than 10^{-14} that of the strongest line. This sum is divided by the sum of the optical thickness τ of all these lines in order to obtain $M_1^B(\tau)$. Mathematically then,

$$M_1^B(\tau_o) = \frac{\sum_i \tau_i M_1(\tau_i) + \sum_j \tau_j M_1(\tau_j) + \sum_k \tau_k M_1(\tau_k)}{\sum_i \tau_i + \sum_j \tau_j + \sum_k \tau_k} \tag{70}$$

where i, j, and k are over lines in the P, Q, and R branches.

The optical thickness τ_o is assigned to be that of the strongest line. This value is determined in the following manner. The line intensity is proportional to the fractional part of molecules in the initial state [*Goody* 1964].

$$\frac{n(J'')}{n} = \frac{g_{J''}}{Q_r(t)} \exp\left[-\frac{E_r(J'')}{kT}\right] \tag{71}$$

where $Q_r(T)$ is the rotational partition function at the temperature T which is given by

$$Q_r(T) = \sum_{J=0}^{\infty} g_J \exp\left[-\frac{E_r(J)}{kT}\right] \tag{72}$$

The term g_J is the multiplicity of the quantum state J. $E_r(J)$ is the rotational energy level of the molecule. For example, the rotational energy levels of a rigid linear molecule are given by [*Goody* 1964]

$$E_r(J) = B_v \, hc \, J(J + 1) \tag{73}$$

The quantium number J" for the strongest line may be found by the maximization process of setting the derivative of n(J)/n with respect to J equal to zero and solving. The result is that the maximum line intensity occurs at

$$J'' = \sqrt{\frac{kT}{2B_v hc}} - \tfrac{1}{2} \tag{74}$$

Thus, by using this value of J" one may determine the relative strength of the strongest line by computing n(J")/n. The value τ_o may then be found using equation (57)

$$\tau_o = \left[\frac{e^2/mc}{2.3795 \times 10^7} \sqrt{\frac{\pi}{2R}}\right] \sqrt{\frac{M}{T}}\, N_1 \cdot \lambda_o \cdot S \cdot S_M \tag{75}$$

where $S \cdot S_M$ is the band strength (S_{1u}) multiplied by the relative strength of the strongest line (n(J")/n).

NLTE Vibrational Populations

In an effort to compute the vibrational populations of the various species, let us first list the possible excitation or de-excitation mechanisms.

Excitation (production terms):

a) collisional T-V excitation
b) collisional V-V excitation
c) radiative absorption of solar flux
d) radiative absorption of terrestrial flux
e) radiative absorption of flux from other levels of the atmosphere
f) chemiluminescence
g) spontaneous radiative transition from a higher state

De-Excitation (loss terms):

a) collisional V-T de-excitation
b) collisional V-V de-excitation
c) spontaneous radiative de-excitation

With these processes in mind it is possible to write a general differential equation for the time rate of change of the number density

of the upper state dN_u/dt in terms of them

$$dN_u/dt = \text{production terms} - \text{loss terms}$$

As in the computation for $N_2^{\ddagger}$ and $O_2^{\ddagger}$ we will assume a case of quasi steady state. That is, we will assume that $dN_u/dt = 0$ and then solve the resulting equation for N_u, the vibrational population of the state under consideration.

Since all of the terms are not present in every case, let us consider a typical example of the computation of a vibrational population. Suppose we consider the population and depopulation of the π_u level of the ν_2 bending mode for CO_2 (see Figure 32). Here one would write:

$$CO_2(\pi_u) = \{(k_{TV} + G_{UP}*N_1^B(\tau) + 2\pi G*N_{eff}*A_1 + G_{DOWN}M_1^B(\tau))([CO_2]) +$$

$$[CO_2(\Sigma_g^+)](A_2 + q_{VT}) + [CO_2(\Delta_g)](A_3 + q_{VT}) +$$

$$[CO_2(\Sigma_g^+(\nu_1))](A_7 + q_{VT})\}/(q_{VT} + A_1) \qquad (76)$$

In this expression k_{TV} and q_{VT} are the proper T-V and V-T collisional energy exchange rate coefficients.

$$G_{UP} = G*\text{terrestrial flux}*2\pi \ (\text{sec}^{-1})$$

$$G_{DOWN} = G*\text{solar flux} \ (\text{sec}^{-1})$$

where $$G = \frac{\pi e^2}{mc^2} f \lambda_o^2 = 3.72 \times 10^{-34} S\lambda_o^2 \ (\text{cm}^2 \cdot \mu)$$

G_{UP} and G_{DOWN} are derived from the general expression of the rate at which a single molecule absorps and radiates infrared radiation. Equation (59) gives their rate as

$$G^1 = \int_o^\infty I_\nu \ (1 - e^{-k\nu}) \ d\nu \qquad (77)$$

on a per unit length basis. To transform this expression to a wavelength basis, we must recall that $d\lambda = \lambda^2/c \ d\nu$. Then one can write this rate as

$$G^1 = \int_o^\infty I(\lambda) \frac{\lambda^2}{c} (1 - e^{-k\lambda}) d\lambda \qquad (78)$$

which upon integration (since N = 1) yields

$$G^1 = I(\lambda_o) \frac{\lambda^2}{c} \left[\frac{\pi e^2}{mc} f\right] = I(\lambda_o) \frac{\pi e^2}{mc^2} f\lambda_o^2 \qquad (79)$$

provided that $I(\lambda_o)$ has not diminished. That is to say, we will account for absorption by multiplying by the appropriate transmission factor as in equation (76) rather than concerning ourselves with it at this point. Thus it can be seen that G_{UP} and G_{DOWN} are just special cases of G^1.

N_{eff} is the effective number of molecules contributing to the radiative flux from other parts of the atmosphere, in a given vibrational-rotational band, multiplied by the factor $N_1^B(\tau)$. N_{eff} has the units photons cm^{-2} μ^{-1}. A_1 is the Einstein A coefficient for spontaneous emission. Note that all of the factors up to this point are multiplied by $[CO_2]$, which gives the resulting units cm^{-3} sec^{-1} as desired. The term $[CO_2(\Sigma_g^+)]*(A_2 + q_{VT})$ and the two succeeding terms give the production rate of the desired level, $CO_2(\pi_u)$, (see Figure 32 for an energy level diagram) from higher levels. This production may be accomplished via spontaneous emissions (A_2) or through collisional energy loss (q_{VT}). The loss terms for the π_u level of the ν_2 bending mode of CO_2 are obvious in light of the previous discussion.

It should be pointed out that all of the equations such as this one are solved by means of an iterative process. The initial values for the number density of the various energy levels used in this process are those as determined from a Boltzman distribution.

Chemiluminescence

Infrared chemiluminescence may be defined as infrared energy radiated as the result of a chemical reaction having taken place. This statement implies that at least one of the product molecules of the chemical reaction is left in an excited vibrational-rotational state which subseuqently radiates in the infrared. This means, for example, that when the following chemical reaction occurs

$$O^+ + N_2 \rightarrow (NO^+)^{\ddagger} + N \qquad (80)$$

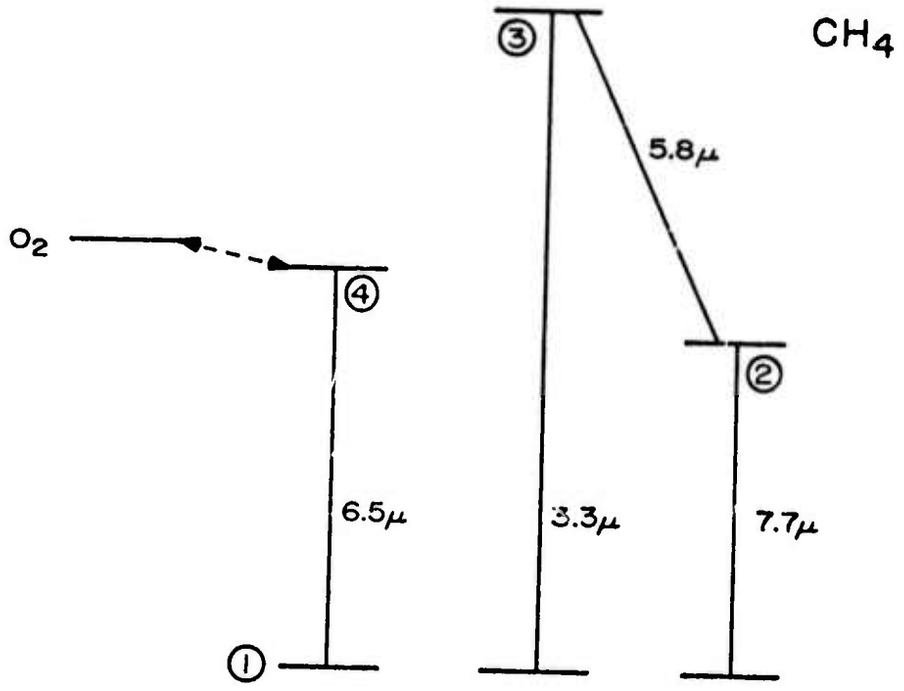

Figure 31. Partial energy level diagram for CH_4.

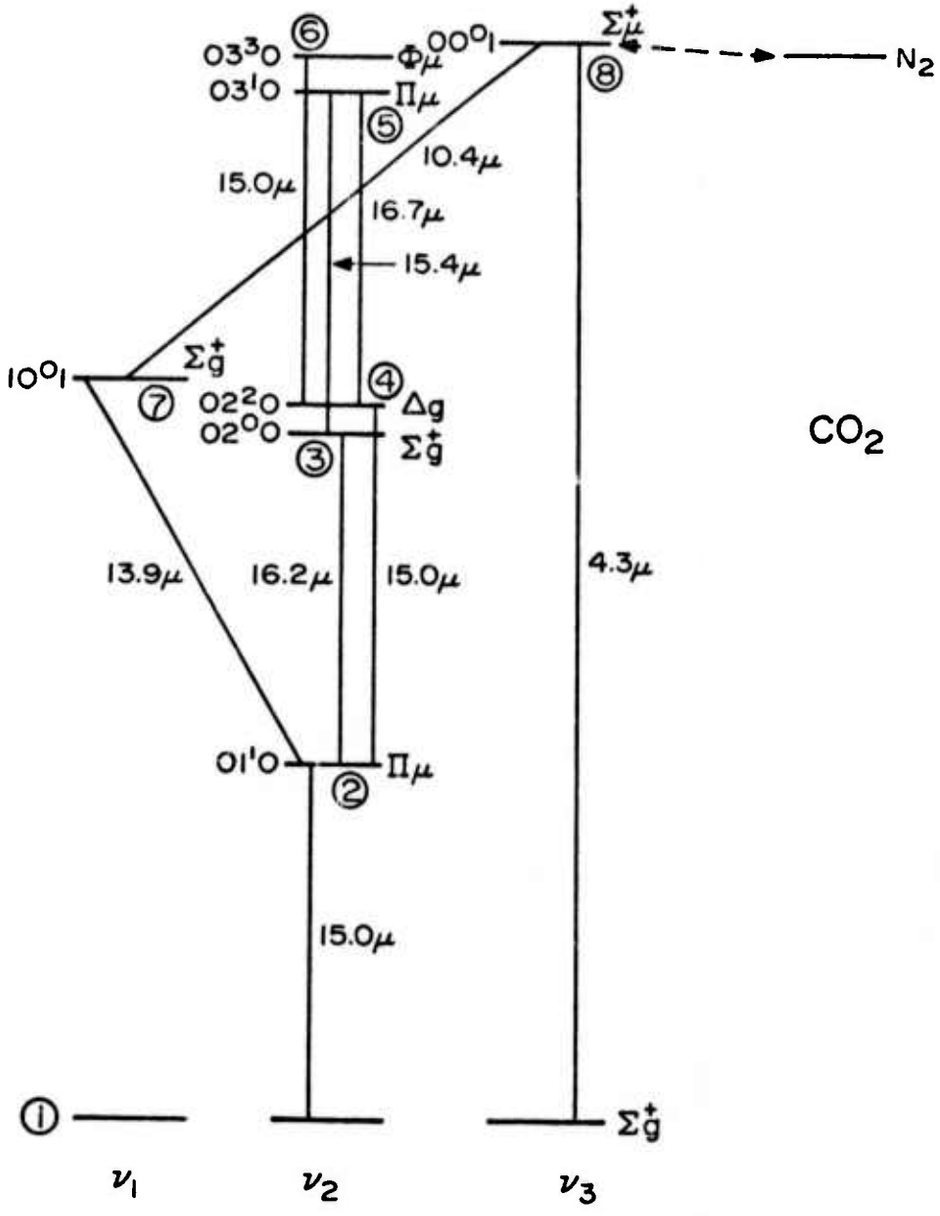

Figure 32. Incomplete energy level diagram for CO_2 showing only the features required in this study.

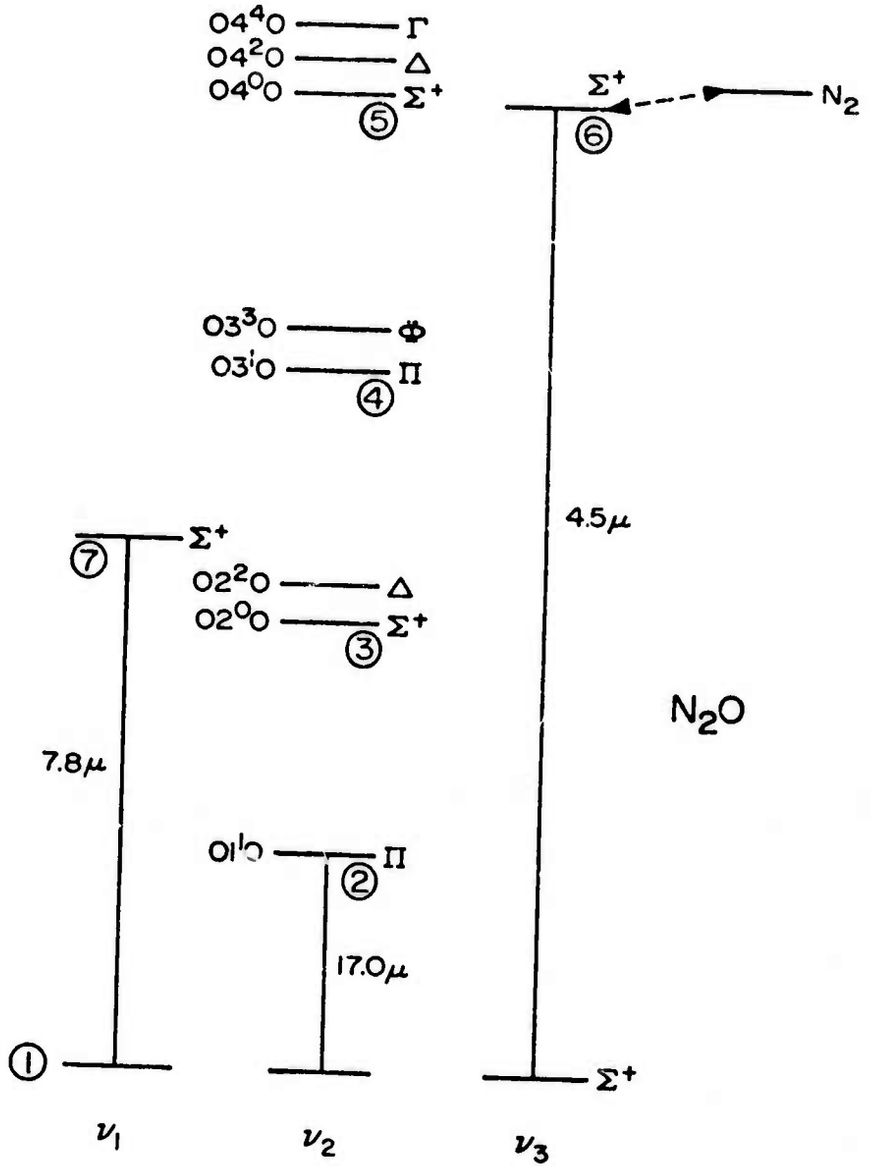

Figure 33. Incomplete energy level diagram of N_2O showing only the features required in this study.

the product molecules have less internal energy in their respective ground states than do the reacting molecules. In order to satisfy the law of conservation of energy, part of this additional energy may go into vibrational-rotational energy and the remaining part into the translational energy of the product molecules. In the case of the above reaction, we have assumed that one quantum of vibrational-rotational energy is obtained per reaction. Further, we assume that 1/3 of this goes into the v=1 vibrational level and 1/3 into the v=2 level. Since the v=2 level is approximately twice the energy of the v=1 level, the total of the two is 1 quantum of energy.

The production rate of NO^+ from this reaction is obtained from the program EXCHNG. This production rate multiplied by the proper factor (1/3 for example) is then included in as an additional production term in the equation used to compute vibrational populations.

Two other chemiluminescent reactions are considered. They are

$$N + O_2 \rightarrow NO^{\ddagger} + O \tag{81}$$

$$H + O_3 \rightarrow OH^{\ddagger} + O_2 \tag{82}$$

In the former, atomic nitrogen may be considered to be in either the $N(^4S)$ or the $N(^2D)$ states. We have taken the production rates given by *Ghosh* [1968] and modified them by multiplying by 0.02. This is done for both the v=1 and the v=2 vibrational levels. This essentially limits us to considering only the $N(^4S)$ reaction. Less is known regarding the $N(^2D)$ reaction and essentially no accounting of it is made in this program.

The hydroxyl radical OH is different than all other species in the program in that the only important nighttime excitation mechanism is through chemiluminescence. This is the result of the nonexistence of a near resonant V-V exchange mechanism and of the fact that the terrestrial flux in this spectral region is relatively very small. In order to compute the vibrational populations of the upper vibrational levels of OH, it was assumed that the above chemical reaction was the only one of any consequence. Further, it should be pointed out that this reaction is capable of populating only the levels up to v=9. A production

rate of 5.69×10^{-12} cm^3 $molecule^{-1}$ sec^{-1} was used for the v=9 vibrational level and a smoothed version of the relative formation rates of *Charters et al.* [1971] was adopted as a means of determining lower vibrational level production rates.

PROGRAM BCKGND (IR BAND MODEL PROGRAM) RESULTS

It is the purpose of this section to present, in graphical form, some of the results of the program BCKGND. It will be recalled that this program has the capability of computing the predicted radiance in watts cm^{-2} $ster^{-1}$ on a band basis. It also has the versatility of computing this radiance for the angles 0°, 20°, 40°, 60°, 70°, 80°, and 90°, as measured from the zenith, as well as for the limb view case. Needless to say, this is a large amount of data. In an effort to reduce the total amount of data presented in this report, and yet, to keep it representative and meaningful, it was decided to present for the most part only data in which the zenith angle is 0°. This is to say, only vertical viewing data will be presented.

The predicted radiance, for the vertical viewing case, is equivalent to predicting what radiance a forward looking radiometer on a rocket would observe. It is still possible to see the effects of optical thickness for this case as compared to an optically thin medium. It is also possible to determine how the increase in electron flux affects the predicted radiance and in particular to observe which bands are enhanced by the auroral activity. The same thing may be said for the case in which the energy input is due to an electric field.

Let us first consider the case in which there is no aurora, no electric fields, but in which an electron drizzle (as previously described) exists. The predicted radiance for vertical viewing is shown in Figures 34 through 44 for the molecules CH_4, CO_2, H_2O vapor, NO, N_2O, O_3, NO^+, OH, and CO. The designation NLTE=3 means that nonthermodynamic equilibrium conditions exist. In this case the 3 means nighttime conditions. The designation aurora = 0 means no auroral conditions exist.

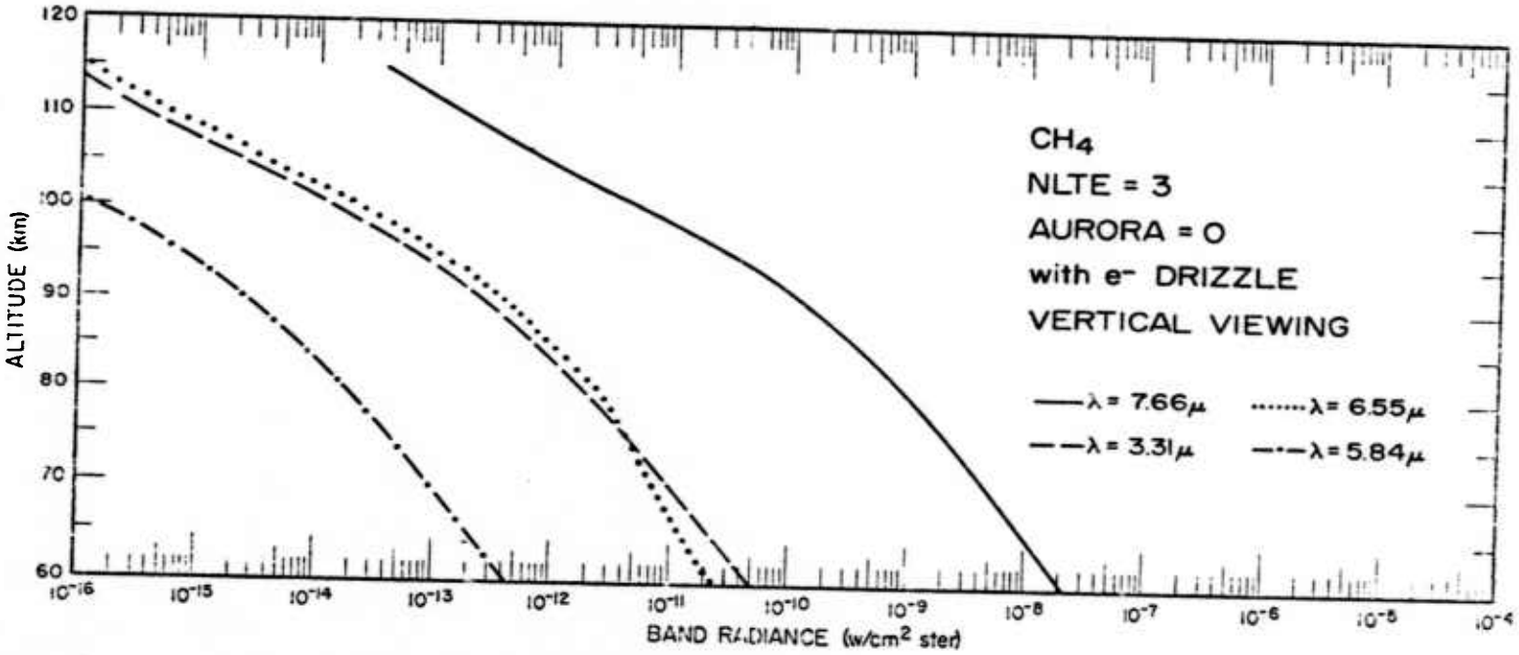

Figure 34. Height profile of the band radiance of CH_4 for the case when an electron drizzle is the only source of ionospheric disturbance.

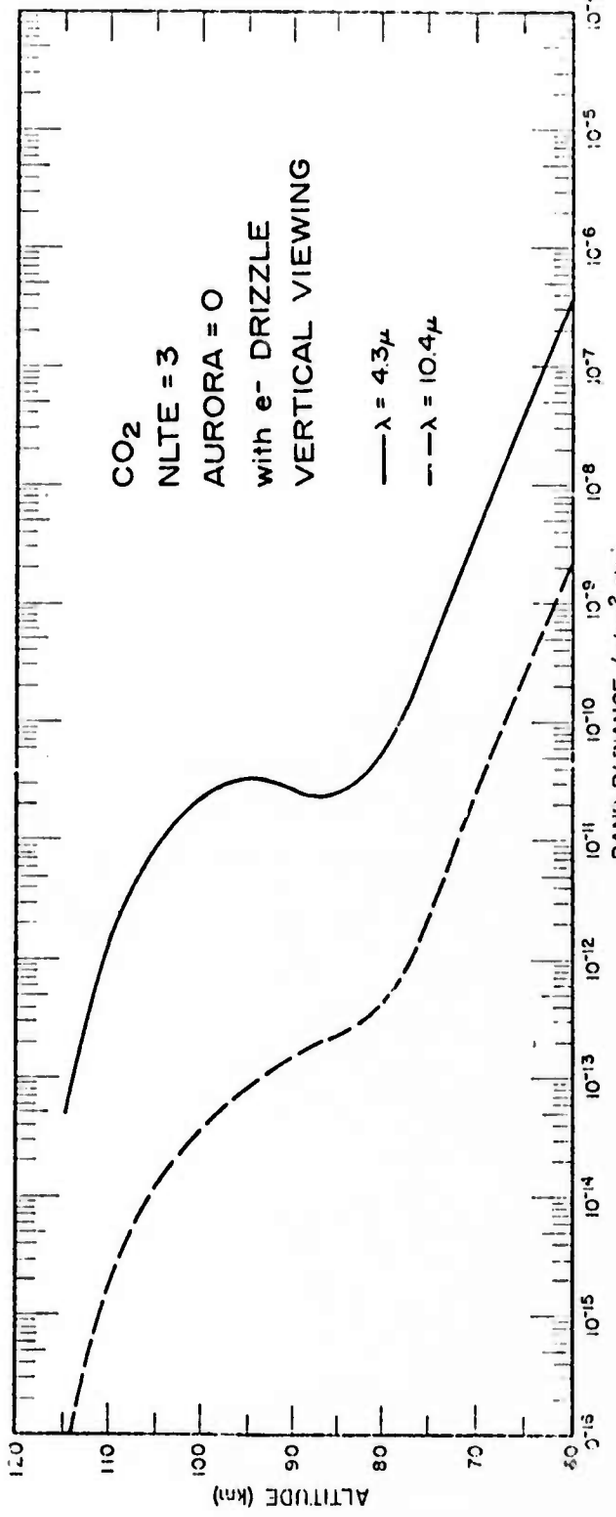

Figure 35. Height profile of the band radiance of CO_2 for the case when an electron drizzle is the only source of ionospheric disturbance.

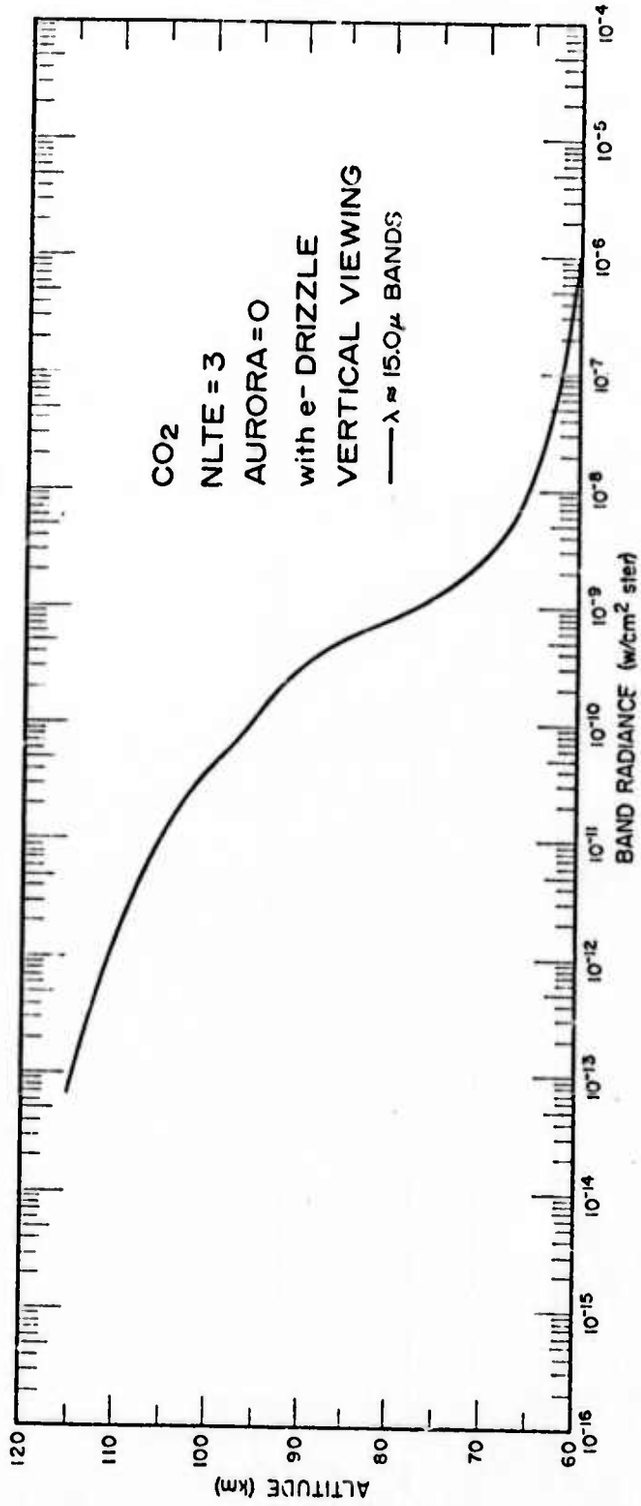

Figure 36. Height profile of the band radiance of all of the 15 μ bands of CO_2 for the case when an electron drizzle is the only source of ionospheric disturbance.

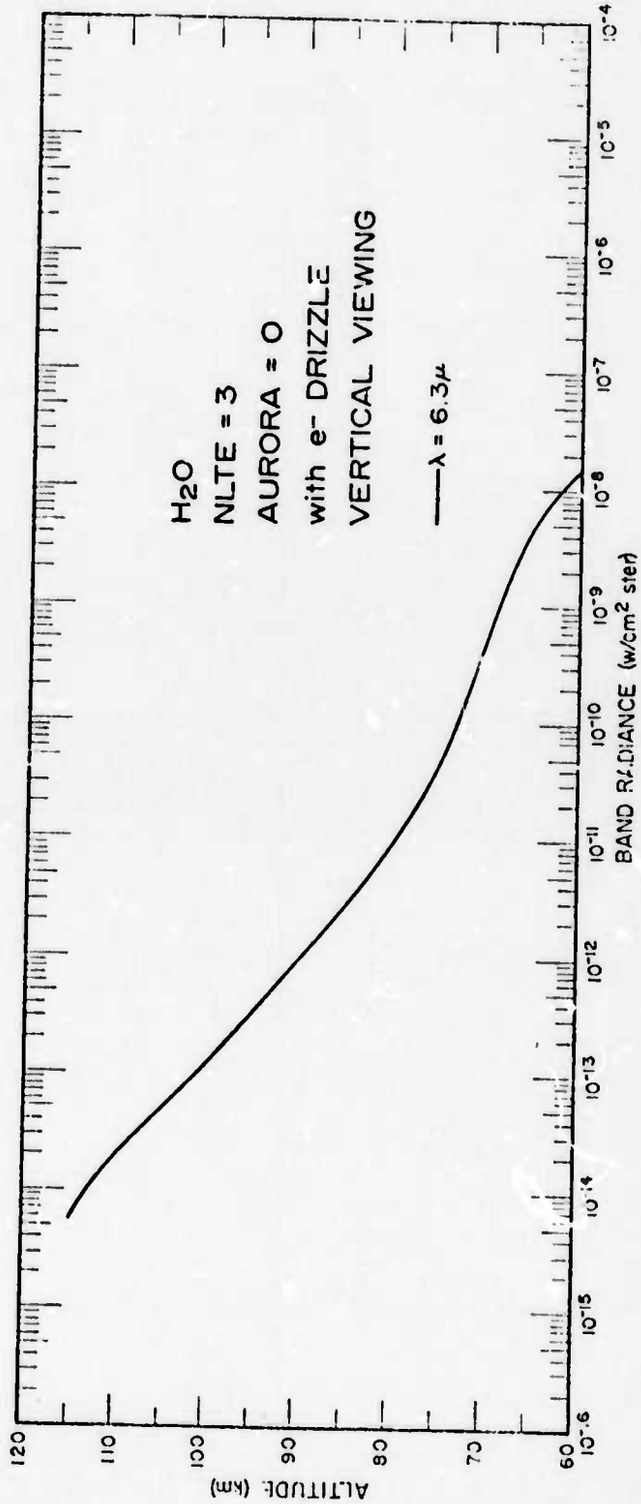

Figure 37. Height profile of the band radiance of H_2O for the case when an electron drizzle is the only source of ionospheric disturbance.

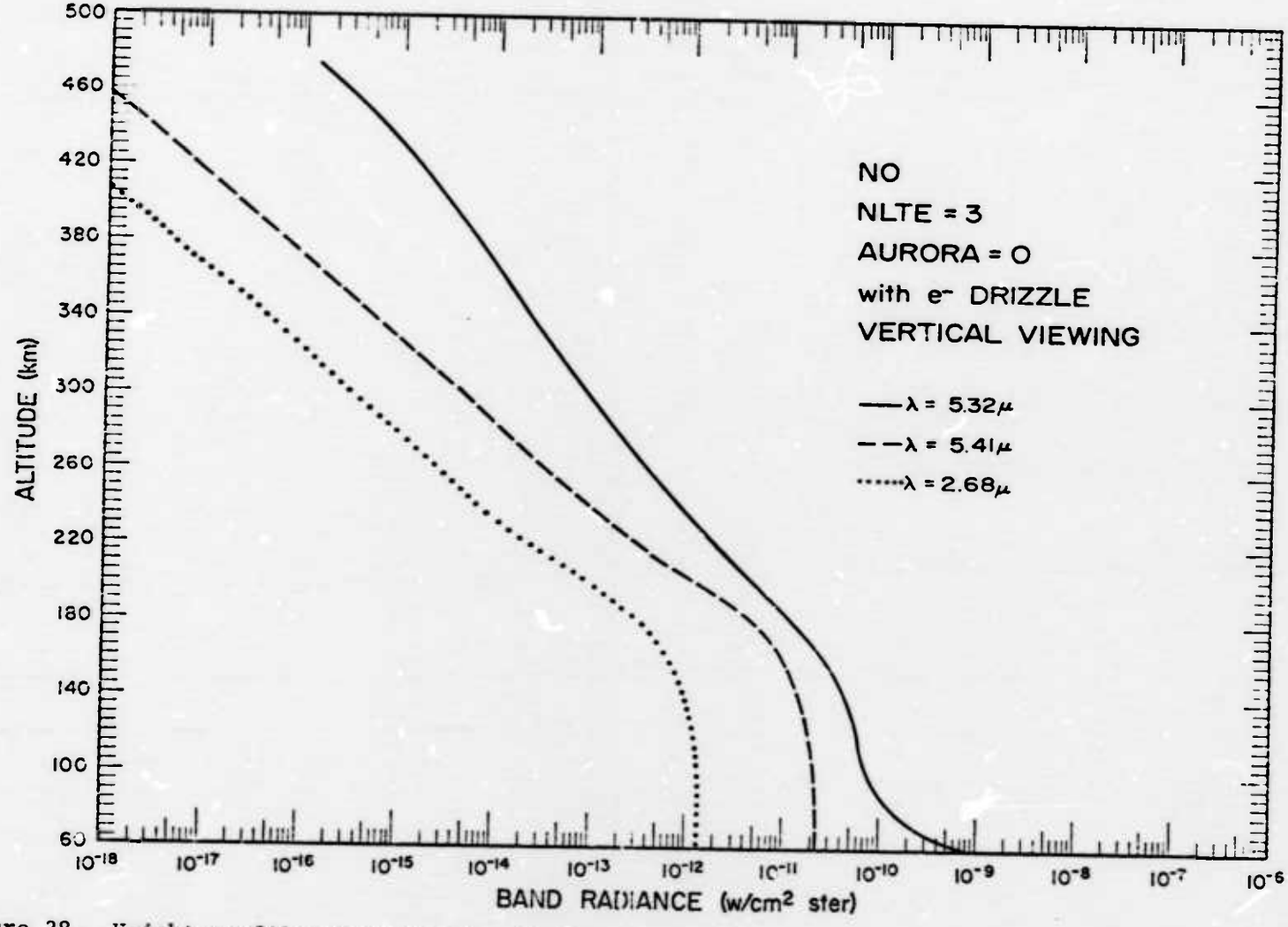

Figure 38. Height profile of the band radiance of NO for the case when an electron drizzle is the only source of ionospheric disturbance.

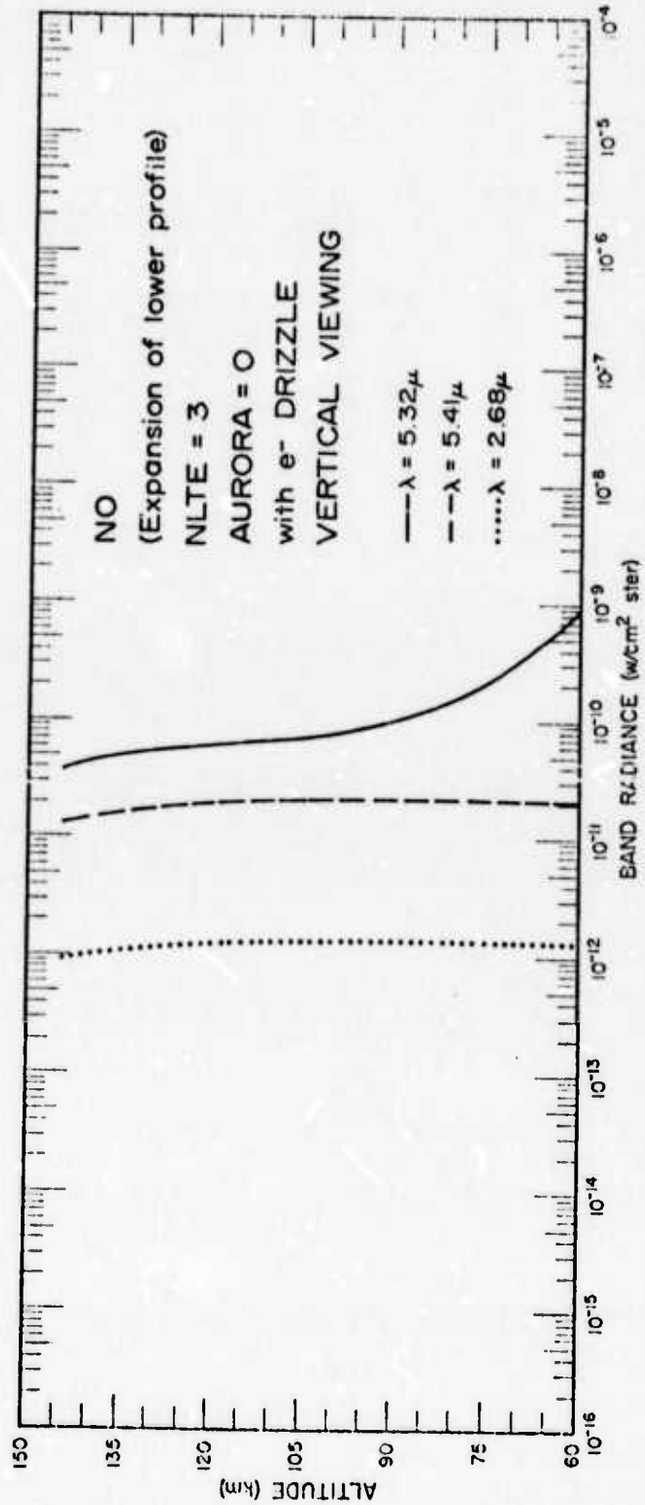

Figure 39. Expansion of the lower altitude band radiance of NO as shown in Figure 38.

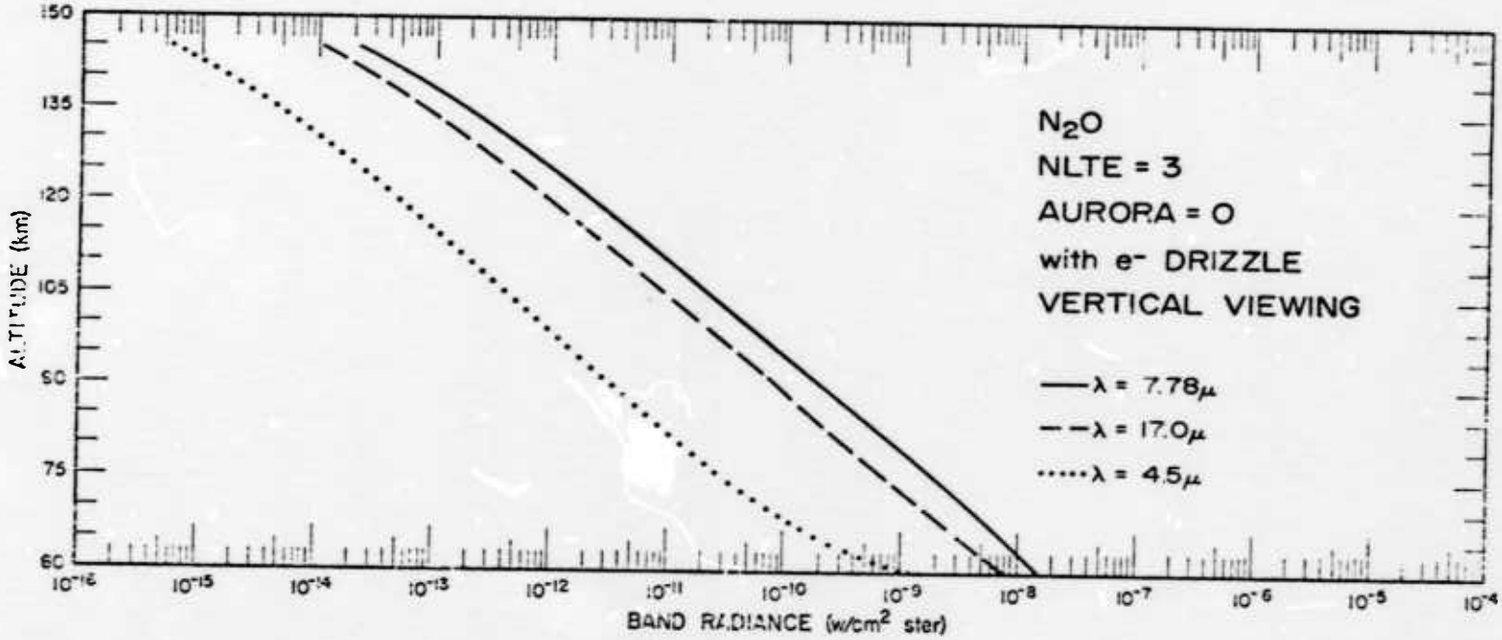

Figure 40. Height profile of the band radiance of N_2O for the case when an electron drizzle is the only source of ionospheric disturbance.

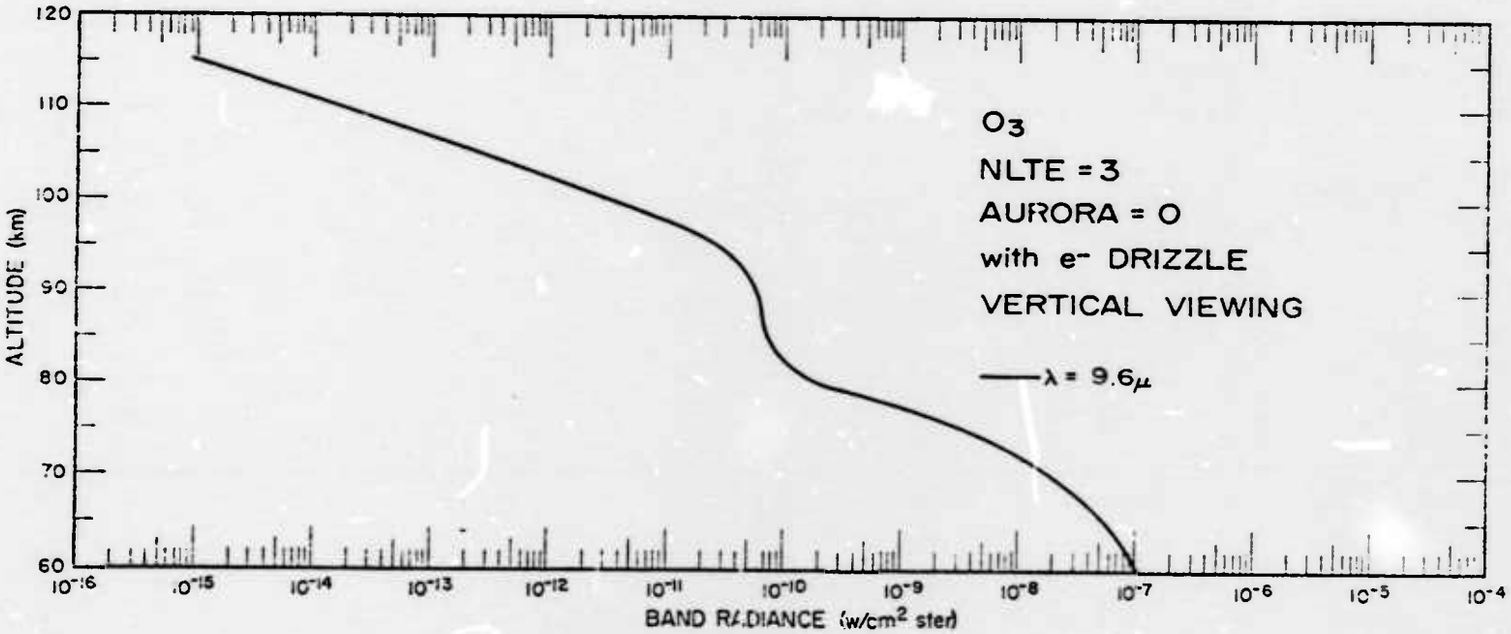

Figure 41. Height profile of the band radiance of O_3 for the case when an electron drizzle is the only source of ionospheric disturbance.

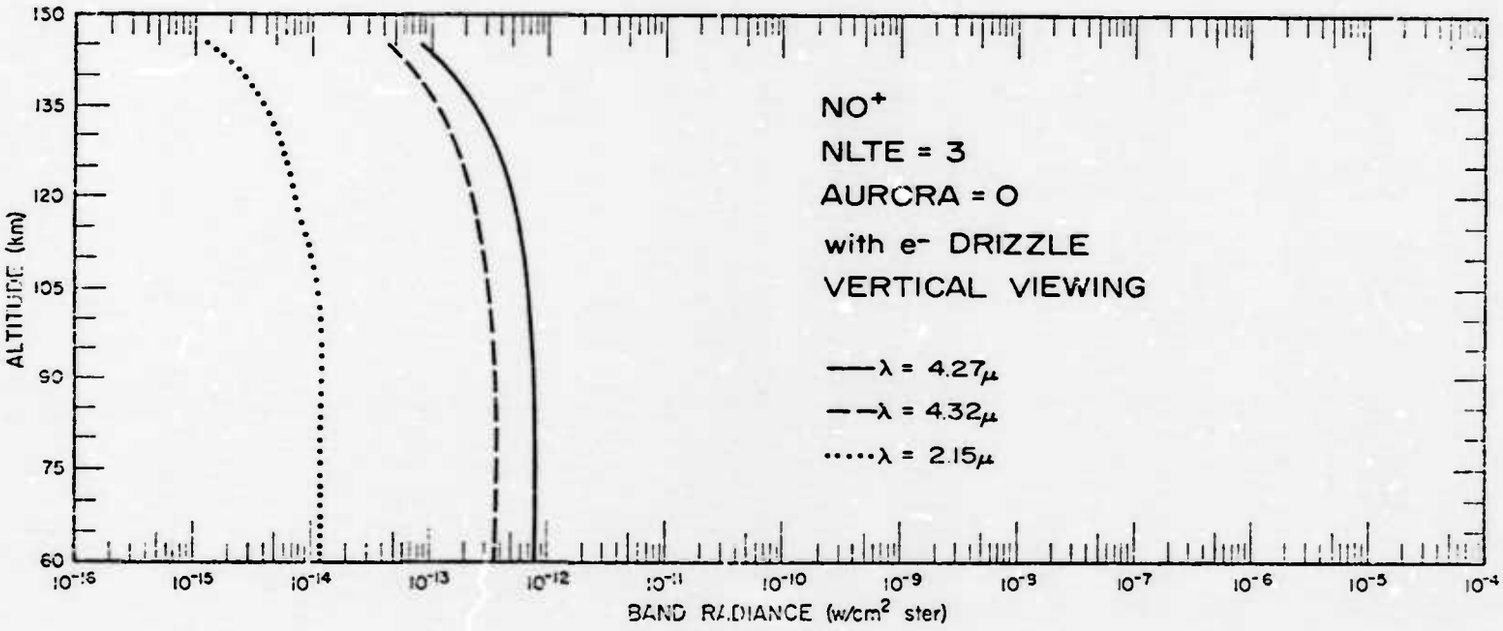

Figure 42. Height profile of the band radiance of NO^+ for the case when an electron drizzle is the only source of ionospheric disturbance.

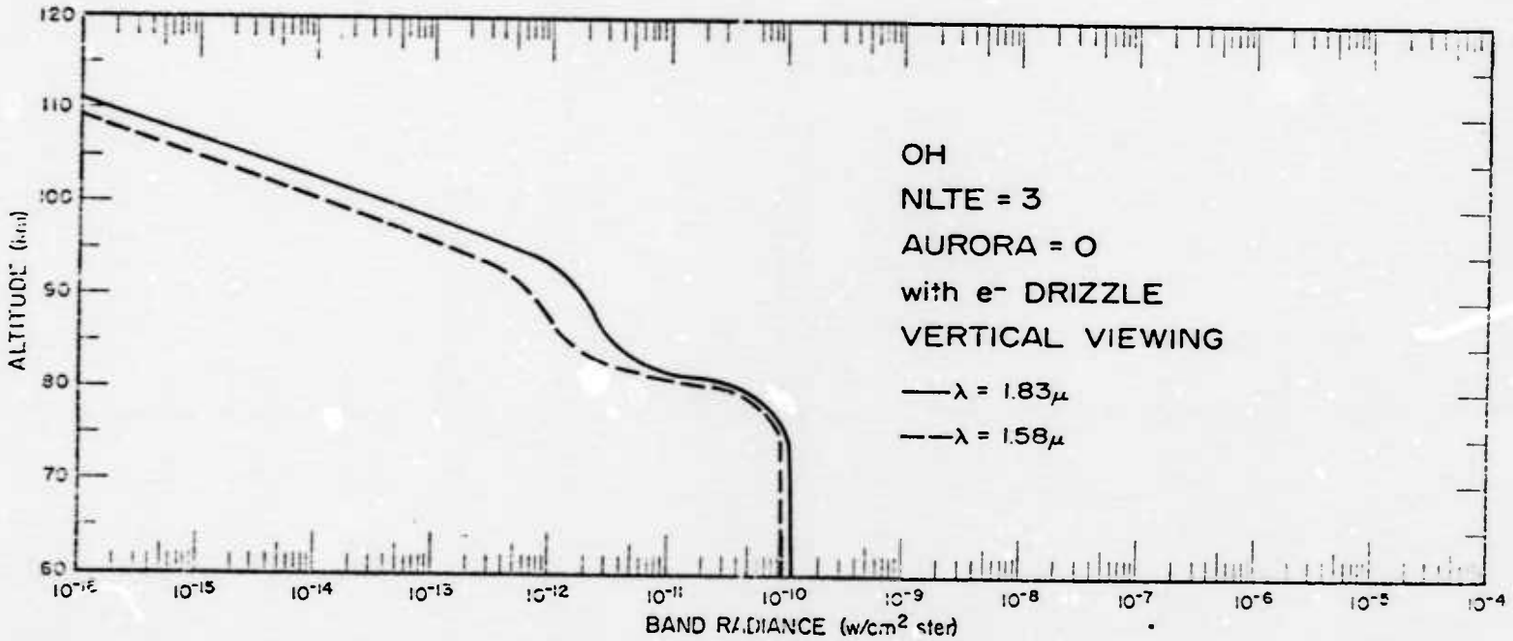

Figure 43. Height profile of the band radiance of 2 bands of OH for the case when an electron drizzle is the only source of ionospheric disturbance.

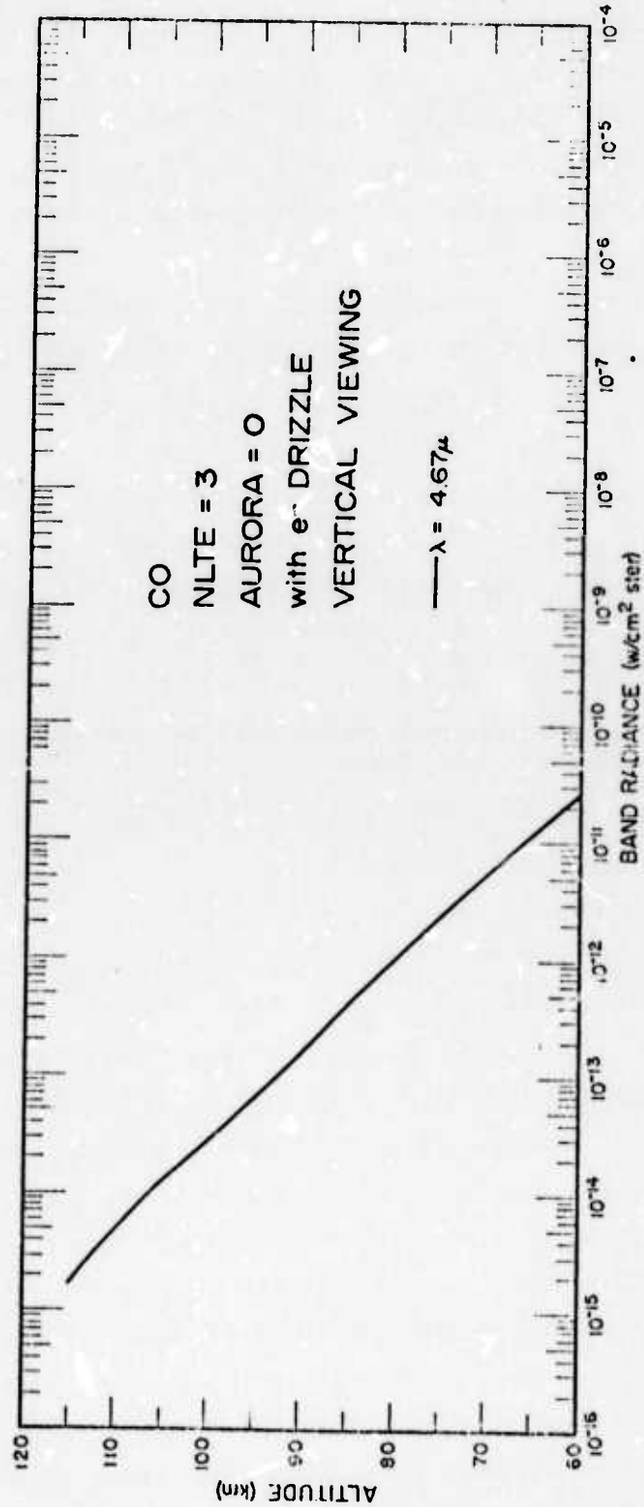

Figure 44. Height profile of the band radiance of CO for the case when an electron drizzle is the only source of ionospheric disturbance.

The radiance from CO_2 is shown in two graphs. Figure 36 indicates that the plot is of the 15 μ bands. This means that all of the bands near 15 μ have summed together and are being plotted as one collective band.

The two plots of NO shown in Figures 38 and 39 are identical plots. The region from 60-150 km is redrawn on an expanded scale to facilitate comparison.

Only two of the $\Delta v = 2$ bands of OH are shown in Figure 43. This is done simply as a means of reducing the total number of bands to be plotted. One could, if desired, include all $\Delta v = 2$ bands as well as the $\Delta v = 1$, etc. This is done in Figure 78.

As a means of determining the effect of the electron drizzle on the radiance of the various bands, let us compare Figures 35 and 40 with Figures 45 and 46. The latter two figures are plots of the predicted radiance of two of the CO_2 bands and the N_2O bands with no aurora, no electric fields, and no electron drizzle. It can be seen that during the electron drizzle both CO_2 bands are somewhat enhanced but that there is only a very slight enhancement of the 4.5 μ band of N_2O. Neither the 7.78 μ band nor the 17.0 μ band of N_2O is enhanced. By referring to the energy level diagrams of Figures 32 and 33, one can see that the cause of the selective enhancement is the near resonant V-V energy exchange with N_2. That is to say, the electron drizzle tends to increase the vibrational energy of N_2 which in turn exchanges part of this energy with selected levels of CO_2 and N_2O. These levels in turn radiate, and having an enhanced population, give rise to an increased radiance.

Next let us see what effect an IBC-II aurora has on the predicted radiance. Figures 47 through 55 are plots of the predicted radiance for the case of an IBC-II aurora five minutes after commencement plus the background electron drizzle but with no electric field. These plots represent the radiance viewing vertically upward. The designation AURORA = 1 simply means that an IBC-II aurora exists. The auroral region was taken to be from 80 km of altitude to 150 km. The integration limits in determining the radiance were taken to be these values. Therefore, it should be pointed out that this represents the total radiance (aurora

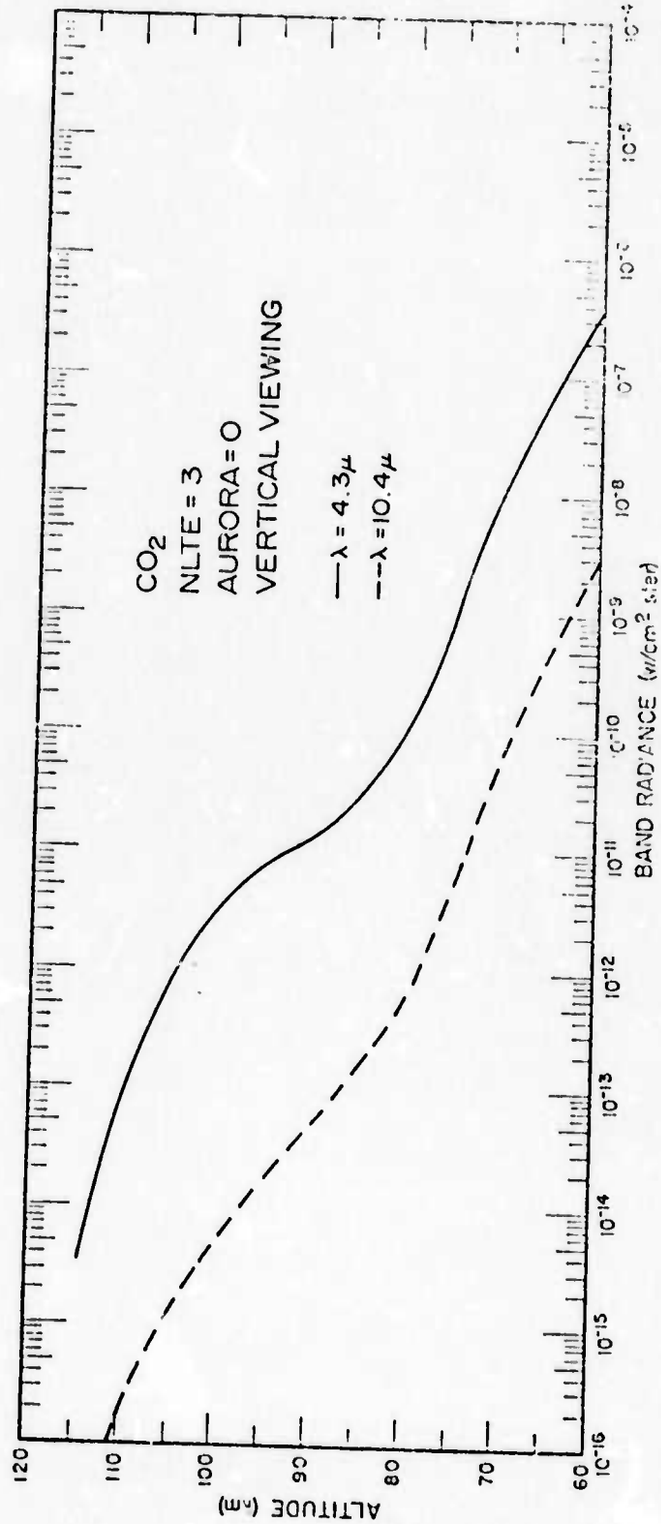

Figure 45. Height profile of the band radiance of CO_2 for the case of *totally quiescent conditions.*

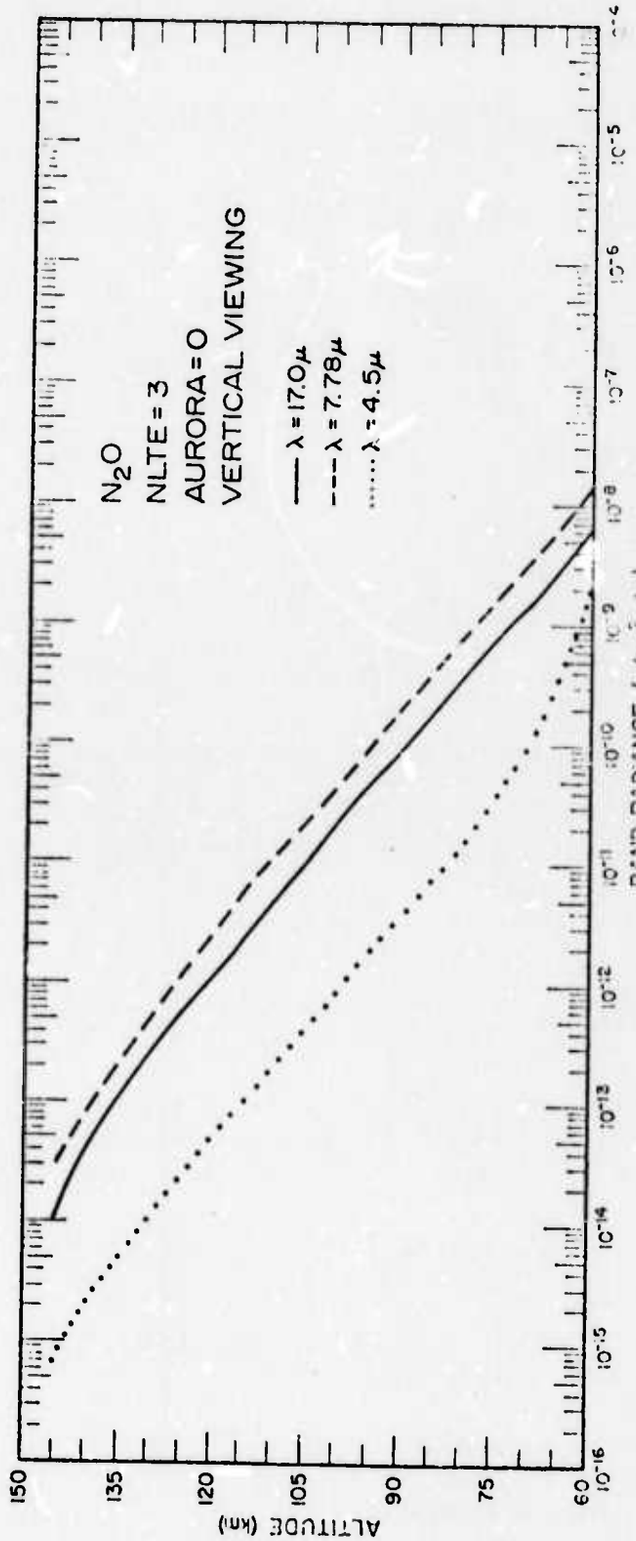

Figure 46. Height profile of the band radiance of N_2O for the case of *totally conditions.*

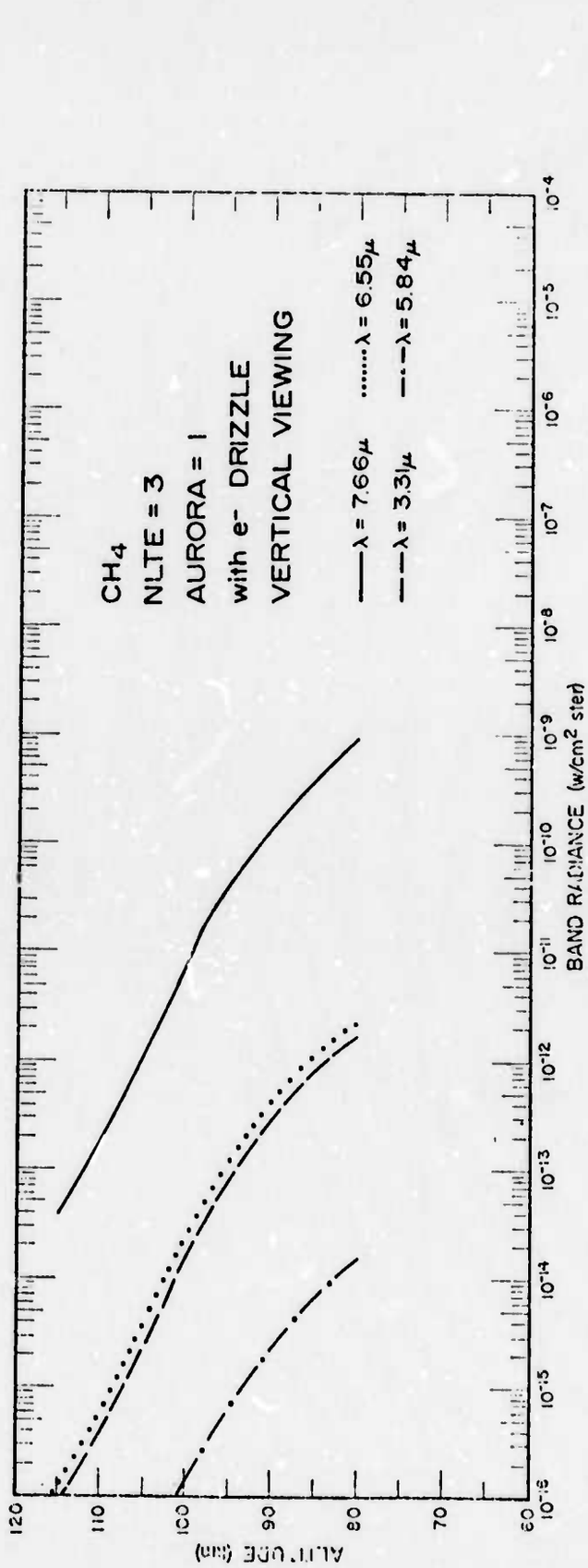

Figure 47. Height profile of the band radiance of CH_4 five minutes after commencement of an IBC-II aurora.

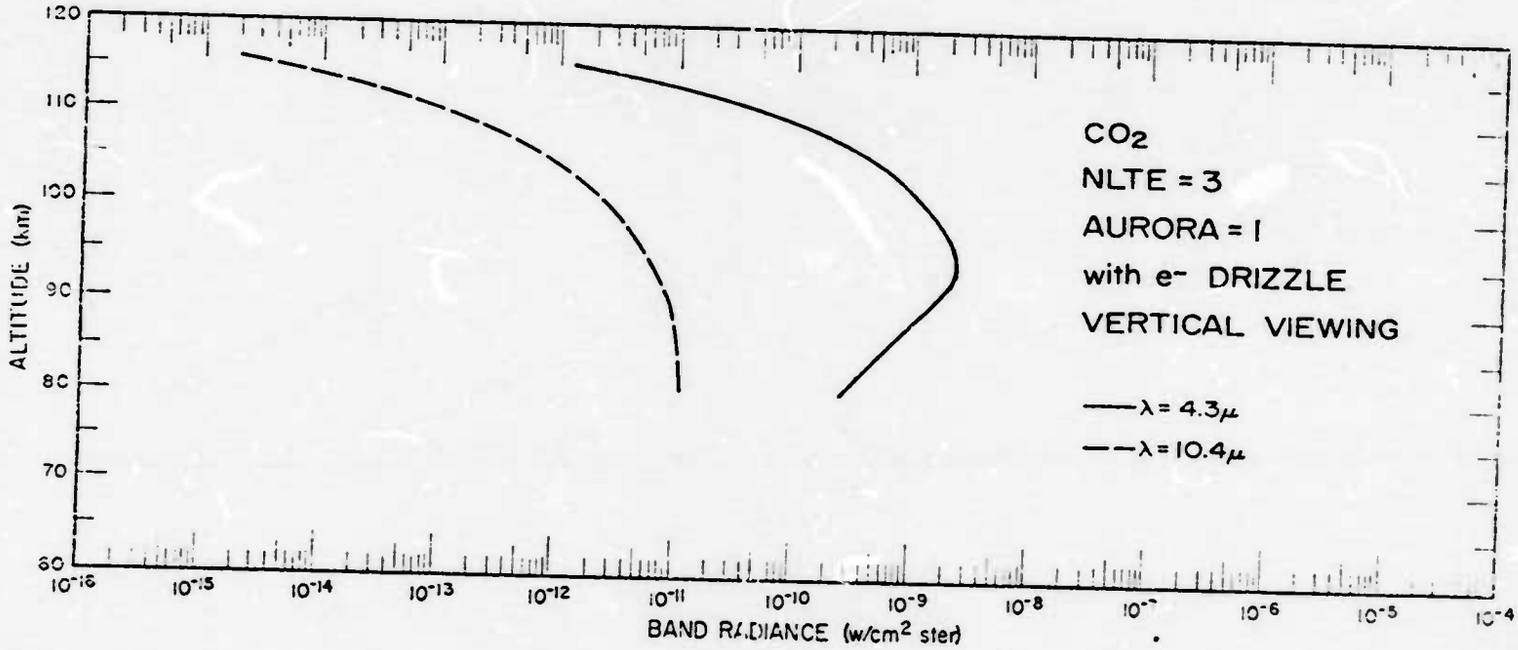

Figure 48. Height profile of the band radiance of CO_2 five minutes after commencement of an IBC-II aurora.

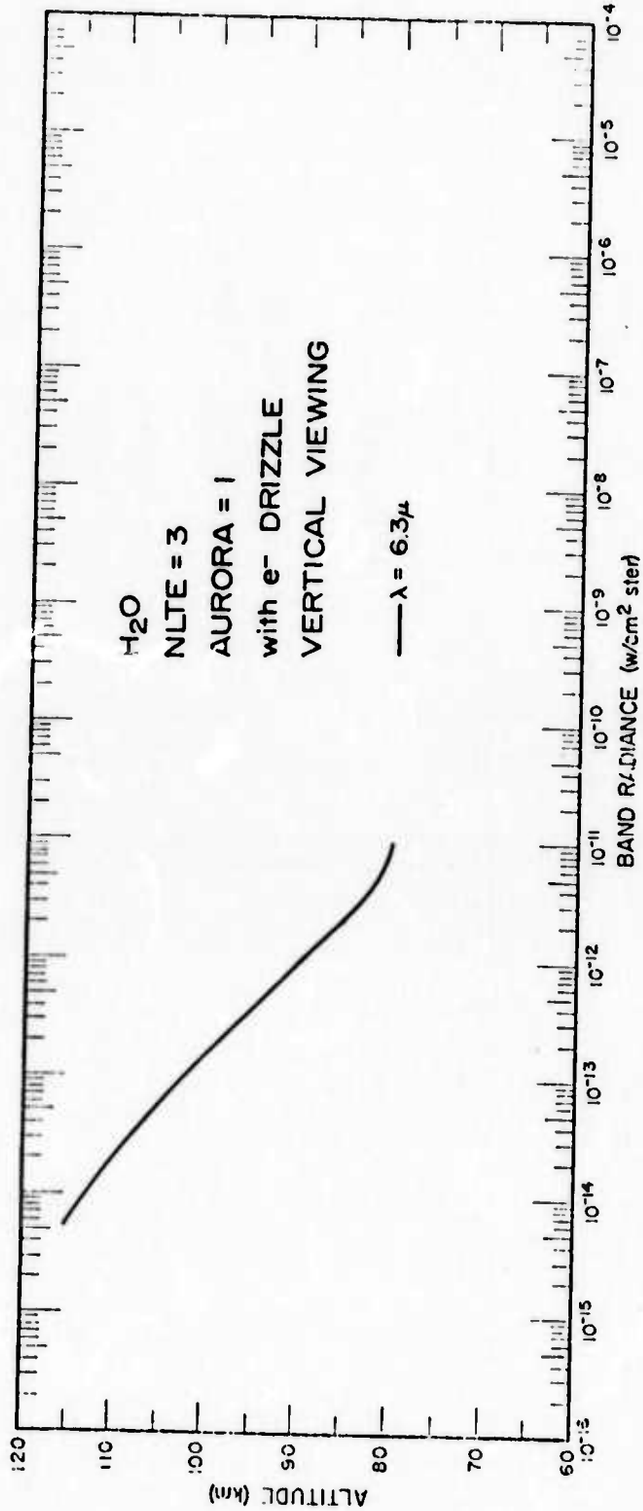

Figure 49. Height profile of the band radiance of H_2O five minutes after commencement of an IBC-II aurora.

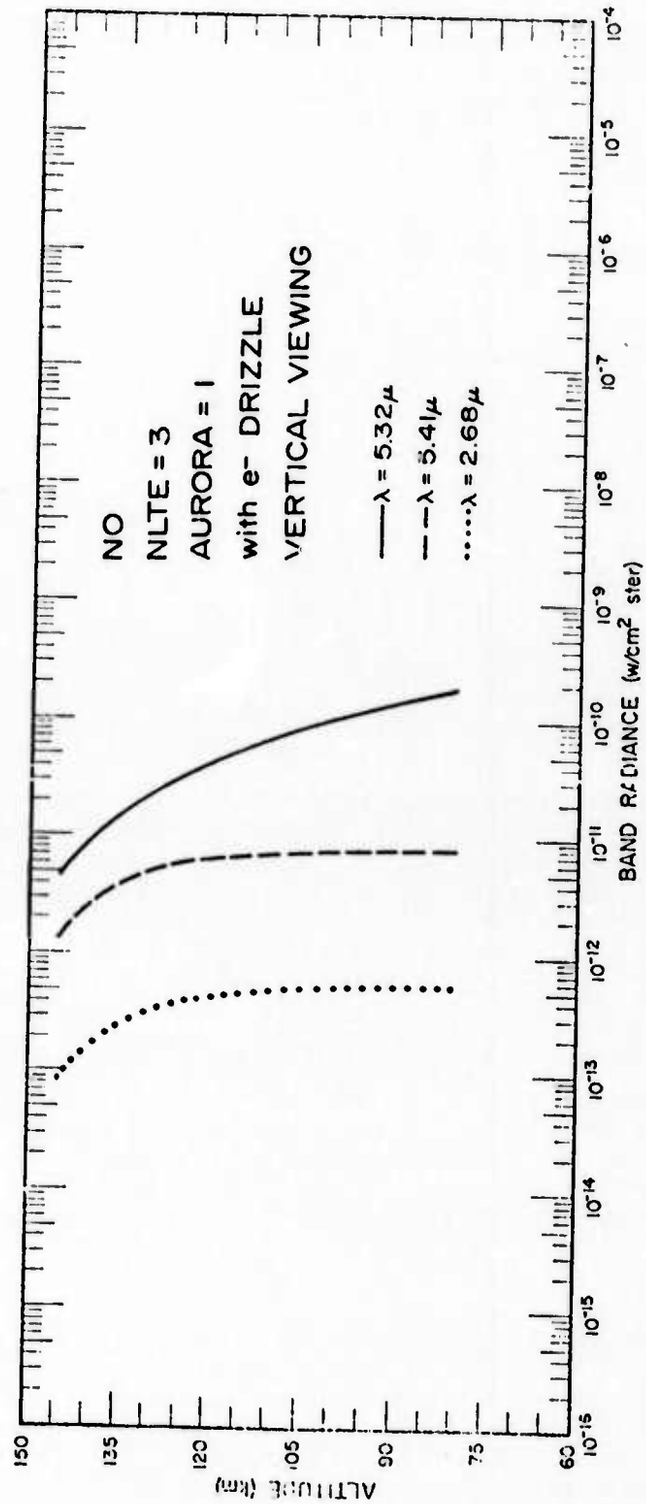

Figure 50. Height profile of the band radiance of NO five minutes after commencement of an IBC-II aurora.

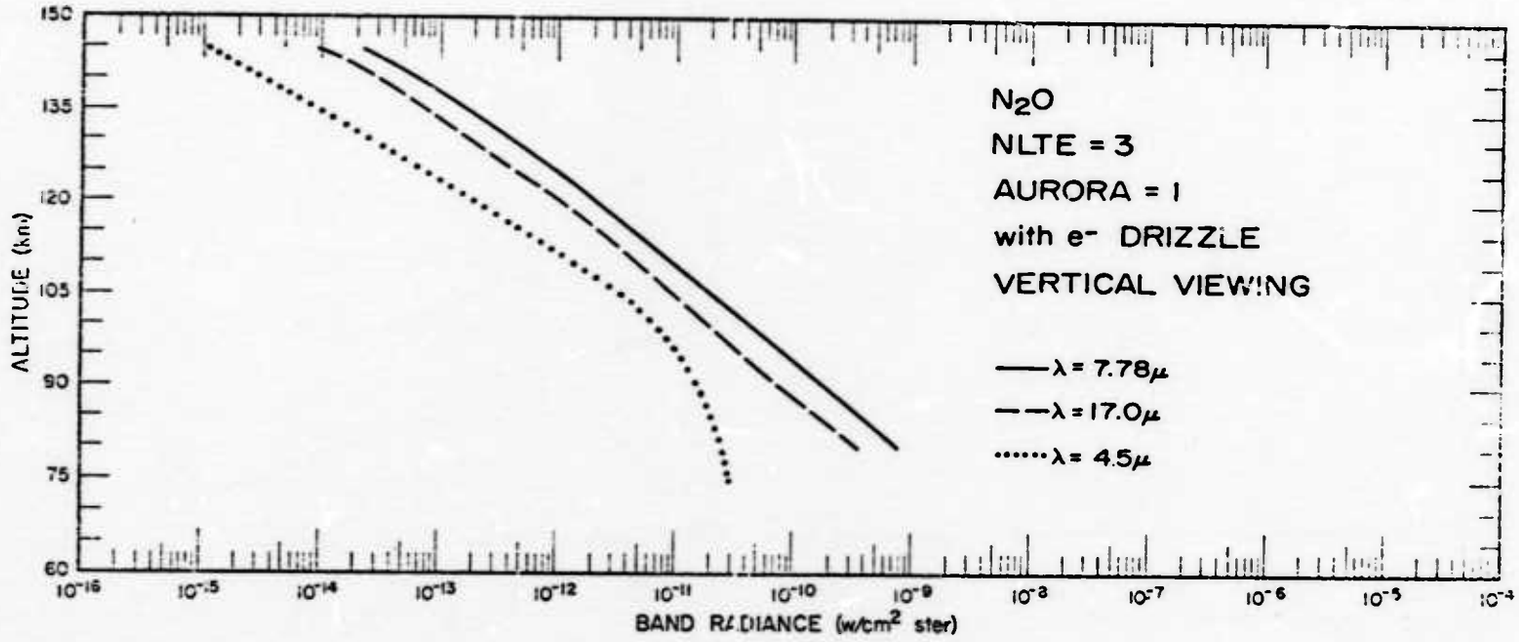

Figure 51. Height profile of the band radiance of N_2O five minutes after commencement of an IBC-II aurora.

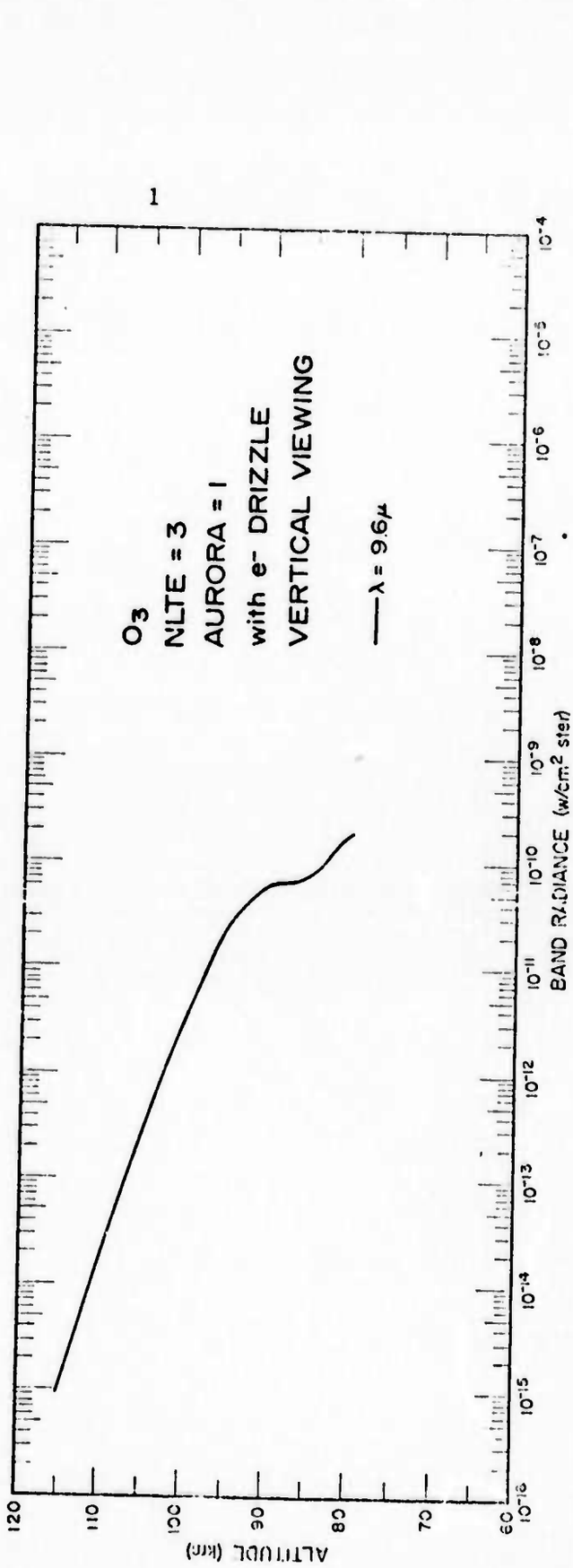

Figure 52. Height profile of the band radiance of O_3 five minutes after commencement of an IBC-II aurora.

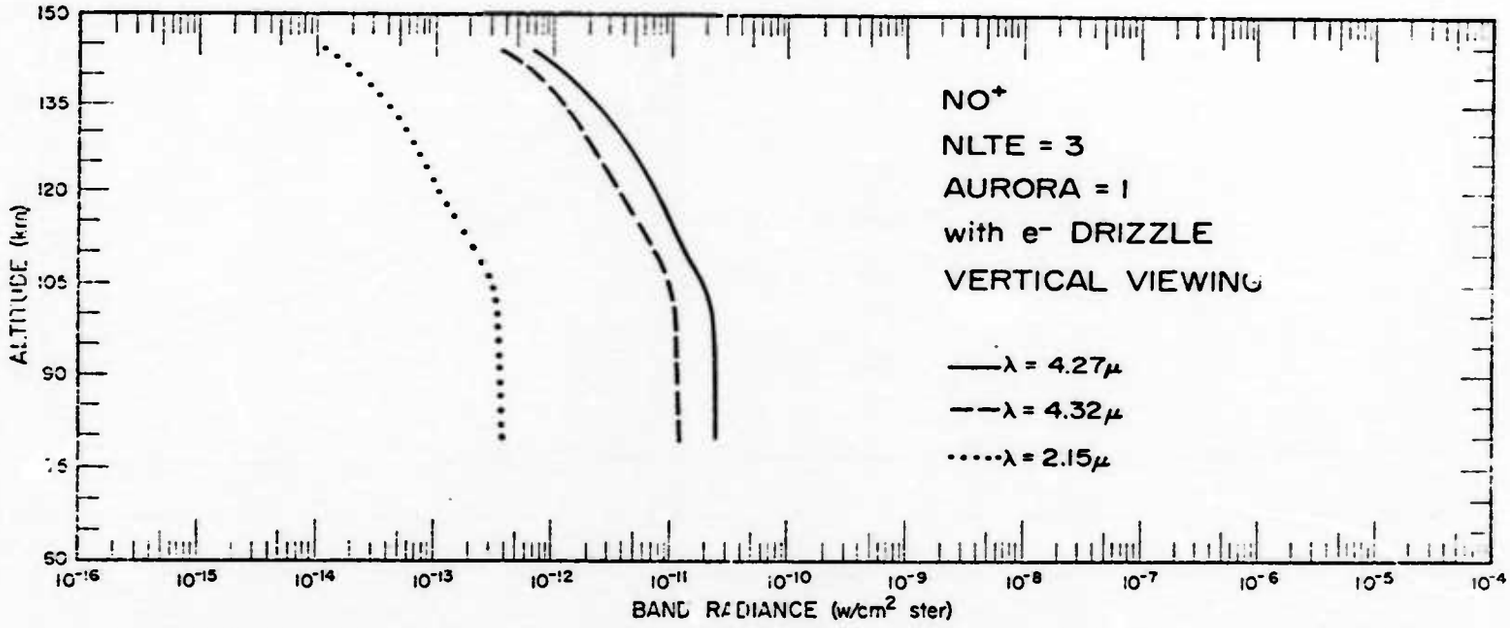

Figure 53. Height profile of the band radiance of NO^+ five minutes after commencement of an IBC-II aurora.

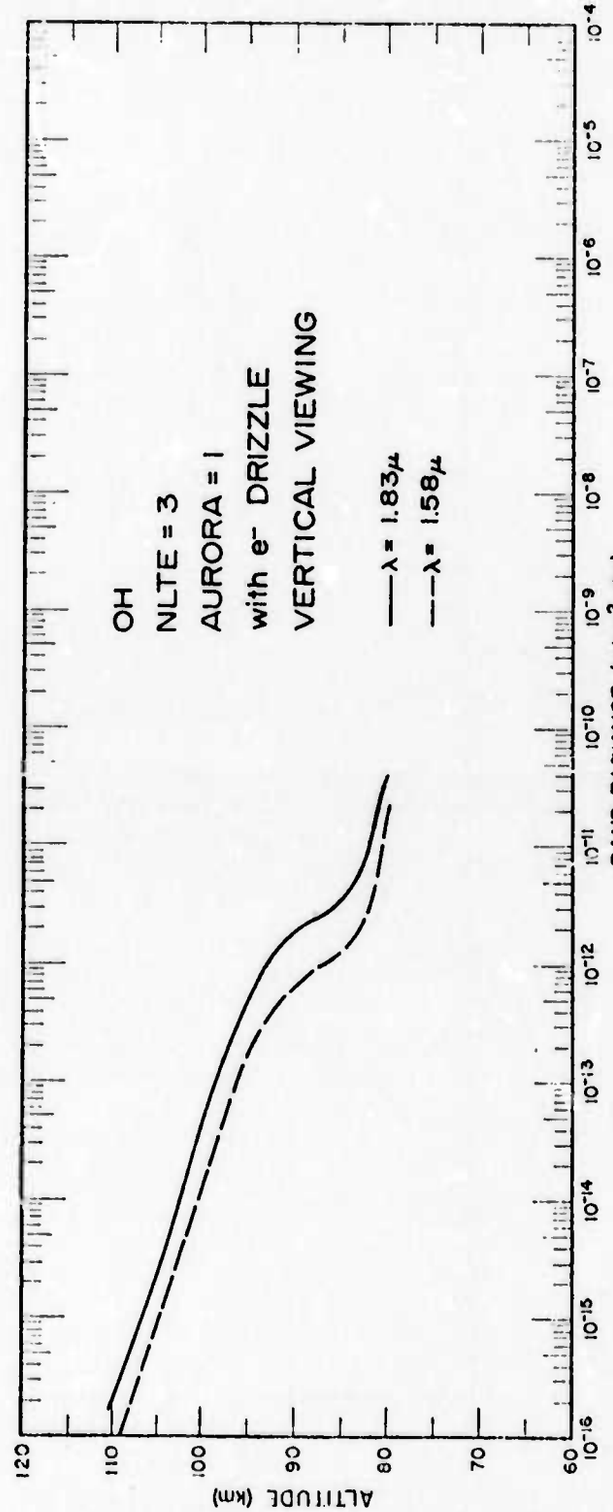

Figure 54. Height profile of the band radiance of two of the bands of OH five minutes after commencement of an IBC-II aurora.

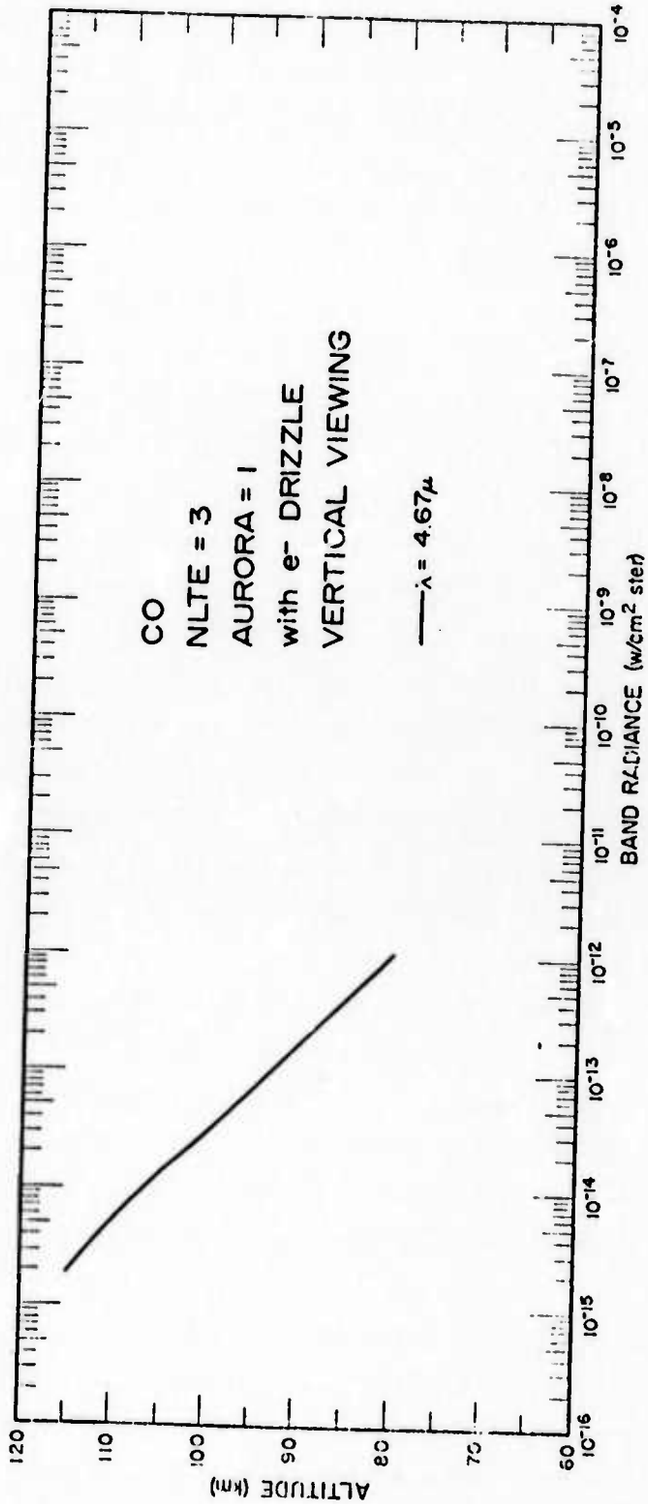

Figure 55. Height profile of the band radiance of CO five minutes after commencement of an IBC-II aurora.

+ background) for every case except NO. The reason for NO being an exception is that it is the only infrared active gas with significant number densities at altitudes greater than 150 km. Hence, in the case of NO the radiance plotted in Figure 50 represents only the auroral contribution; i.e., the background contribution from molecules at altitudes greater than 150 km is not included.

It can be seen that the aurorally enhanced bands include CO_2 at 4.3 μ, 10.4 μ (and some of the 15 μ band group), NO at 5.32 μ, N_2O at 4.5 μ, and all of the NO^+ bands. The molecule CO has a near resonant V-V exchange with N_2 but the number densities of this gas at auroral altitudes is not sufficient to cause significant auroral enhancement. Of the remaining gases, CH_4, H_2O, and O_3 have a near resonant V-V exchange with O_2 rather than N_2, and OH has no near resonant V-V exchange with either of these molecules. The much smaller cross sections for an electron-O_2 collision (as compared with N_2) make the auroral enhancement of the latter gases insignificant.

Next let us increase the auroral activity to that of an IBC-III aurora (AURORA = 3) and compare the predicted radiance with previous results. Figures 56 through 65 show the predicted radiance of an IBC-III aurora five minutes after commencement with the background electron drizzle but with no electric fields. As before, the NLTE = 3 designation means nighttime NLTE conditions. Again, one may note that there is a further enhancement of CO_2 bands, the NO band at 5.32 μ, the N_2O band at 4.5 μ, and all of the NO^+ bands.

For the next case let us go back to quiescent conditions but add an electric field. Figures 66 through 74 show the predicted radiance when no aurora or electron drizzle is occurring but where an electric field of 0.1 volts/meter is present. The electric field, as described in a previous section. leads to a vibrational excitation of both N_2 and O_2. Again the near resonant V-V exchange process becomes important and leads to an enhancement of various bands. In the case of an electric field as the disturbing element, the $O_2(v=1)$ level is more heavily populated leading to some enhancement of CH_4 at 6.55 μ, H_2O, and O_3 in addition to the enhancement of CO_2, NO, N_2O, and NO^+ as before. One

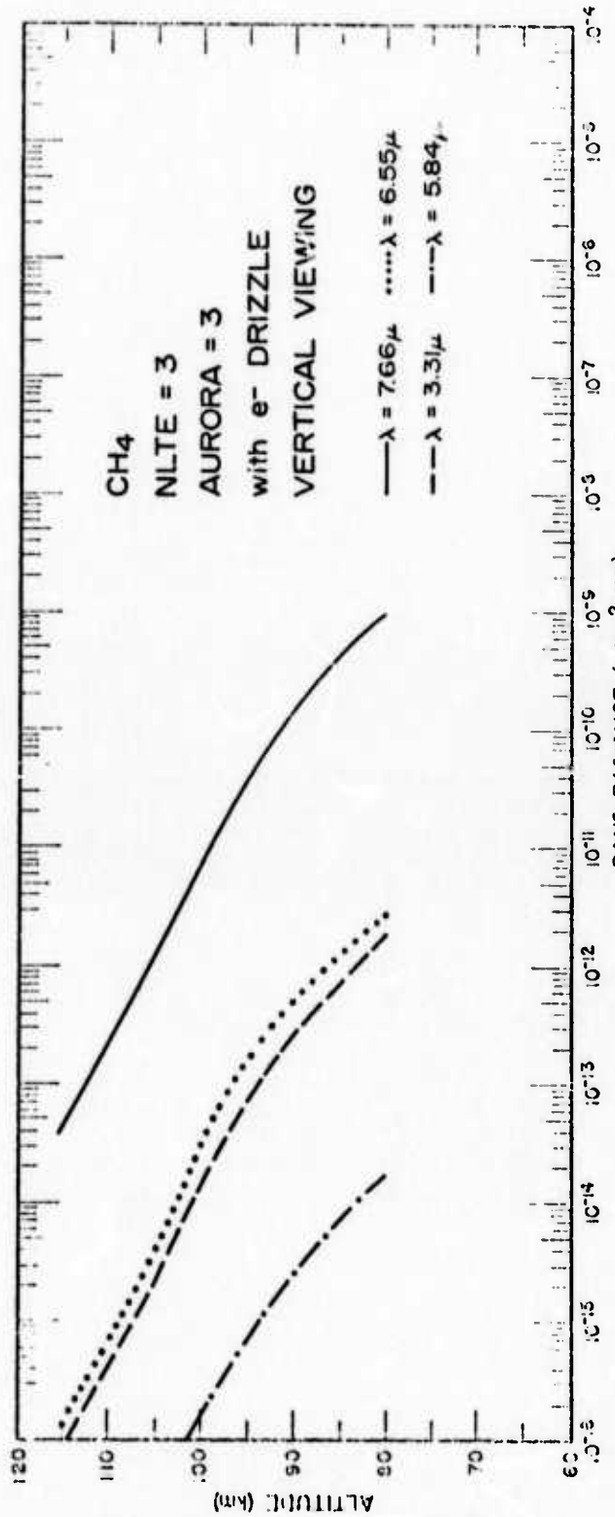

Figure 56. Height profile of the band radiance of CH_4 five minutes after commencement of an IBC-III aurora.

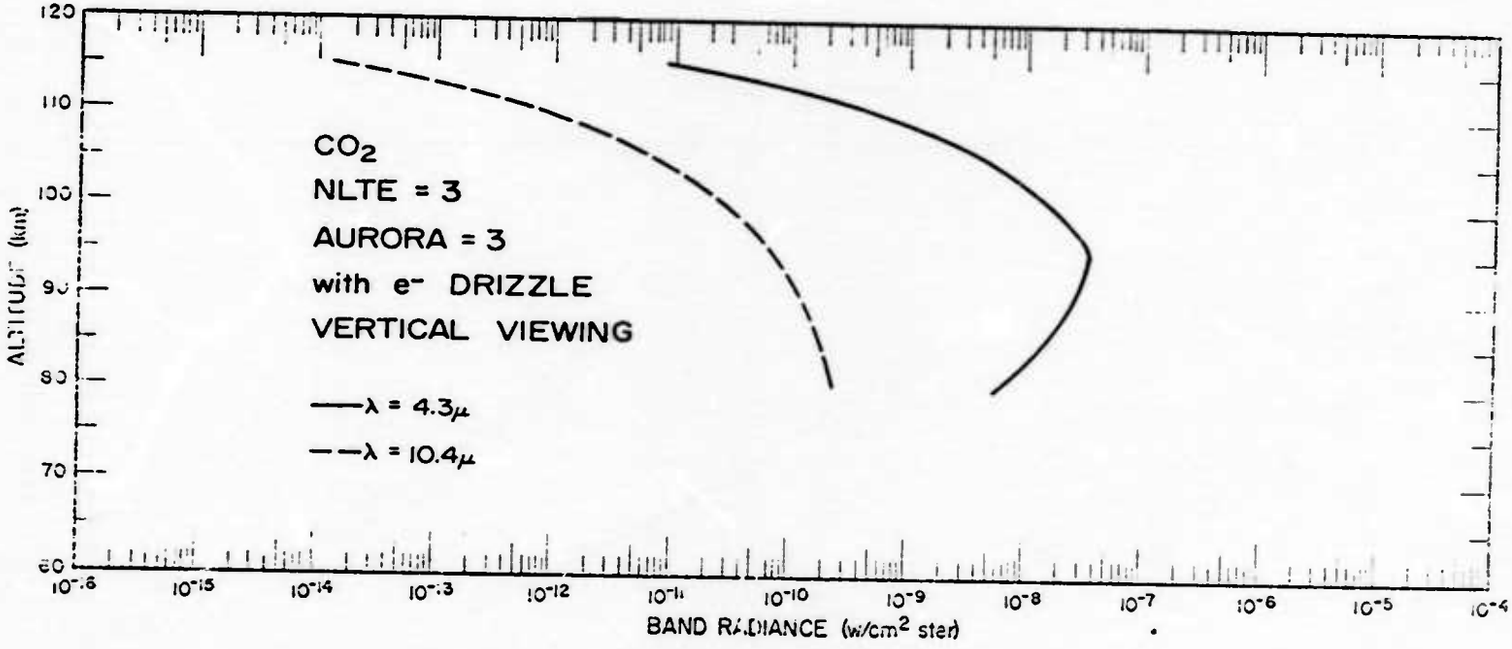

Figure 57. Height profile of the band radiance of CO_2 five minutes after commencement of an IBC-III aurora.

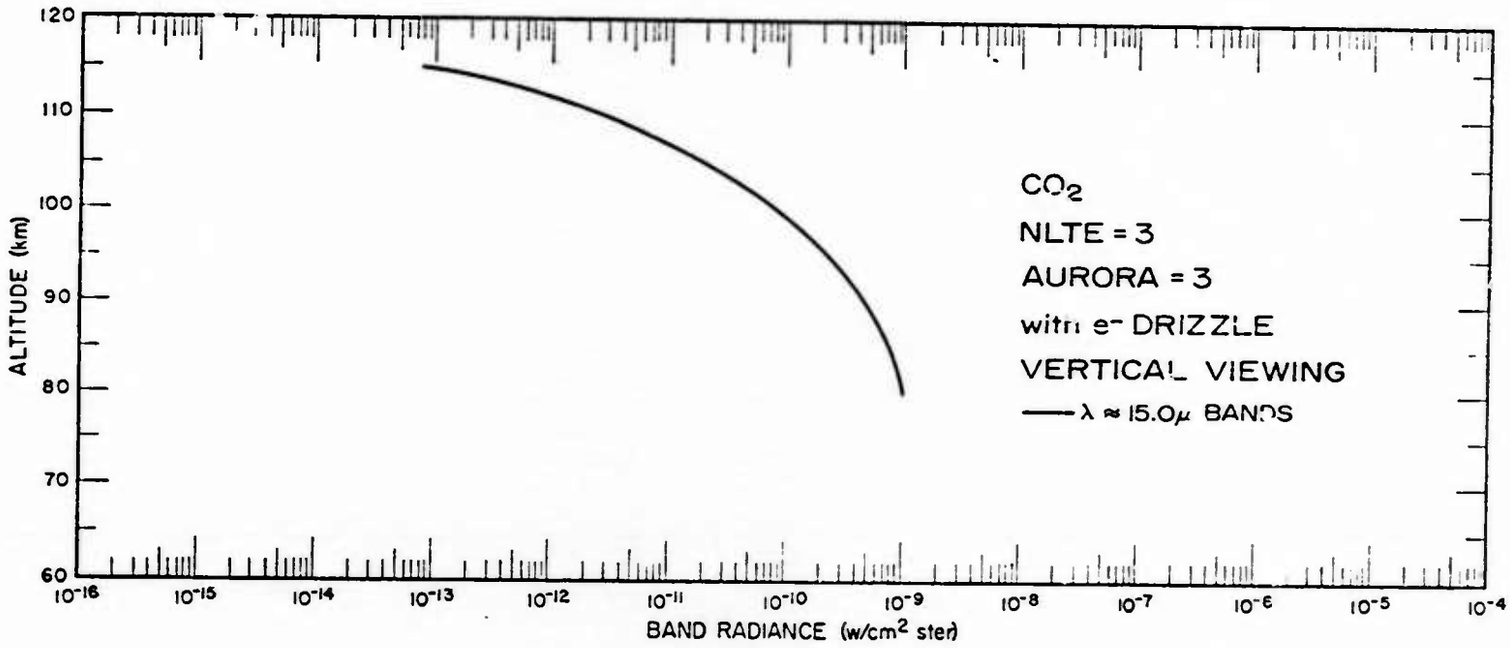

Figure 58. Height profile of the band radiance of all the 15 μ bands of CO_2 five minutes after commencement of an IBC-III aurora.

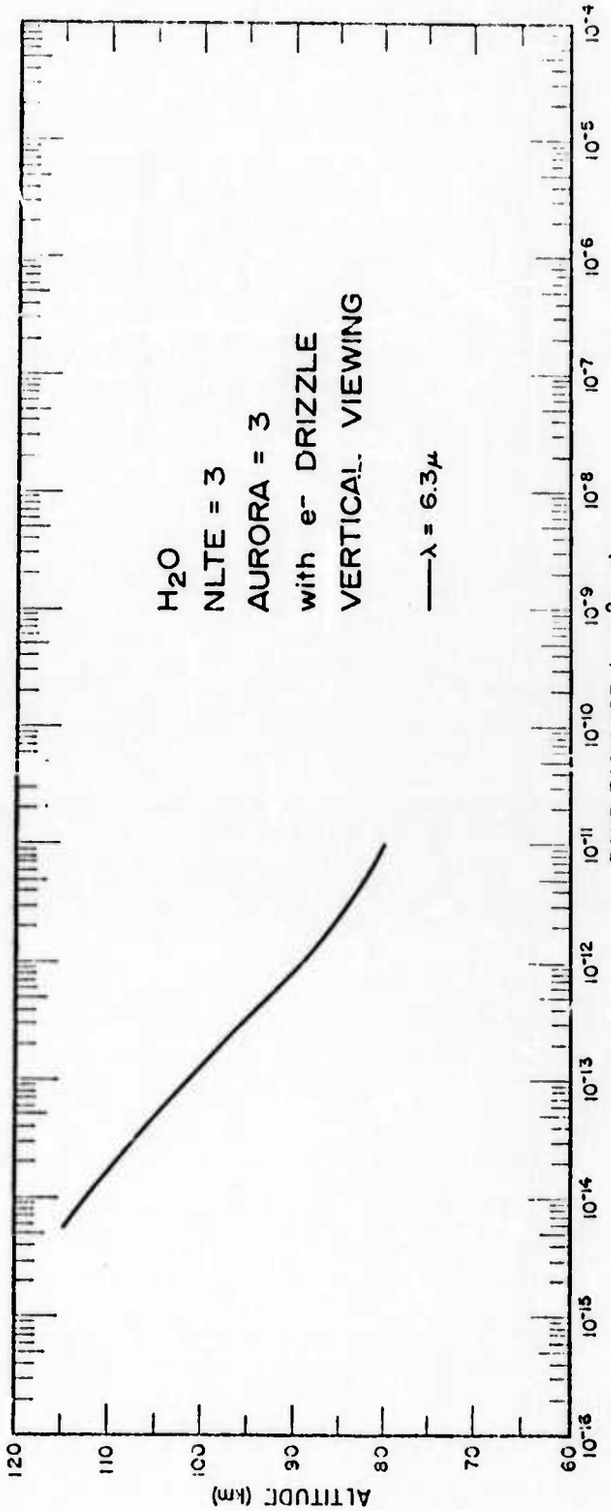

Figure 59. Height profile of the band radiance of H_2O five minutes after commencement of an IBC-II aurora.

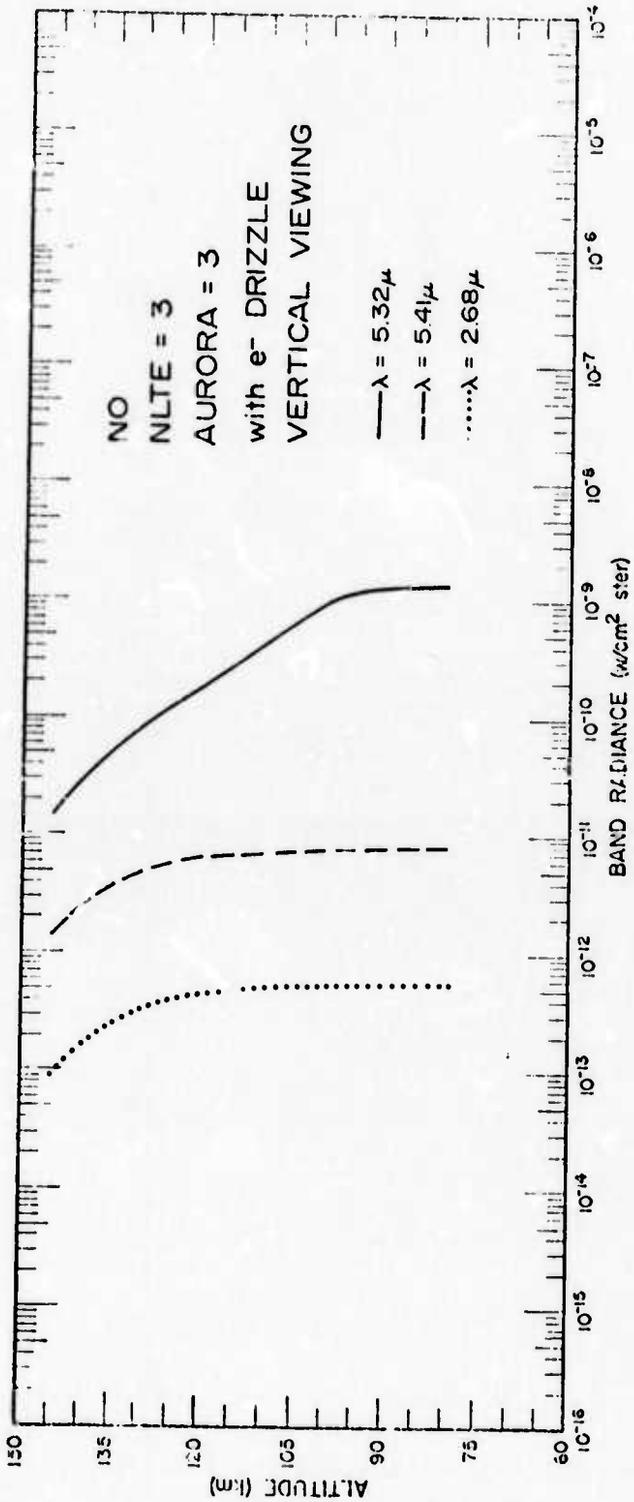

Figure 60. Height profile of the band radiance of NO five minutes after commencement of an IBC-III aurora.

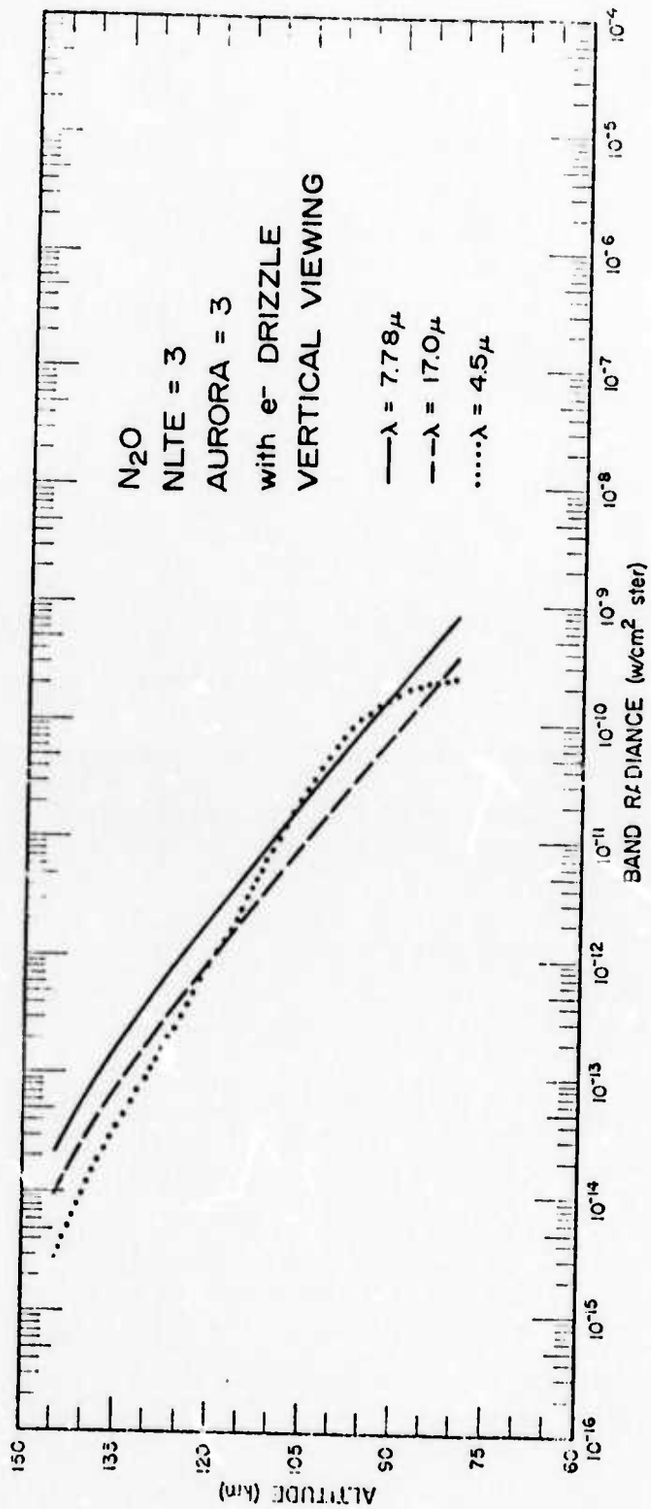

Figure 61. Height profile of the band radiance of N_2O five minutes after commencement of an IBC-III aurora.

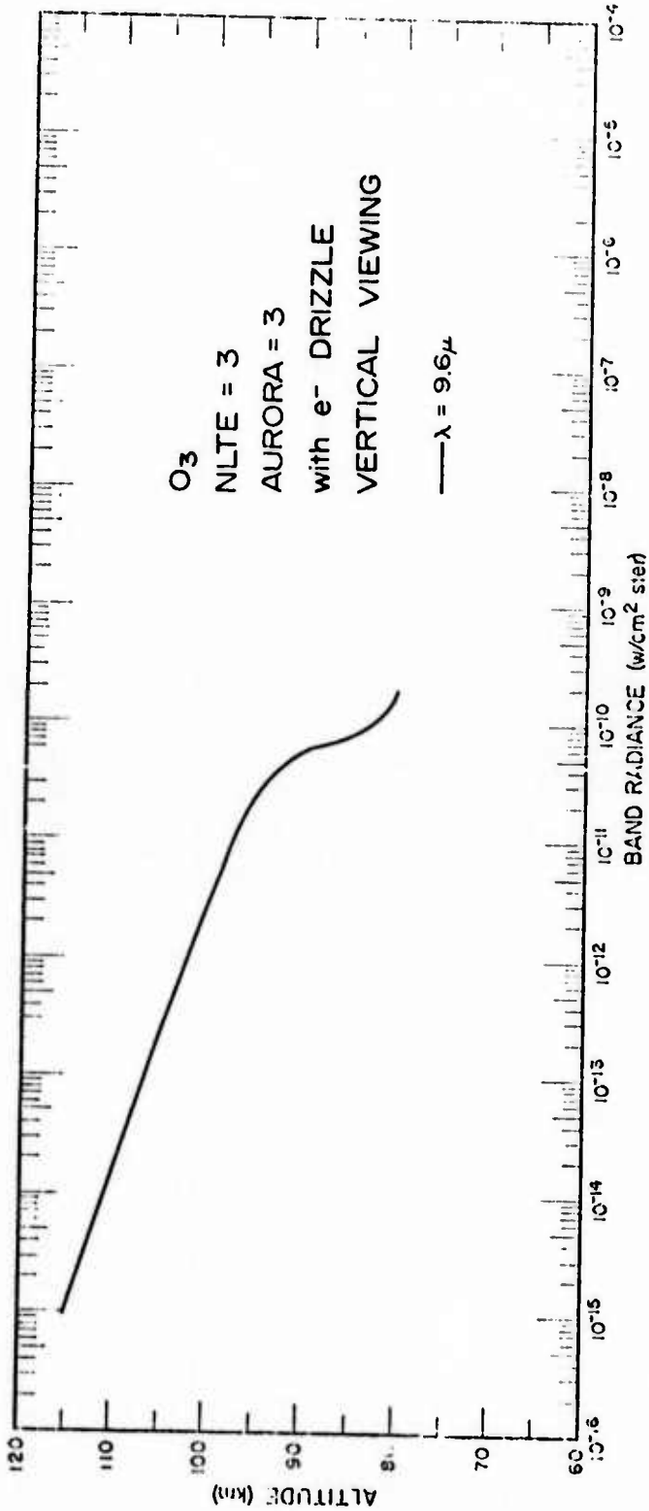

Figure 62. Height profile of the band radiance of O_3 five minutes after commencement of an IBC-III aurora.

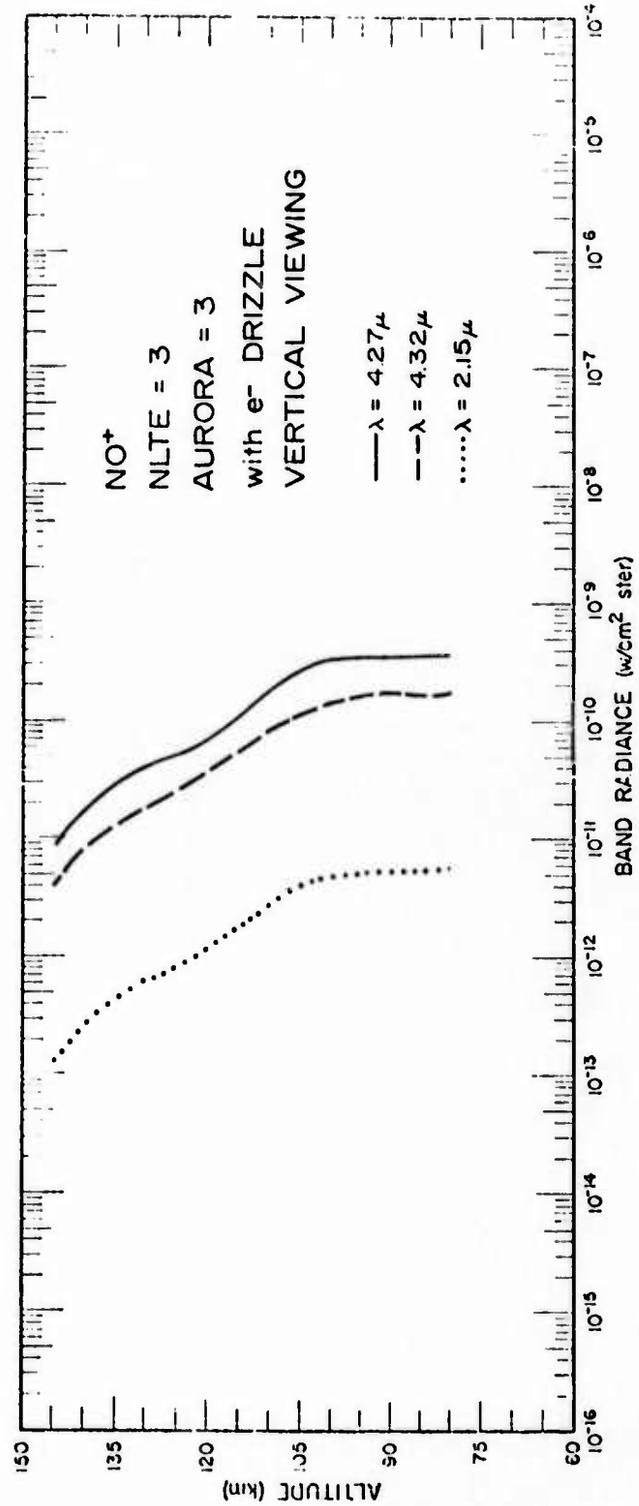

Figure 63. Height profile of the band radiance of NO^+ five minutes after commencement of an IBC-III aurora.

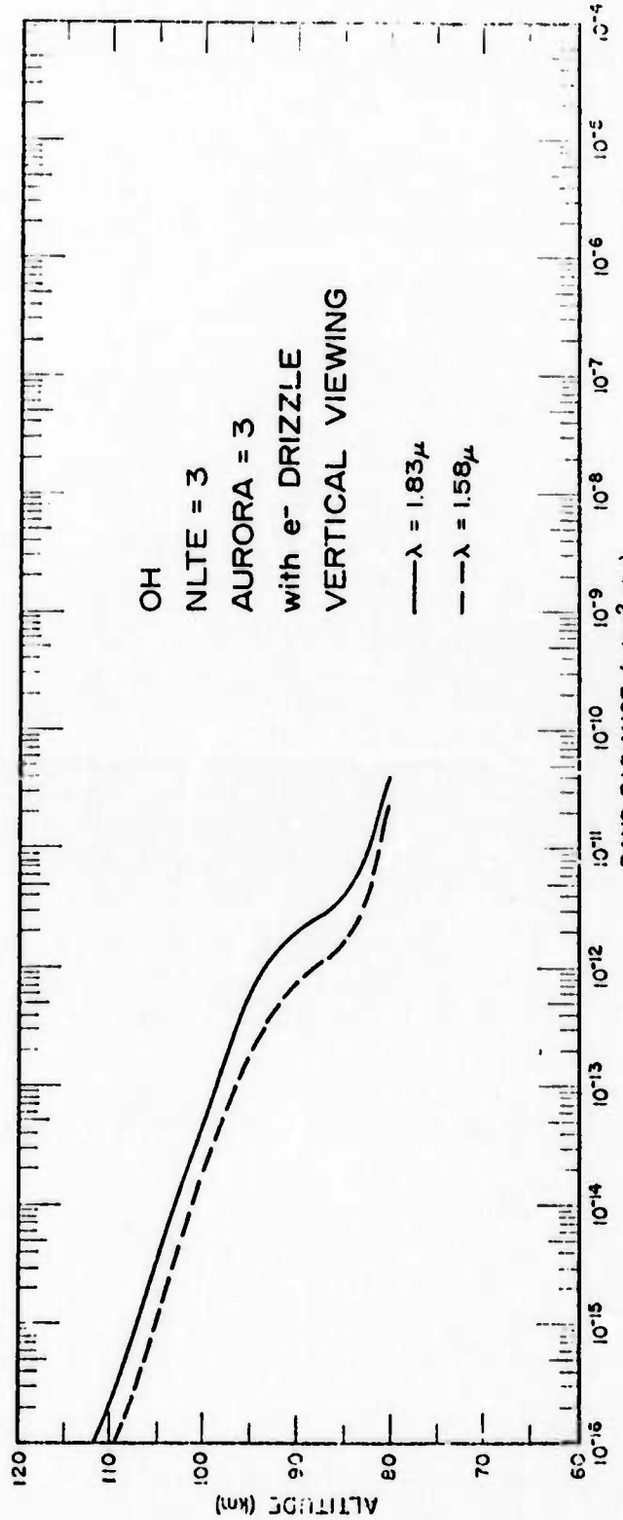

Figure 64. Height profile of the band radiance of two of the bands of OH five mintues after commencement of an IBC-III aurora.

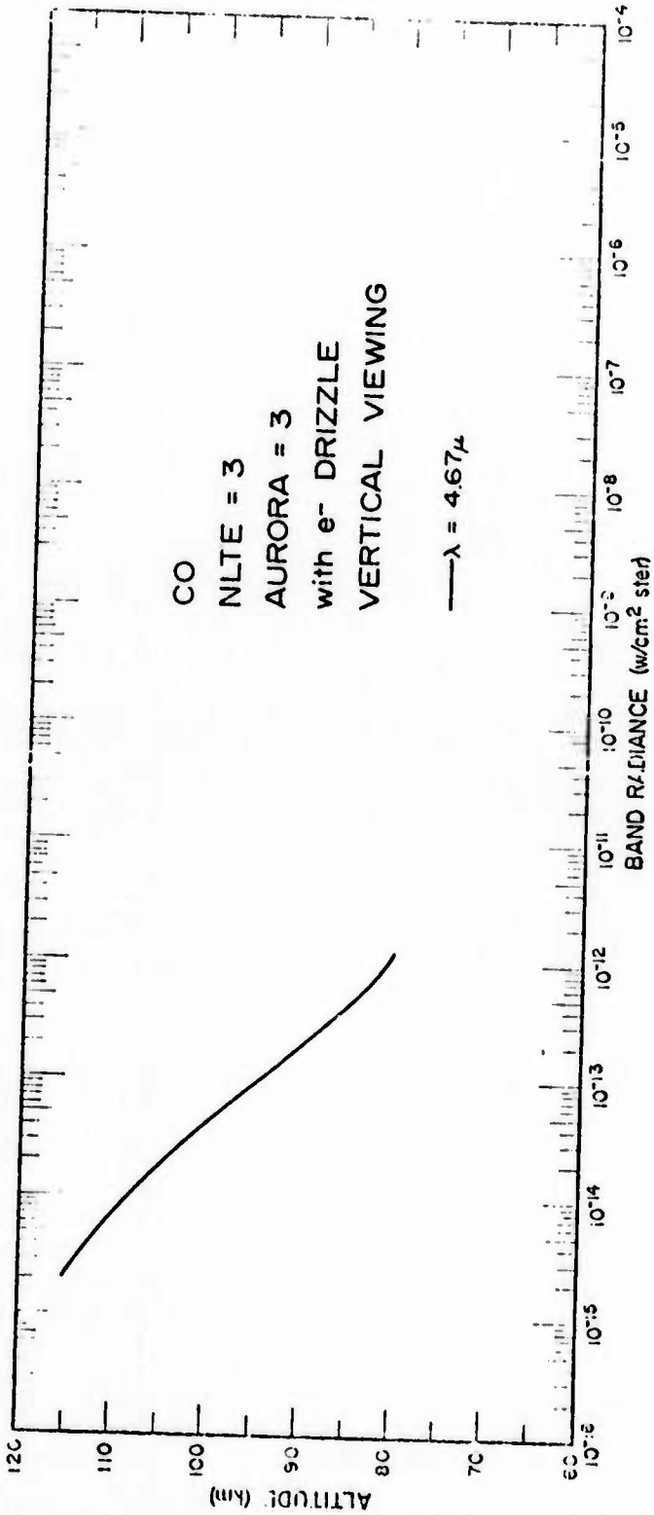

Figure 65. Height profile of the band radiance of CO five minutes after commencement of an IBC-III aurora.

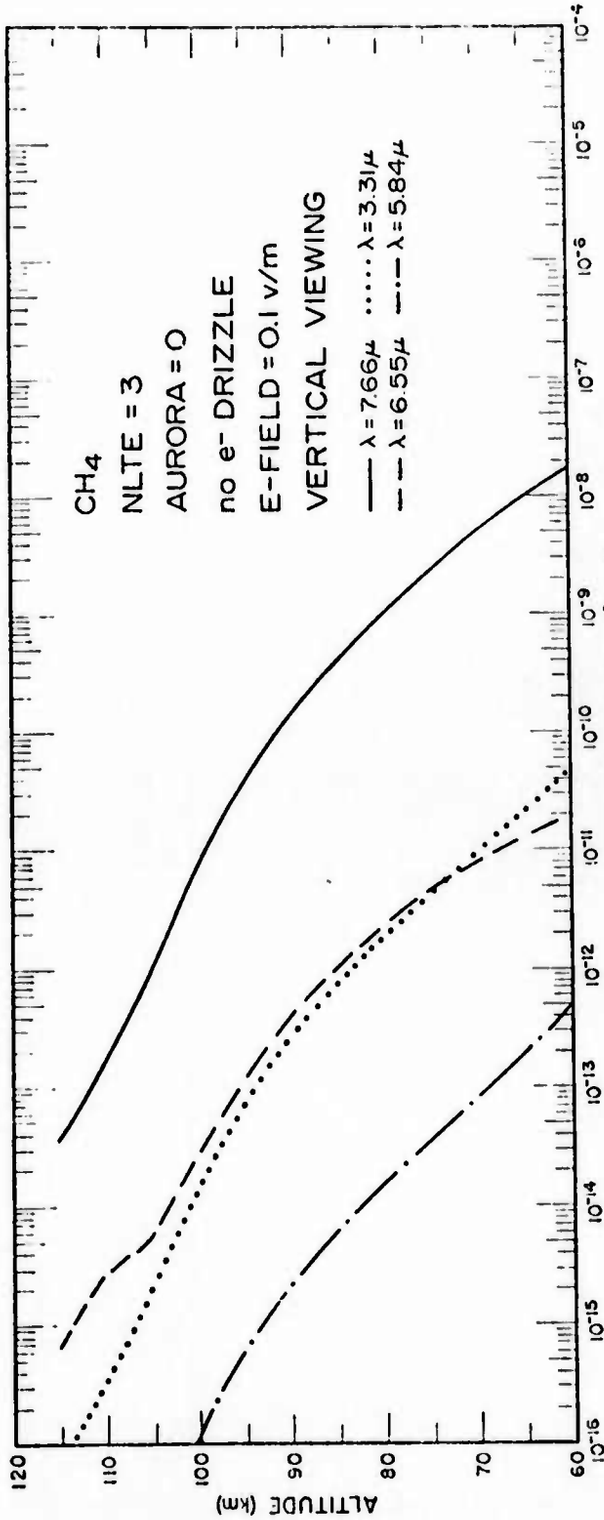

Figure 66. Height profile of the band radiance of CH_4 for the case when the only source of ionospheric disturbance is an electric field of 0.1 v/m.

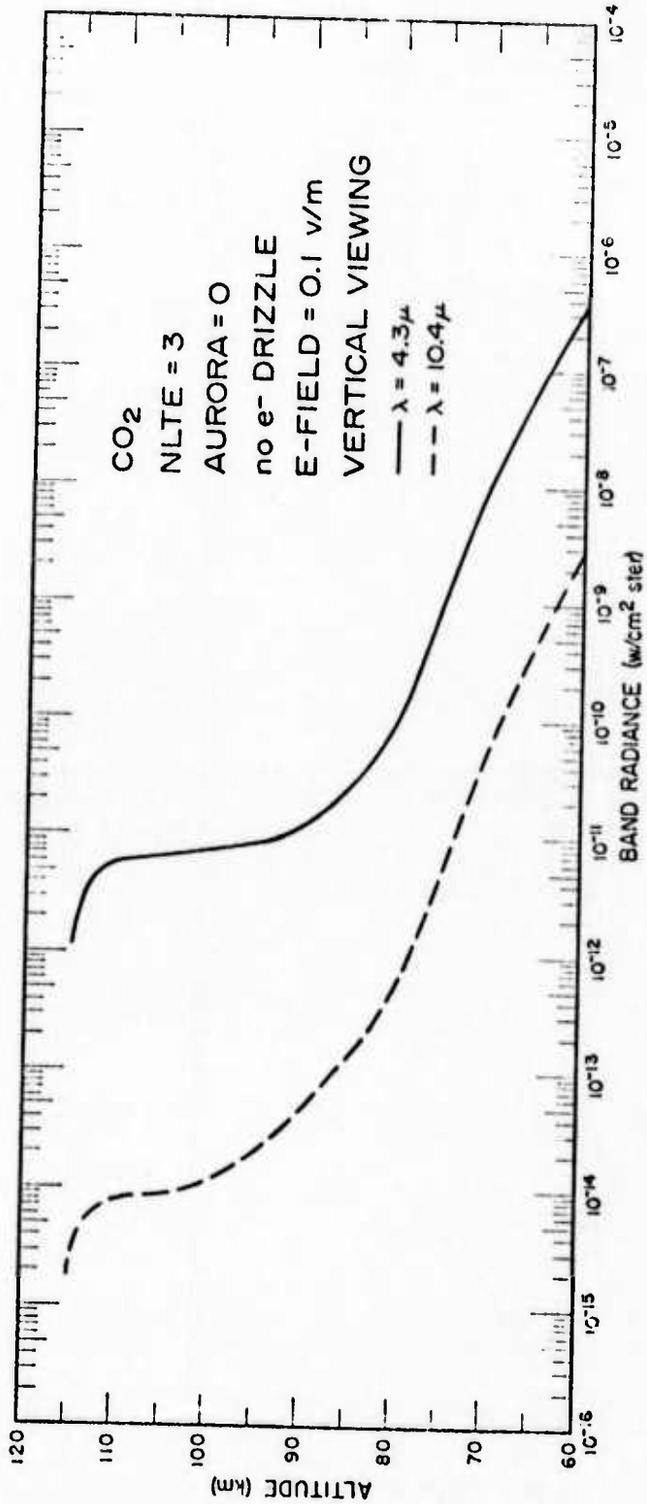

Figure 67. Height profile of the band radiance of CO_2 for the case when the only source of ionospheric disturbance is an electric field of 0.1 v/m.

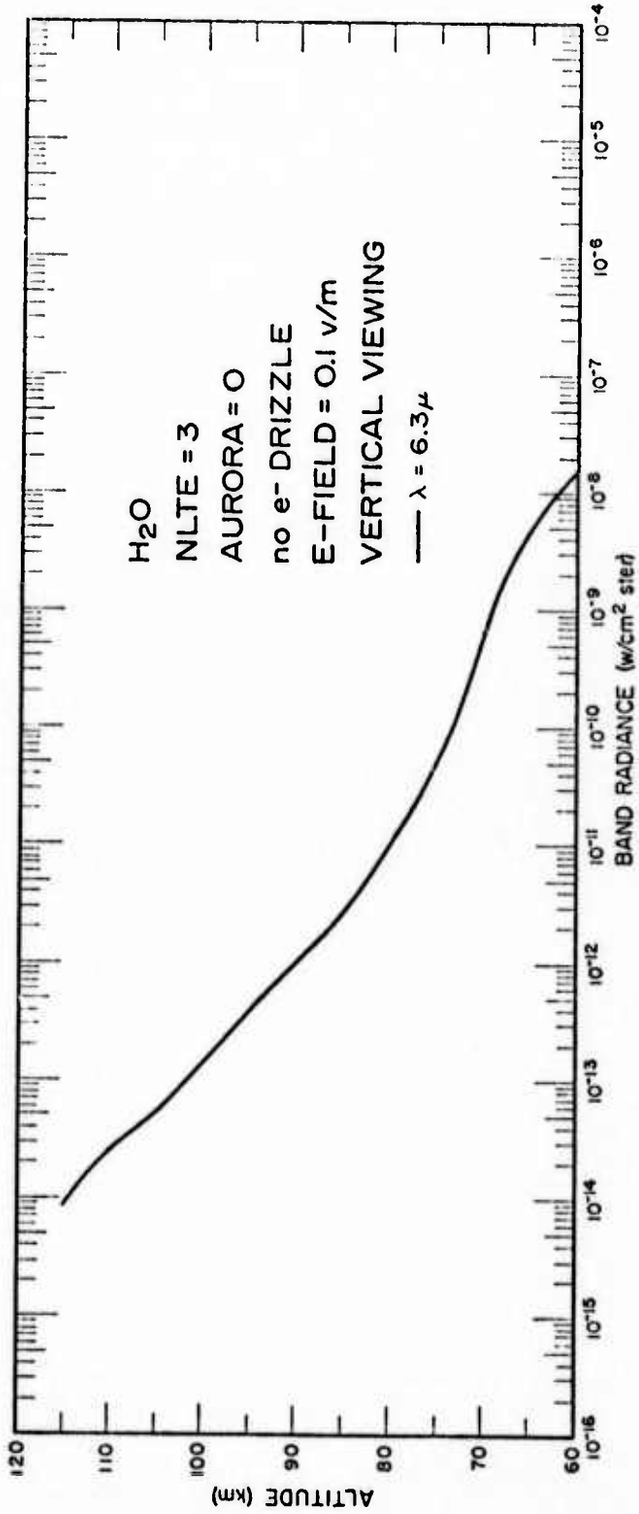

Figure 68. Height profile of the band radiance of H_2O for the case when the only source of ionospheric disturbance is an electric field of 0.1 v/m.

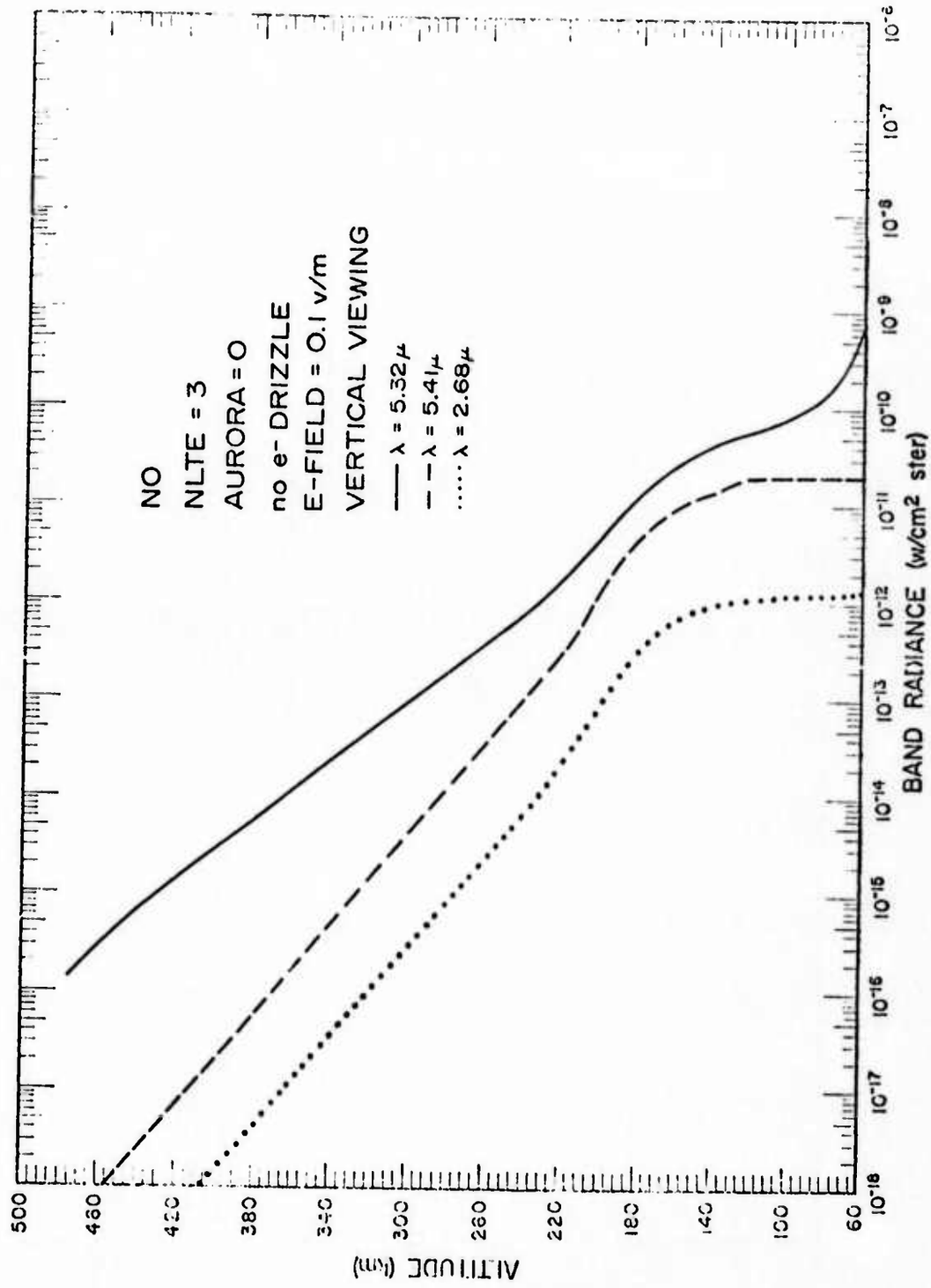

Figure 69. Height profile of the band radiance of NO for the case when the only source of ionospheric disturbance is an electric field of 0.1 v/m.

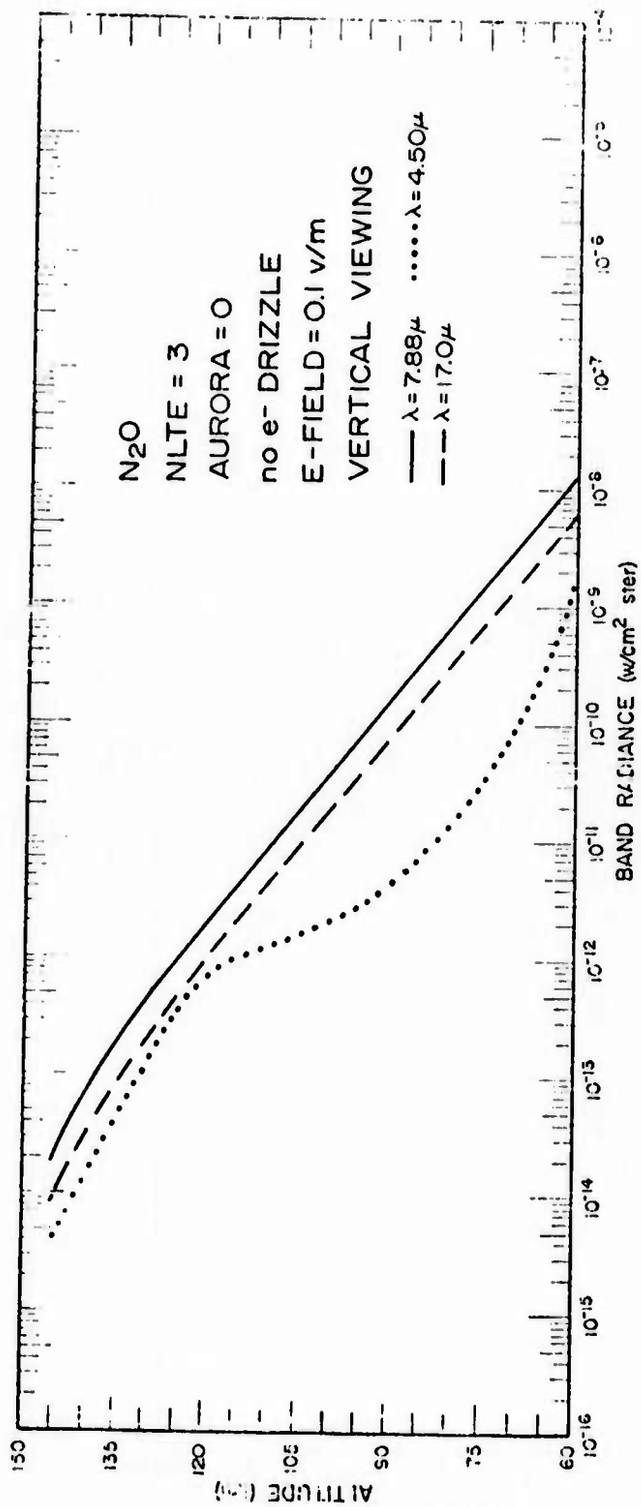

Figure 70. Height profile of the band radiance of N_2O for the case when the only source of ionospheric disturbance is an electric field of 0.1 v/m.

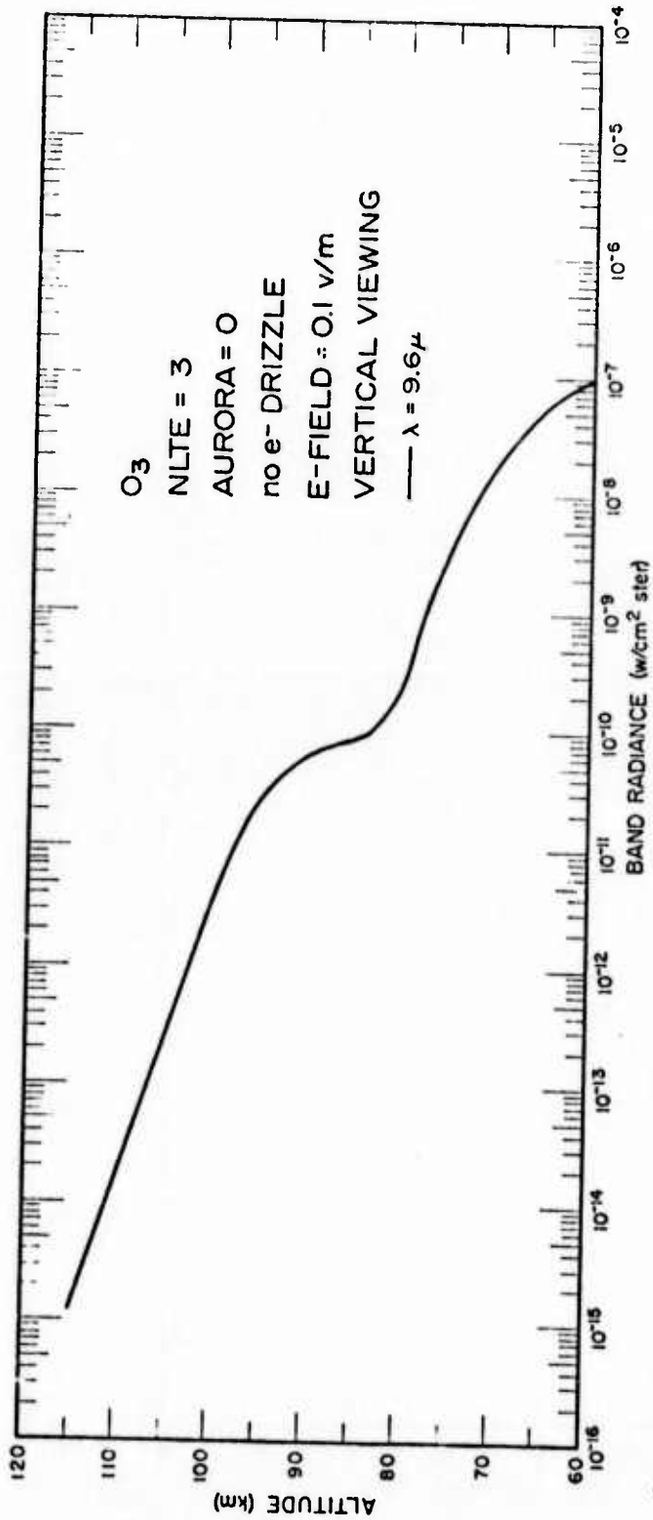

Figure 71. Height profile of the band radiance of O_3 for the case when the only source of ionospheric disturbance is an electric field of 0.1 v/m.

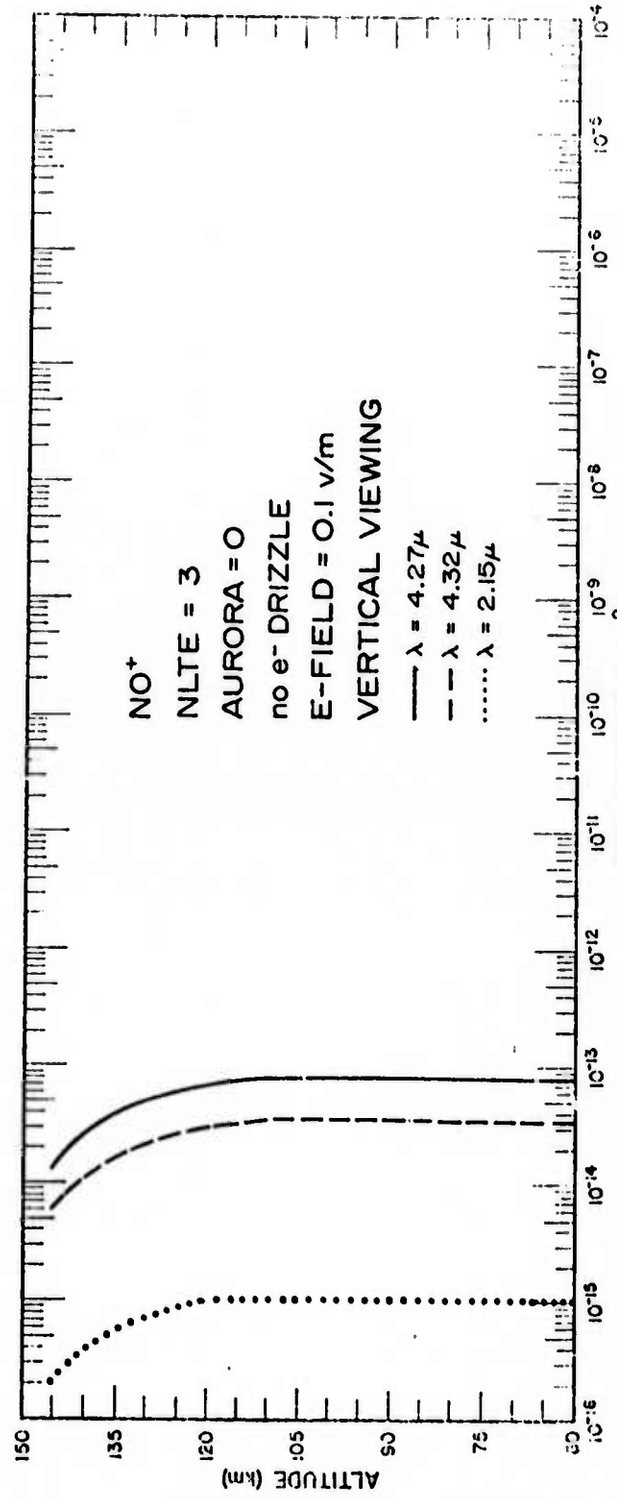

Figure 72. Height profile of the band radiance of NO^+ for the case when the only source of ionospheric disturbance is an electric field of .0.1 v/m.

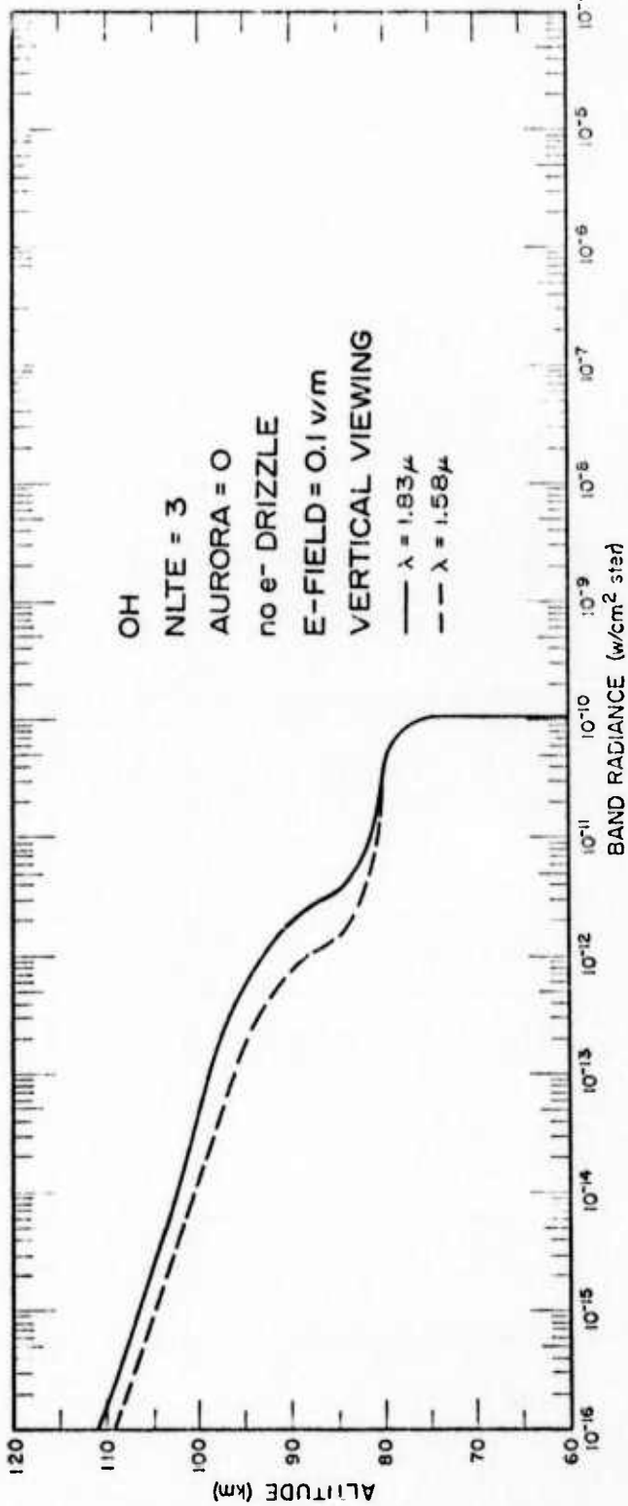

Figure 73. Height profile of the band radiance of two of the bands of OH for the case when the only source of ionospheric disturbance is an electric field of 0.1 v/m.

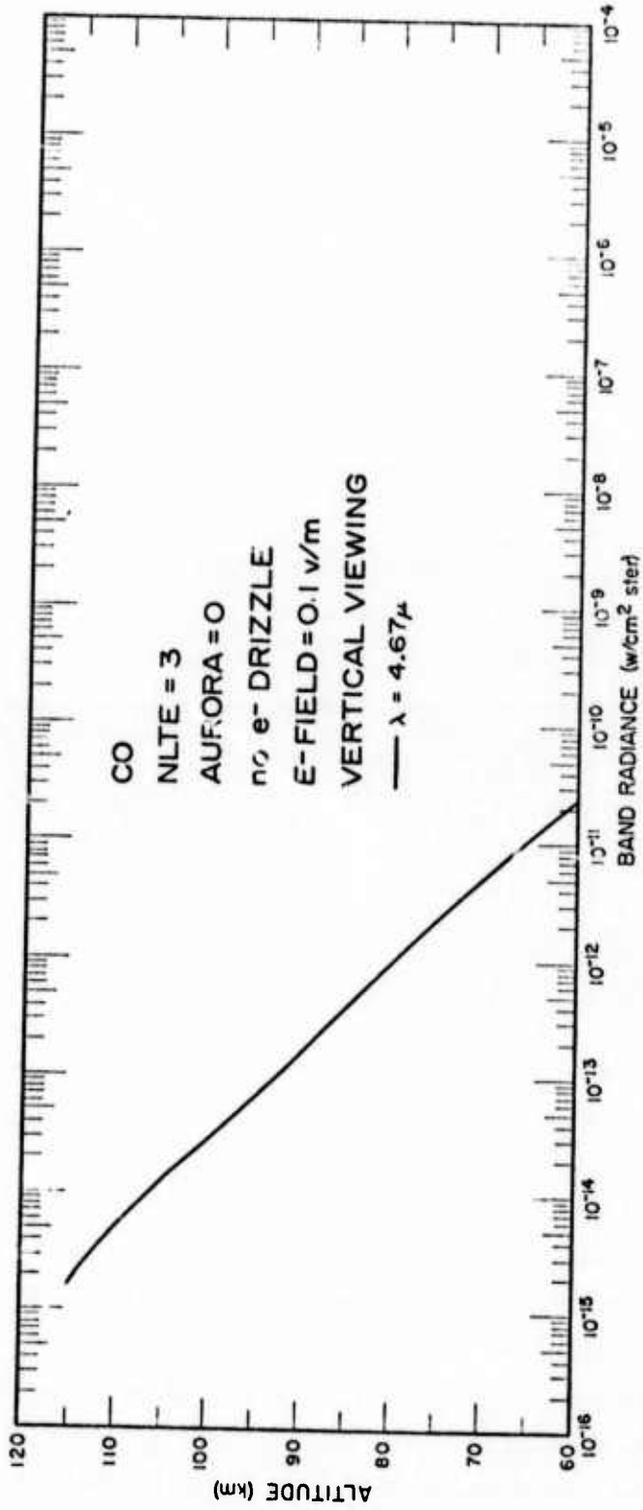

Figure 74. Height profile of the band radiance of CO for the case when the only source of ionospheric disturbance is an electric field of 0.1 v/m.

might note that the altitude regime for enhancement is somewhat different than that of the aurorally disturbed cases. This is because the electric field excitation process cannot produce $O_2(v=1)$ or $N_2(v=2)$ at altitudes where the mean free path is below some threshold length. That is to say, the electric field excitation process has a threshold altitude of somewhere near 100-110 km or so.

As a comparison, Figures 75 and 76 show the predicted radiance of CO_2 at 4.3 μ and 10.4 μ and the bands of NO^+ when the electric field has been increased to 0.2 volts/meter.

Much has been said about the near resonant V-V exchange process being the means of enhancing certain vibration populations of the infrared active species. The amount of energy exchange to the minor constituents, therefore, is proportional to the vibrational population of the v=1 state of N_2 (or O_2 as the case may be). Figure 77 is a plot of the ratio of the predicted v=1 level population of N_2 to the Boltzman population of that level. Five different cases are presented in this plot. They are (1) totally quiescent conditions, (2) that of only a background electron drizzle, (3) IBC-II aurora five minutes after commencement with electron drizzle, (4) IBC-III aurora five minutes after commencement with electron drizzle, and (5) that with an electric field of 0.1 volts/meter but no aurora or electron drizzle. Needless to say, the N (v=1) population significantly increases with auroral activity. One might also note the altitude dependence of this population with the excitation mechanism.

SPECTRUM COMPUTATION PROGRAM (PROGRAM SPCTRA) PHYSICS

The data presented in the previous section was on a band-by-band basis. This is informative if one is interested in only one particular band. Very often, however, it is of interest to know the predicted infrared radiance throughout some spectral region. In this case one would need to know the radiance contribution of each and every band which radiates in that particular region.

It is the purpose of program SPCTRA to compute a predicted radiance throughout the spectral region 1-25 μ. This is done by using the output

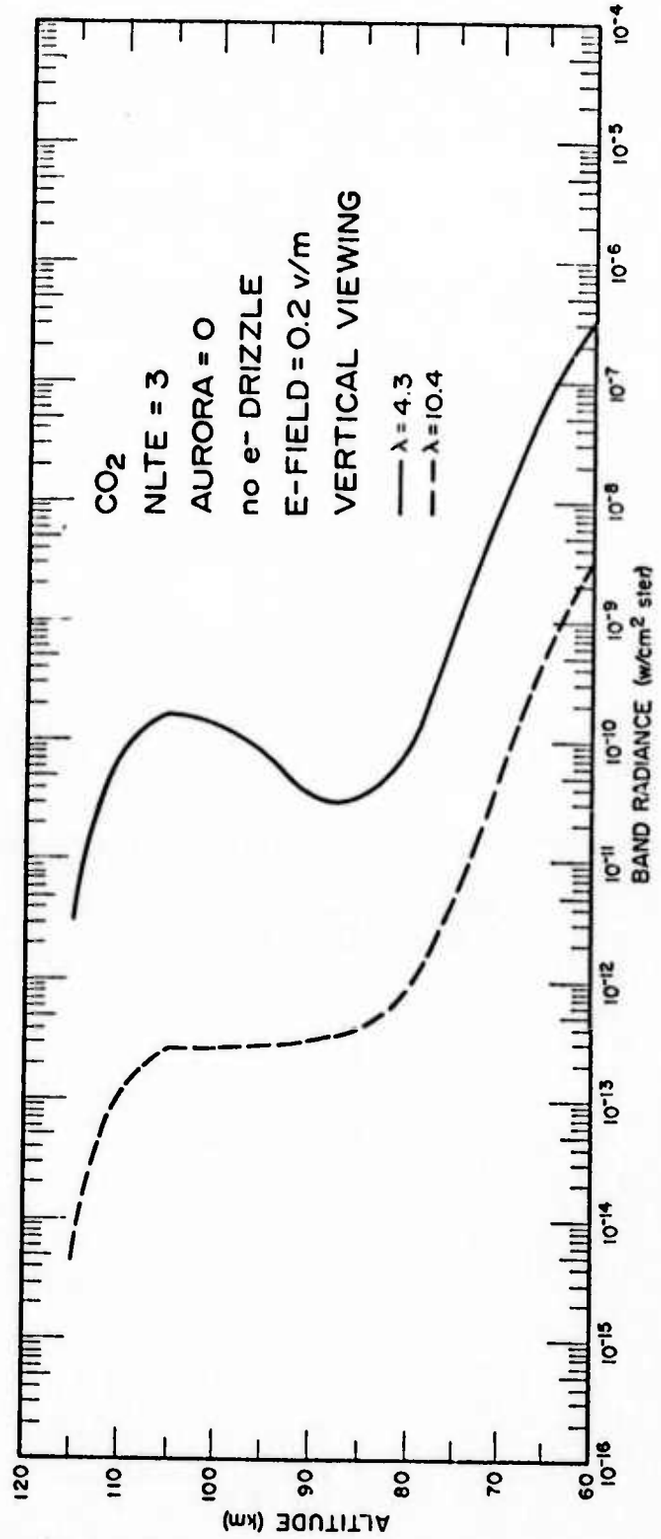

Figure 75. Height profile of the band radiance of CO_2 for the case when the only source of ionospheric disturbance is an electric field of 0.2 v/m.

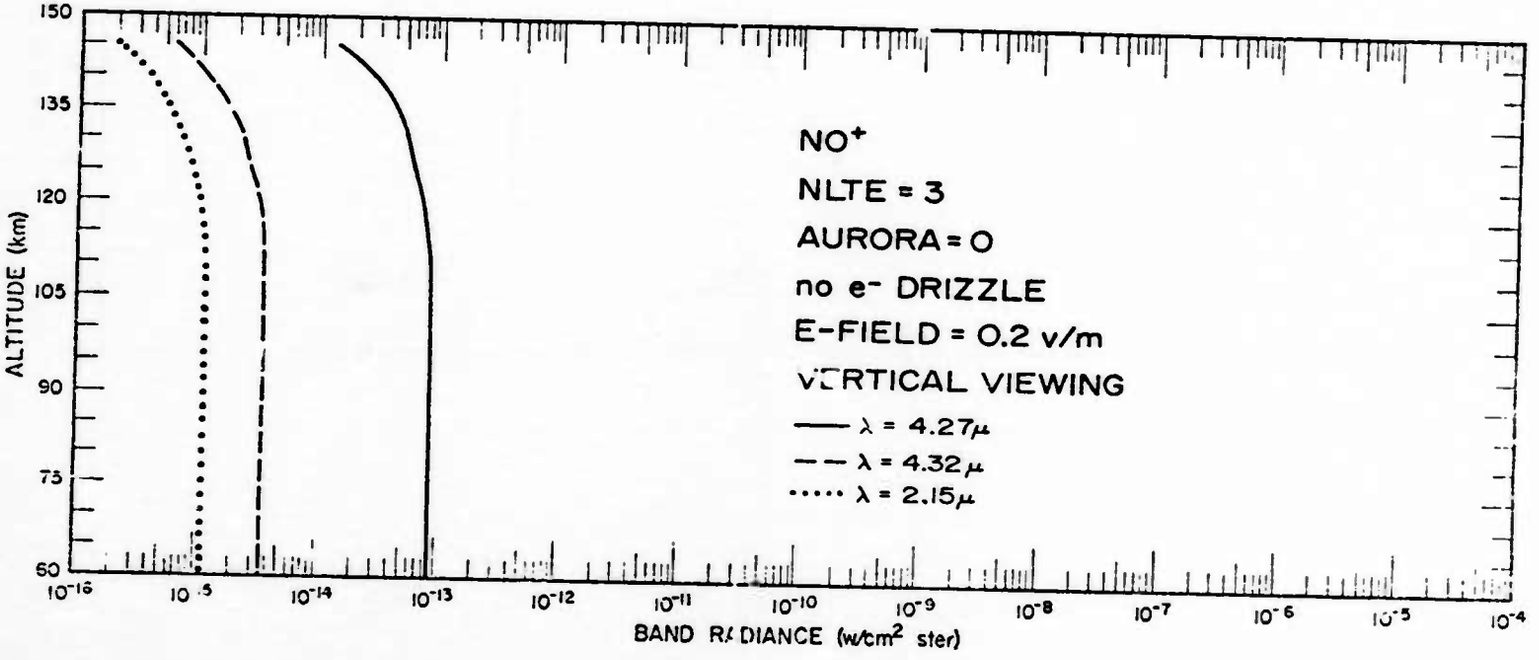

Figure 76. Height profile of the band radiance of NO^+ for the case when the only source of ionospheric disturbance is an electric field of 0.2 v/m.

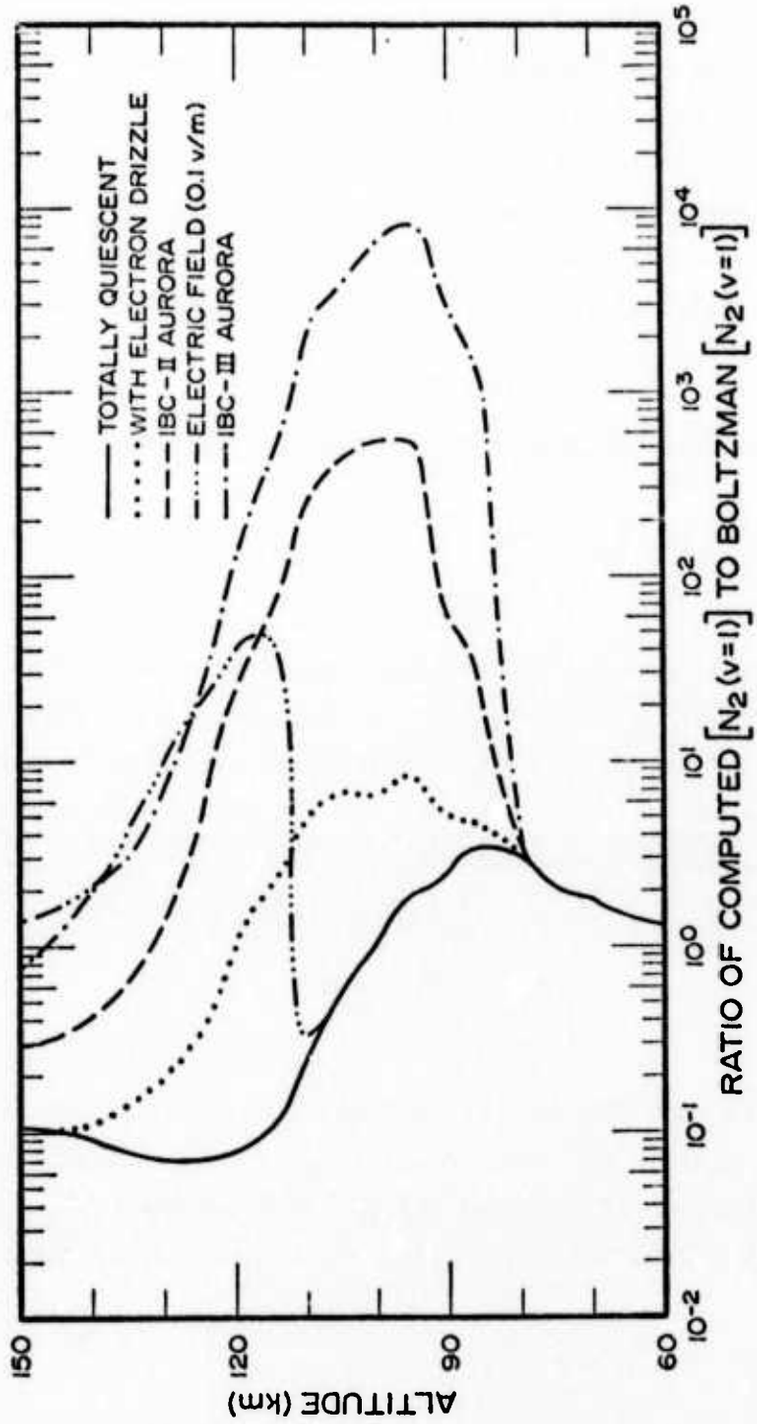

Figure 77. Height profile of the ratio of the predicted number density of excited N_2 to the number density of excited N_2 as determined by the Boltzman equation for various disturbed states of the ionosphere.

of program BCKGND as an input to this program. That is, each of the predicted band radiances for each of the minor constituents is redistributed on a line by line basis. All of the myriad of lines from all of the bands of all of the minor constituents are then summed together and printed out every 0.1 μ from 1.0 μ to 25.0 μ. Three different viewing geometries are considered. The observer may be looking vertically upwards, horizontally, or he may be observing in limb view fashion.

Line Position Determination

The rotational energy levels for a rigid linear molecule are given as

$$E = hc\, F(J) \tag{83}$$

where

$$F(J) = B(J + 1)J \tag{84}$$

B is the rotational constant for that particular vibrational level under consideration and J is the rotational quantum number. For this type of molecule (if we ignore any selection rules associated with symmetry properties) the line positions, in wave numbers, for a vibrational-rotational band are given as [*Goody* 1964]

$$P(J'') = \nu_o/c - (B' - B'')J'' + (B' - B'')J''^2 \tag{85}$$

$$Q(J'') = \nu_o/c + (B' - B'')J'' + (B' - B'')J''^2 \tag{86}$$

$$R(J'') = \nu_o/c + 2B' + (3B' - B'')J'' + (B' - B'')J''^2 \tag{87}$$

where B' and J' (B" and J") are the rotational constant and the rotational quantum number in the upper (lower) energy state respectively and ν_o is the frequency of the band center. The letters P, Q, and R define the branch of the band. That is, if $\Delta J = J' - J''$ is taken as

$\Delta J = -1$	P-Branch
$\Delta J = 0$	Q-Branch
$\Delta J = +1$	R-Branch

In addition to the above, the vibrational angular momentum quantum number plays an important role. Transitions with regard to this quantum number fall into one of two categories: $\Delta\ell = 0$ or $\Delta\ell = \pm 1$.

If $\Delta\ell = 0$ the transition is called a parallel band. If in addition $\ell = 0$ in both the upper and lower states it is called a Σ-Σ transition and has no Q-branch. Both the P-branch and the R-branch turn out to be regular arrays of lines with fairly constant spacing. A gap occurs at the band center frequency ν_o. The R-branch lies on the high frequency side of ν_o and the P-branch on the low frequency side. The intensities of these two branches are not symmetrical due to the fact that the first line on either side of ν_o (R(0) and P(1)) have different initial states; i.e., J is different, and hence have different populations and also the fact that the intensity varies with the fourth power of the frequency. If $\ell \neq 0$ in the upper and lower states, a parallel band still results but it is no longer a Σ-Σ transition. In this case a weak Q-branch will be exhibited. No fundamentals are of this type [*Herzberg* 1945].

If $\Delta\ell = \pm 1$, the transition is called a perpendicular band. Bands of this type exhibit a Q-branch which is stronger than either the P-branch or the R-branch.

Of the molecules examined in this report, all are linear with the exception of CH_4, H_2O, and O_3. Therefore, the line positions of all but these may be computed using the method outlined earlier in this section. The remaining are dealt with in one of two ways. Either the line positions are obtained from experimental measurement and used as an input parameter, or individual line positions are not computed. In the latter case, a technique of computing the total radiance of all lines in certain spectral intervals is used.

Line Strength Determination

In a previous section it was stated that the line intensity is proportional to the fractional part of molecules in the initial state which is given by

$$\frac{n(J'')}{n} = \frac{g_{J''}}{Q_r(T)} \exp\left[-\frac{E_r(J'')}{kT}\right] \tag{88}$$

Therefore the individual line intensities are proportional to

$$\exp\left[-\frac{hc\, B_v}{kT} J(J+1)\right] \tag{89}$$

multipiied by a degeneracy factor. By computing this intensity for each line and summing over all lines a total relative line strength for all lines of all branches may be computed.

The spectral absorption coefficient τ_L for each line may be found in the same manner as equation (75) with the exception that a line strength and position must be used rather than a band strength and position. That is,

$$\tau_L = 4.8815 \times 10^{-18} \sqrt{M/T}\, N\, S_L \lambda_L \qquad (90)$$

where for example if a line in the P-branch is under consideration

$$S_L = \frac{PS}{\sum_i PS_i} S_B$$

Here

PS = relative line strength

$\sum_i PS_i$ = total relative line strength

S_B = band strength

The predicted radiance for a particular line is computed as follows. First, all of the relative line strengths are corrected for the effective optical thickness. The corrected line strengths are then summed over all lines and all branches of the band. The predicted line radiance R_L is then found as

$$R_L = \frac{LS}{\sum_i LS_i} R$$

where LS = the corrected relative line strength

$\sum_i LS_i$ = the total corrected relative line strength

R = the band radiance (watts-cm^{-2} -ster^{-1}) from the program BCKGND

In the case of nonlinear molecules either the individual line strengths or representative line strengths throughout the band intervals are given as input variables. That is to say, actual computation of individual line strengths is not done except in the case of linear molecules.

Spectrum Computation

Once the computation of all of the individual line positions and their predicted radiance has been completed for all of the bands, it is a simple matter to compute the total spectrum. The spectral region from 1 μ to 25 μ is essentially broken up into intervals of 0.1 μ. The radiance contributions for each of these intervals is summed over all lines of all bands of all molecules. As mentioned earlier, this is done for three different viewing geometries.

RESULTS OF PROGRAM SPCTRA

The output of program SPCTRA, which computes the predicted radiance spectrum from 1.0 μ to 25.0 μ, takes three different geometries into consideration. These geometries are the vertical viewing case, the horizontal viewing case, and the limb viewing case. Each of these cases is done for the altitudes from 60 km to 120 km in 5-km increments. As in a previous section, it is not necessary to present all of this data in order to gain some insight into the radiance changes due to auroral activity. Instead, two representative cases are illustrated. To be consistent with the data presented from program BCKGND, the vertical viewing case was chosen; and since the auroral activity was not modeled below 80 km, this altitude was chosen as the viewing altitude.

Figure 78 shows the predicted radiance spectrum for an instrument at 80 km, viewing in the vertical direction, under conditions of an electron drizzle but no aurora and also for an IBC-III aurora five minutes after commencement. The figure illustrates how the predicted radiance changes when auroral conditions prevail. The electric field intensity is assumed to be zero.

One may note that the enhancement due to the auroral energy input apperas in the bands of CO_2 at 4.3 μ and 10.4 μ, the NO band at 5.3 μ, the N_2O band at 4.5 μ, and the NO^+ bands at 4.32 μ, 4.27 μ, and 2.15 μ as predicted by the band model program. In addition there is an enhancement at 13.9 μ. This may be explained as follows.

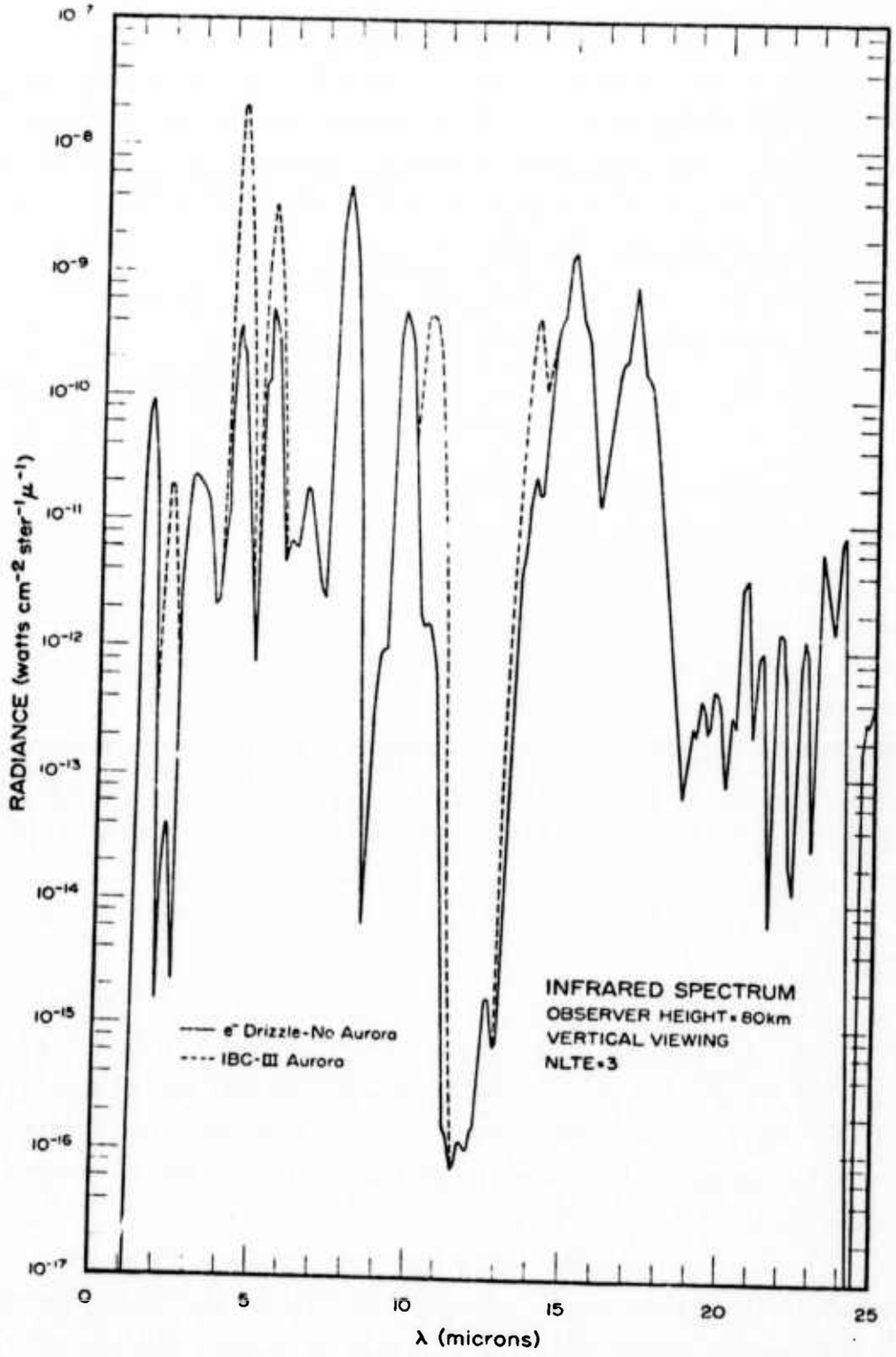

Figure 78. The solid line shows the radiance of the infrared spectrum from 1-25 μ under conditions of an electron drizzle only. The dashed line indicates the enhancement due to an IBC-III aurora. The predicted radiance for the auroral case is for five minutes after auroral commencement. Both cases are for nighttime conditions.

Figure 36 is a plot of the 15 μ bands of CO_2. This is a collection of seven different bands all grouped around 15 μ. Of these, the most aurorally enhanced is the band at 13.9 μ. The total radiance of this band, however, is considerably less than one of the 14.98 μ bands during quiescent conditions. The radiance is still slightly smaller than this 14.98 μ band, even though greatly enhanced by the IBC-III aurora. One would, therefore, expect to see an enhancement at 13.9 μ on the spectrum plot whereas this enhancement is hidden from view in grouping all of the bands around 15.0 μ together.

Plots such as those in Figure 78 are helpful in the design of scanning radiometers such as those using circularly variable filters. They are also helpful in determining filter requirements for single channel radiometers.

REFERENCES

Adams, G. W., Species densities in the lower thermosphere compatible with the U.S. Standard Atmosphere, *NOAA Technical Report ERL 193-SDL 20*, 1970.

Adams, G. W. and L. R. Megill, SIXBIT -- A generalized reaction kinetics program, *ESSA Technical Report ERL 177-SDL 15*, 1970.

Albritton, D. L., *private communication*, 1973.

Biondi, M. A., Atmospheric electron-ion and ion-ion recombination processes, *Com. J. Chem.*, *47*, 1711, 1969.

Bloomfield, C. H. and J. B. Hasted, Interconversion of ions drifting in a gas, *Brit. J. Appl. Phys.*, *17*, 499-460, 1966.

Burch, James L., Low-energy electron fluxes at latitudes above the auroral zone, *J. Geophys. Res.*, *73*, 3585-3591, 1968.

Charters, P. E., R. G. MacDonald, and J. C. Polanyi, Formation of vibrationally excited OH by the reaction H + O_3, *Applied Optics*, *10*, 1747-1754, 1971.

Chen, Joseph C. Y., Theory of subexcitation electron scattering by molecules, II. Excitation and de-excitation of molecular vibration, *J. Chem. Phys.*, *40*, 3513-3520, 1964.

Corbin, V. L., A. Dalgarno, T. C. Deggs, F. B. House, P. Lilienfeld, G. Ohring, and G. E. Oppel, Atmospheric radiance models for limb-viewing geometry in the 5 - 25 μ spectral region, *Honeywell, Inc. Scientific Report No. 1*, AFCRL Contract F19628-69-C-0268, 1970.

DASA, Reaction Rate Handbook, *DASA Information and Analysis Center*, 1967.

Deggs, T. C., A high altitude radiance model, *Final Report*, AFCRL Contract F19628-71-C-0156, 1972.

Deggs, T. C., Vibrationally excited nitric oxide in the upper atmosphere, *Applied Optics*, *10*, 1856-1860, 1971.

Dunkin, D. B., F. C. Fehsenfeld, A. L. Schmeltekipf, and E. E. Ferguson, Ion-molecule reaction studies from 300°K to 600°K in a temperature controlled flowing afterglow system, *J. Chem. Phys.*, *49*, 1365, 1968.

Fehsenfeld, F. C., D. B. Dunkin, and E. E. Ferguson, Rate constants for the reaction of CO_2 with O, O_2, and NL; N_2 with O and NO; and O_2 with NO, *Planet. Space Sci.*, *18*, 1267, 1970.

REFERENCES (cont.)

Fehsenfeld, F. C., P. D. Goldan, A. L. Schmeltekipf, and E. E. Ferguson, Laboratory measurement of the rate of the reaction $O^+ + O_2 \rightarrow O_2^+ + O$ at thermal energy, *Planet. Space Sci.*, *13*, 579-582, 1965.

Ferguson, E. E., Ionospheric ion-molecule reaction rates, *Rev. of Geophysics*, *5*, 305, 1967.

Field, R. W., The valence states of NO^+, *to be published.*

Gast, P. R., A. S. Jurso, J. Castelli, S. Basu, and J. Aarons, Solar Electromagnetic Radiation in *Handbook of Geophysics and Space Environments*, edited by S. L. Valley, McGraw-Hill Book Co., 1965.

Gerard, J. C., Metastable oxygen ions distribution and related optical emission in the aurora, *Ann. Geophys. 26*, 777-781, 1970.

Ghosh, S. N., Distributions and lifetimes of N and NO between 100 and 280 kilometers, *J. Geophys. Res.*, *73*, 309-318, 1968.

Goldan, P. D., A. L. Schmeltekopf, F. C. Fehsenfeld, H. I. Schiff, and E. E. Ferguson, Thermal energy ion-neutral reaction rates, II. Some reactions of ionospheric interest, *J. Chem. Phys.*, *44*, 4095, 1966.

Goody, R. M., *Atmospheric Radiation*, Oxford University Press, 436 pp., 1964.

Green, A. E. S. and L. R. Peterson, Energy loss functions for electrons and protons in planetary gases, *J. Geophys. Res.*, *73*, 233-241, 1968.

Green, A. E. S., *private communication*, 1972.

Harris, R. D., *private communication*, 1972.

Heaps, M. G., *Circulation in the high latitude thermosphere due to electric fields and joule heating*, 176 pp., Center for Research in Aeronomy, Utah State University, Logan, 1972.

Heppner, J. P., J. P. Stalarik, and E. M. Wescott, Electric-field measurements and identification of currents causing magnetic disturbances in the polar cap, *J. Geophys. Res.*, *76*, 6028-6053, 1971.

Herzberg, G., *Infrared and Raman Spectra of Polyatomic Molecules*, 632 pp., D. Van Nostrand, Princeton, New Jersey, 1945.

Herzberg, G., *The Spectra and Structures of Simple Free Radicals*, 226 pp., Cornell University Press, 1971.

Ivanov, V. V. and V. T. Shcherbakov, Tables of functions encountered in the theory of resonance radiation transfer, *Astrofizika*, *1*, 10-12, 1965.

REFERENCES (cont.)

Jones, R. A. and M. H. Rees, Time dependent studies of the aurora: I. Ion density and composition, *private communication*, 1972.

Kuhn, W. R. and J. London, Infrared radiative cooling in the middle stratosphere, *J. Atmos. Sci.*, *26*, 189-204, 1969.

Lazarev, V. I., Absorption of the energy of an electron beam in the upper atmosphere, *Geomagnetizm i Aeronomiya*, *7*, 219-223, 1967.

Lin, C. L. and F. Kaufman, Deactivation and reaction of $N(^2D)$, *J. Chem. Phys. (in press)*, 1971.

Linder, F. and H. Schmidt, Experimental study of low energy e - O_2 collision processes, report from *Fachbereich Physik der Universitat, Trier-Kaiserslautern, W. Germany*, 1971.

Mantz, A. W., J. K. G. Watson, K. N. Rao, D. L. Albritton, A. L. Schmeltekopf, and R. N. Zare, Rydberg-Klein-Rees potential for the $\chi^1\Sigma^+$ state of the CO molecule, *Jour. Molecular Spectroscopy*, *39*, 1971.

Megill, L. R., Self distortion of radio signals in the D-region, *Radio Science*, *69D*, *No.* ?, 367-373, 1965.

Megill, L. R. and N. P. Carleton, Excitation by local electric fields in the aurora and airglow, *J. of Geophys. Res.*, *69*, *No. 1*, 101-122, 1964.

Michels, H. H., A report of Air Force Weapon Laboratories, *AFWL-TRA-72-1* (1970).

Mitchell, A. C. G. and M. W. Zemansky, *Resonance Radiation and Excited Atoms*, 338 pp., Cambridge University Press, 1971.

Penner, S. S., *Quantitative Molecular Spectroscopy and Gas Emissivities*, 587 pp., Addison-Wesley Publishing Co., 1959.

Phillips, L. F. and H. I. Schiff, Mass spectrometric studies of atom reactions. I. Reactions in the atomic nitrogen-ozone system, *J. Chem. Phys*, *36*, 1509, 1962.

Rees, M. H., Auroral ionization and excitation by incident energetic electrons, *Planet. Space Sci.*, *11*, 1209-1218, 1963.

Rees, M. H., A. I. Stewart, and J. C. G. Walker, Secondary electrons in aurora, *Planet. Space Sci.*, *17*, 1997-2008, 1969.

Shimazaki, T. and A. R. Laird, A model calculation of the diurnal variation in minor neutral constituents in the mesosphere and the lower thermosphere including transport effects, *J. Geophys. Res.*, *75*, 3221-3225, 1970.

REFERENCES (cont.)

Stair, A. T. Jr. and H. P. Gauvin, Research on Optical Infrared Characteristics of Aurora and Airglow, Artificial and Naturan, in *Aurora and Airglow*, edited by B. M. McCormac, 365 pp., Reinhold Publishing Corp., 1967.

Taylor, R. L. and S. Bitterman, Survey of vibrational relaxation data for processes important in the CO_2 - N_2 laser system, *Reviews of Modern Physics*, 41, 26-47, 1969.

Thomson, H. W. and R. L. Williams, Vibration bands and molecular rotational constants of nitrous oxide, *Pro. Royal Soc.*, *220*, 435-445, 1953.

Ulwick, J. C., W. P. Reidy, and K. D. Baker, Direct measurements of the ionizing flux in different types of auroral forms, *Space Research VII*, 656-664, 1967.

U.S. Standard Atmosphere Supplement, 1966.

Wescott, E. M., J. D. Stolarik, and J. P. Heppner, Electric fields in the vicinity of auroral forms from motions of barium vapor releases, *J. Geophys. Res.*, *74*, 3469-3487, 1969.

Young, R. A., G. Black, and T. G. Slanger, Reaction and deactivation of $O(^1D)$, *Jour. of Chem. Physics*, *49*, 4758-4768, 1968.